Spectroelectrochemistry and voltammetry of metalloporphinones

Florentina Tutunea
Marquette University

SPECTROELECTROCHEMISTRY AND VOLTAMMETRY OF METALLOPORPHINONES

By

Florentina Tutunea, M.S.

A Dissertation submitted to the Faculty of the Graduate School,
Marquette University,
in Partial Fulfillment of the Requirements for
the Degree of Doctor of Philosophy

Milwaukee, Wisconsin

August 2011

ABSTRACT
SPECTROELECTROCHEMISTRY AND VOLTAMMETRY OF METALLOPORPHINONES

Florentina Tutunea, M.S.

Marquette University, 2011

Metalloporphinones have been found in a number of enzymes involved in nitrogen metabolism. The emphasis of this research project has been to develop spectroscopic markers in order to identify metal versus porphinone reduction. The carbonyl group in the porphinone has a very strong signal which is quite sensitive to the extent of reduction of the porphinone macrocycle.

The spectral change makes IR an important tool in the process of structure determination of metalloporphyrins because the carbonyl group shift can be correlated with the metal oxidation state. It was observed from previously published studies that a higher metal oxidation state moves the carbonyl group at a higher frequency while a lower oxidation state will shift the carbonyl vibration to a lower frequency.

Previous work in our laboratory has focused on iron porphinones, but the lack of empirical relationships for the spectroscopic data has made it difficult to clearly interpret the results. Consequently, previous students' work was extended to include zinc, cobalt and manganese complexes. It has been postulated that zinc and manganese complexes would lead to primarily macrocycle reduction while cobalt complexes would be more similar to iron. By using a combination of spectroscopic techniques (visible and infrared spectroscopy), it has been possible to separate metal from macrocycle reduction. Additional information is now being gathered using oxygen isotopic substitution. This information can be quite useful in understanding both the enzymatic process and the use of these compounds for catalysis.

Based on this information, our studies will be focused on the mentioned correlation and bring supplementary evidence for the problem addressed by researchers in the last 25 years concerning the oxidation state of iron(II) upon reduction.

ACKNOWLEDGEMENTS

I would like to thank to research adviser, Dr. Michael D. Ryan for his guidance and encouragement throughout the course of this research and for his suggestions and corrections of this dissertation.

I also would like to express appreciation to my research committee members, Dr. James R. Kincaid, Dr. Adam Fiedler for their guidance and support. I am thankful to Dr. Rajendra Rathore, Dr. Sergey Lindeman and Dr. Sheng Cai for their help. I am very thankful to the graduate students, the faculty and the staff of the Chemistry Department of Marquette University for all their help.

I am very thankful for the support and encouragement of my friends in Romania, my parents for their love and understanding.

TABLE OF CONTENTS

TABLE OF FIGURES

LIST OF TABLES

Chapter 1 INTRODUCTION

The origin of "porphyrin" term is from ancient Greece, when the word *porphura* was used to describe the color purple. In those days, due to their colors, the porphyrins were usually used as pigments. One of the characteristics that make porphyrins special is that they are associated with blood, and many of the redox enzymes involved in metabolic processes. The main function of porphyrins in nature is to bind metal atoms, which act as centers for significant biochemical events[1].

1. Background: Structure and Nomenclature of Porphyrins

Porphyrins are 16-atom conjugated macrocycles with planar geometry[2] which can form complexes with almost all transition and main group metals[3]. Figure 1-1 shows the numbering scheme of the carbon atoms of the macrocycle, as well as the conventional labeling system (Cα, Cβ and Cm). The electronic structure is based on conjugated π-electron system with twenty-two electrons, eighteen of which can be included in one cyclic path. Different types of groups or side chains can be attached to the β carbons of the pyrrole rings or the methine carbons (C_m).

Octaethylporphyrin (OEP) is the most commonly synthesized etio-type porphyrin (containing alkyl substituents at the β-pyrrole positions). The porphyrins having substituents only at the four methine bridges are known as meso-type porphyrins. The four substituents are usually derivatives of benzene or pyridine. Tetraphenylporphyrin (TPP)

is the most encountered, as it is easily synthesized. It does not occur in nature. Models of porphyrin, chlorin and isobacteriochlorin have been examined with regards to the structure of the compounds formed between these metal complexes and intermediates of enzymes found in biological systems[4].

Chlorins, bacteriochlorins, and isobacteriochlorins (Figure 1-1) are all derived from a parent porphyrin by the hydrogenation of one or two pyrrolic double bonds[5]. The parent porphyrin is a tetradentate ligand which consists of four pyrrole molecules linked together as a ring by four methine bridges. The reduction of one pyrrole double bond gives chlorin, while the saturation of double bonds on two opposite pyrrole yields a bacteriochlorin. An isobacteriochlorin results from the reduction of double bonds on two adjacent pyrroles. Another common name of these compounds is hydroporphyrins. The oxidation of octaalkylporphyrins with hydrogen peroxide or osmium tetroxide leads to structures containing one or two oxygens in the molecule. These compounds are named porphinones and porphinediones (Figure 1-1).

The metal complexes of porphyrin ligands (metalloporphyrins) are a large class of coordination compounds which can be found in many biological systems in nature. For instance, chlorophylls which are involved in the photosynthesis of green plants are magnesium chlorins. Heme proteins, compounds containing an iron-porphyrin moiety, play important functions in oxygen transport and storage in human body. The four coordinated complexes have two vacant axial sites for binding additional ligands and can form both five and six coordinated compounds[6].

The reduction and oxidation of metalloporphyrins can occur either at the porphyrin center to generate π anion and π cation radicals (the energy of HOMO or LUMO π orbital

can be altered) or it may occur at the metal center (the change in molecular orbitals involves metal-centered atomic wavefunctions)[7]. The redox reactions can also occur at the axial ligand. The site of reaction depends on the porphyrin macrocycle, central metal ion, axial ligand, solvent and supporting electrolyte[8,9].

Metal centered reductions occur for the metalloporphyrins with vacancies in the dπ orbitals while porphyrin ring centered reductions occur for metalloporphyrins having d^8, d^9, d^{10} central metals. The site of the electron transfer depends on the shape of the LUMO (reduction) or HOMO (oxidation). If the orbital resides mostly on the metal, the reduction is considered metal centered[10].

Electron donating substituents facilitate oxidation of the molecule by raising the HOMO towards the non-bonding level, and cause the same molecule to be hard to reduce by lifting the LUMO energy. The more extended is the porphyrin conjugated system, the closer will be the frontier orbitals to each other and to the non-bonding level and the compound will be easier oxidized or easier reduced[10].

The site of electron transfer can be characterized by UV-visible, IR or EPR spectroscopy[11,12,13,14,15,16]. Spectra with two bands between 500-600 nm are generally obtained for compounds with an uncharged ring system, while those with a broad band covering the whole visible range and extending into the near infrared are typical of species with singly oxidized porphyrin ring[17]. The one-electron reduction products of the porphyrins macrocycle have a spectrum with strong absorptions above 800 nm and a broad Soret band.

Electrochemical techniques are used in order to produce a controlled addition or abstraction of electrons to or from a compound which will result in a short-lived or stable species for study. Techniques such as UV-Visible, IR, NMR, Raman spectroscopy have

been used to better understand the electrochemical process. Electronic absorption spectroscopy can be used to clarify where the electrochemical process takes place (ring or metal). The IR technique is useful to evaluate and identify the site of unpaired electrons, but there are no general guidelines in order to determine which technique is the most efficient.

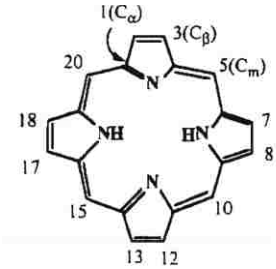

Structure 1

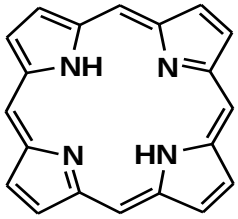

Porphyrin

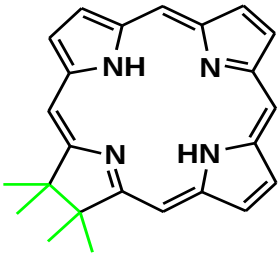

Chlorin

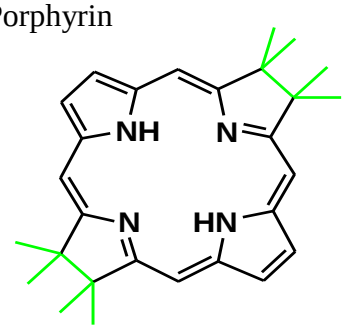

Bacteriochlorin

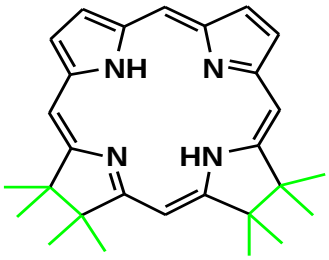

Isobacteriochlorin

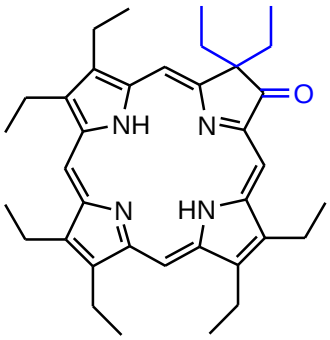

Octaethylporphinone (OEPone)

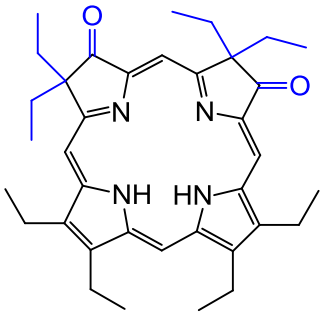

Octaethylporphinedione (OEPdione)

Figure 1-1.Structures of Porphyrin ,Chlorin, Bacteriochlorin, Isobacteriochlorin, Octaethylporphinone, Octaethylporphinedione

2. Electrochemistry of metallo-porphyrin complexes

The redox behavior of porphyrins has been extensively investigated because of their relevance to several biological processes and high number of literature reviews have been published in this area[18,19,20]. Metalloporphyrins containing iron and cobalt have been used as model compounds for hemoproteins and vitamin B_{12}, nickel porphyrins have served as models for coenzyme F_{430} while other metalloporphyrins have been used to study inherent reactivity and function relationships. Thousands of metalloporphyrins have been investigated during last three decades. These include compounds with hundreds of different porphyrin macrocycle, dozen of different coordinated axial ligands and close to 80 metals ions.

Most of metalloporphyrins electrochemistry involves either the central metal ion or the conjugated π system. Therefore the electrochemistry of metalloporphyrins can be described from two points of view: the nature of central metal ion and the nature of macrocycle. However, electrochemistry of metalloporphyrins can be influenced by the structural factors related to the number and type of substituents attached to the macrocycle or to the number of axial ligands bound to the central metal ion.

In the reviews published by Kadish[21], Felton[22], Davis[23], and Buchler[24,25] the authors discussed the electrochemistry of octaethylporphyrin (OEP) and tetraphenylporphyrin (TPP) derivatives. The compounds of these two series have always been used as comparison compounds against values of other newly synthesized metalloporphyrins. Although a number of hydroporphyrin complexes have been synthesized[26], their poor yield, stability and purity strongly limited the electrochemical

and spectroscopic studies of these complexes. The electrochemical studies of some free-base [27,28,29,30,31,32,33,34] and iron hydroporphyrin complexes[27,28,29] have involved the measurements of the redox potentials, and little information is available on the details of electron transfer.

Electrochemical studies of some free-base hydroporphyrins[35,36,37,38] (including, chlorins, bacteriochlorins and isobacteriochlorins) reported previously, have concluded that the oxidation of free-base hydroporphyrins becomes easier as the porphyrin pyrrolic ring are progressively saturated. Isobacteriochlorin complexes are 250-300 mV easier to oxidize than the corresponding chlorins, and 500-600 mV easier than porphyrins[33]. The sensitivity of the half-wave potentials of the macrocycle structure suggested that the oxidation occurred at ring systems. The effect of macrocycle structure on the reduction of hydroporphyrins is complex.

Calculated energy levels for the highest occupied (HOMO) and lowest unoccupied (LUMO) MOs of porphyrin, porphinone, porphinedione complexes of Zn(II) were performed by Chang et al[29]. As more carbonyls are added to the porphyrin ring, the energy required for oxidation should parallel the energy of the HOMOs and decrease in the order: (hard) porphine> porphinone > porphinedione (easy), as it was observed in their experiments. On the other hand, the energy levels diagram of HOMOs and LUMOs of zinc complexes studied by this group, suggested that porphinedione will be the hardest to reduce and that the other three complexes should have nearly equal reduction potentials. In a later study, Chang et al[33], showed that extended calculations of Huckel MO helped rationalize redox trends. They calculated the LUMOs of porphyrins,

porphinones and porphinediones which revealed that the ease of reduction increased in the order: (hard) porphyrin(-9.195)>porphinedione (-9.276)>porphinone(-9.394) (easy).

The half wave potentials of some free-base porphinones[34,38] and their iron complexes[33,36] were reported in the published literature. Unlike what was observed for hydroporphyrins, the porphinone complexes (porphinone and porphinedione) oxidize at about the same potentials[33,34,36,38]. The reduction for both free-base and iron complexes appears to be easier with progressive hydrogenation of pyrrolic double bonds and the reduction potentials were strongly dependant on the location of the oxygen atoms.

One of the first comprehensive comparisons between electrode reactions involving formation of metalloporphyrin π-anion radicals and those involving π-cation radicals was published by Fuhrhop et al.[39]. The authors measured the potentials of 25 octaethylporphyrins with different metal ions using cyclic voltammetry to evaluate $E_{1/2}$ for the oxidation or reduction, and concluded that the potential difference between the first porphyrin oxidation to form π-cation radical and the first reduction to form a π-anion radical was a constant 2.25±0.15 V. In addition, the difference in potential between the first and second reduction of the macrocycle was reported to be 0.42 ±0.05 V. The results further suggested the use of these electrochemical ”diagnostic criteria” to distinguish between metal-centered and ring centered reactions of metalloporphyrins.[40,41,42]. Fuhrhop et al.[39], constructed plots of $E_{1/2}$ for the first porphyrin centered ring reduction vs $E_{1/2}$ for the first porphyrin-centered ring oxidation and showed that there is an inverse linear relationship between the ease of metalloporphyrin ring oxidation and the ease of metalloporphyrins ring reduction. The inverse trend was explained as resulting from a variation in the electrostatic forces introduced into the cavity of the porphyrin by the

different metal ions. The potentials for the reversible ring first oxidation and the reversible first ring reduction were also linearly related to the divalent central metal ion electronegativity. In addition, the half wave potentials for the oxidation or reduction were roughly linear with respect to the charge on the porphyrin macrocycle, as calculated by Gouterman and coworkers[43,44,45,46,47]. Several conclusions were drawn from the large number of literature studies of metalloporphyrins containing OEP or TPP macrocycles and the majority seems to have held up over the last 20 years independent of the nature of the central metal ion and/or nature of any bound axial ligand. The first conclusion is that metalloporphyrins can be reduced by two electrons at the conjugated macrocycle to give porphyrin π-anion radicals and dianions. Metal centered reactions can be observed for the compounds containing an electroactive central metal ion. One diagnostic criterion which surfaced from early electrochemical studies is the experimentally determined HOMO-LUMO gap of 2.25± 0.15 V, which could be compared with the theoretical value of 2.18 V calculated by Zerner and Gouterman[43]. Another important finding in the porphyrin research field is the constant potential difference between the first and second macrocycle centered reduction. Large deviation from these values have been often used to suggest an electrode reaction which did not involve the conjugated macrocycle, with early examples being given for the case of Co, Fe, Ag, Cr-centered oxidation and reduction[39,48]. Other deviations from the well-accepted values were used to suggest an increased interaction between the central metal ion and the macrocycle[39] or a substantial difference in axial ligand-metal interaction between oxidized and reduced forms of the porphyrin.

2.1. Zinc porphyrin complexes

The chemical and electrochemical oxidations of Zn(OEP)[49,50,51,52] and Zn(TPP) [49,53,54,55,56] have been well-studied in non-aqueous media. The electrochemical or chemical oxidations of Zn(OEP) with Br_2 in $CHCl_3$, CH_3OH or CH_2Cl_2 lead to $[(OEP)Zn]^{+\cdot}$, a π cation radical. Zn(TPP) can also be chemically or electrochemically oxidized to yield $[(TPP)Zn]^{+\cdot}$ [49,52, 53,54,55,56]. Previous literature data of ZnTPP reduction illustrates two processes observed at -1.34 V and -1.74 V vs Standard Calomel Electrode (SCE). The complex displays reversible two-one electron step reductions of ZnTPP, first one to its anion radical and second one being the reduction to the dianion species[57]. The $ZnTPP^{-2}$ dianion was not stable during the thin layer spectroelectrochemical experiment. The specified intermediate accepts one proton from the reaction medium which binds to one of the meso-carbons, leading to the phlorin anion complex[58].

2.2. Manganese porphyrin complexes

As discussed below, manganese porphyrin electrochemistry involve reactions of Mn(III) derivatives, which are easily reduced to Mn(II), followed at more negative potentials by the possible formation of the π-anion radical and dianion depending upon the solvent and macrocycle. Manganese porphyrins have been characterized as stable derivatives with metal oxidation states of 2^+, 3^+, 4^+ and 5^+. Early electrochemistry and spectroscopic characterization of Mn(III) and Mn(II) porphyrins was reported by the

groups of Boucher, Davis and Calvin in the 60's, Felton, Fuhrhop, Basolo/Hoffman and Kadish in the 70's and Kadish, Schultz and others in the 1980-1990s.

Extensive measurements of Mn(III)/Mn(II) redox potentials and spectroscopic characterization of Mn(III) and Mn(II) porphyrins under varying solution conditions were published starting in 1970's. Mn(III) may be electrochemically reduced by up to three one electron transfer steps yielding initially a Mn(II) complex, followed by π-anion radicals and dianions of Mn(II). The potentials and site of electron transfer for each electrode reaction of a given manganese(III) porphyrin will depend upon porphine basicity or planarity, the nature of the solvent, the counterion on Mn(III) and the basicity and/or steric effects of any bound axial ligands. Several studies which elucidated the effect of solvent and counterion on manganese porphyrin redox potentials began to appear in the late 70s. The Kadish group reported (TPP)MnCl reduction potentials at -0.23 V in DMSO and pyridine and -0.3 V in CH_2Cl_2. In 1982 Kelly and Kadish published one of the most systematic investigation of (TPP)MnX redox potentials, measured in twelve different solvents for compounds with six different counterions. The results of this study indicated that the Mn(III) counterion binding strength increased in the order ClO_4^-< I^-<SCN^-<Br^-<Cl^-<N_3^-, which reflected an increased stabilization of the Mn(III) over the Mn(II) form of the porphyrin as one progressed along the series[59].

2.3. Cobalt porphyrin complexes

Another commonly studied metal in porphyrin complexes is cobalt. The electrochemistry of cobalt porphyrins is dominated by metal- centered reactions, the most

common of which involve Co(II)/Co(III) and Co(II)/Co(I) transitions which occur at potentials easily accessible within the range of most non-aqueous electrochemical solvents[60,61,62,63]. Two additional less studied electrode reactions involve the Co(I) to Co(I) π - anion radical and Co(I) π-anion radical to dianion transitions to negative potentials. One of the most studied of all cobalt porphyrins is (TPP)Co which was first characterized as to its oxidation and reduction properties in the mid 1960's[64,65].

The electrochemical[66,67,68] or chemical[69] reduction of (TPP)Co(II) leads to a Co(I) porphyrin which has been isolated as (TPP)Co(Na)·5THF[71] The electrochemical reduction of TPPCo(II) has been reported to occur in different solvents but the further reduction of electrogenerated $TPPCo(I)^-$ takes place outside the range of most electrochemical solvents as is located at approximately -1.9 V vs SCE in DMF or DMSO and - 2.03 V in toluene or benzene. The half-wave potentials for reduction of cobalt(II) porphyrins are generally not dependent on the solvent and supporting electrolyte, with the only exception in pyridine.

The reduction of CoTPP has been reported to occur at -0.81 V to -0.82 V on DMSO[41,67,70] and in the range -0.76 V to -0.77 V in DMF[67]. Both DMF and DMSO form mono-adducts with CoTPP in CH_2Cl_2 but no solvent binding to the Co(I) form of the porphyrin is observed under these conditions. The mechanism for electroreduction or electrooxidaton of a given cobalt porphyrin will depend in large extent on the nature of the axial-ligand coordination[71].

2.4. Iron porphyrin complexes

The electrochemistry of iron porphyrins has been extensively studied in non-aqueous and aqueous media[72,73,74]. Iron porphyrins can be oxidized or reduced at three distinct sites: metal, porphyrin ring, or axial ligand. Six redox reactions have been observed for iron porphyrins, without destroying the integrity of the conjugated ring system[70]. The iron(III) electroreduction could be represented as occurring in three-one electron transfer steps; the first two redox reactions take place at central metal, and the latter occur within the macrocycle. The oxidation states are easy to be assigned to the central metal for the complexes of iron(III) and iron(II), but it has been difficult to specify the degree of delocalization of electron in the other steps.

All iron porphyrins with halide or perchlorate axial ligands contain Fe(III) in their air-stable structures but a conversion of Fe(III) to Fe(II) is readily accomplished at potentials generally located between -0.2 V and -0.5 V vs. SCE. The potential value of the metal centered reduction will depend in large part upon the solvent conditions, the type of counterion and the type of porphyrin macrocycle as demonstrated in the published literature[59].

The effect of solvent on half-wave potentials was investigated by Davis in 1975,[75] Kadish and Davis et al. in 1976,[76,77] Based on all these early studies, it could be concluded that strongly coordinating anions shift the potential for the Fe(III)/Fe(II) reduction in a negative (cathodic) direction while weakly coordinating anions result in a positive(anodic) shift, or an easier reduction. The well studied iron tetraphenylporphyrin

chloride (TPPFeCl) was reduced at -0.11 V in DMSO and +0.15 V in DMF, but the half wave potential was shifted to -0.29 V in poorly coordinating solvent such as CH_2Cl_2.

Bottomley and Kadish[76,77] published a study of Fe(II) reduction potentials as a function of solvent and counterion. The reduction of TPPFeX with five different counterions was investigated in ten different non-aqueous solvents. The study showed an increased sensitivity of $E_{1/2}$ to the counterion on a specific solvent.

The presence of porphinediones in nitrogen cycle has open interest in recent years. Timkovich et al[78] determined the chemical structure of the heme prosthetic group (heme d_1, an iron porphinone) of the nitrite reductase. This finding brought considerable interest in the last decade consequently many research groups have examined the properties of the porphinedione complexes in order to further investigate the structure of the macrocycle and their properties[79] .

Voltammetric studies of free base hydroporphyrins and their iron complexes were previously reported and they have shown that the redox potentials of hydroporphyrins are shifted to more negative values. They are easier to oxidize and harder to reduce. Also the separation between the first ring oxidation and reduction potentials that reflect the HOMO-LUMO energy gap is constant between porphyrin-porphinones-porphinediones series. Yet not many studies have been found to examine the complete electrochemistry of these complexes on a larger potential interval. Because THF can be purified with very low levels of trace water, this solvent is ideal for the spectroelectrochemical study of reduction products.

Experimental studies performed in our laboratory on iron porphinones showed two electrochemical processes, the first being a metal centered reaction while the second

electron process was influenced by the presence of the carbonyl group in the porphinone rings. The reduction potential for the second process becomes more negative in the following order: porphinedione, porphinone, porphyrin[80].

Redox potentials of free base porphyrins were reported from this laboratory (Table 1-1). It was observed that the first oxidation becomes easier with hydroporphines and harder for porphinones. The $E_{1/2}$ for the first oxidation of porphinediones was 250 mV positive of porphinone which was 250 mV positive of OEP.

The electrochemical results reported previously from this laboratory on porphinones and porphinediones shows that reduction and oxidation is a two-one electron process and the porphinedione (-1.62 V) reduce at similar potential to octaethylporphinone (-1.66 V). It was also shown that they are easier to reduce and harder to oxidize in comparison with H_2OEP.

The results from this laboratory on iron porphinones showed that the reduction potential of FeOEPCl was more negative than that of FeOEPoneCl and FeOEPdioneCl by 0.1 V and 0.3 V, respectively. For the oxidation process, the $E_{1/2}$ values shifted to more negative potentials with progressive increasing of carbonyl groups in the molecule.

When electrochemistry is used to characterize the site of reaction in the porphyrin complexes, a rough estimate based on potential difference can be assessed. One can use a comparison between series of complexes in order to infer a metal or a porphyrin ring reaction site but the assessment cannot be made based only on these results. A decision should be confirmed involving other measurements (spectroscopic methods).

The main advantages of the electrochemical techniques are: the ability to reduce or oxidize species selectively, the ability to be combined in-situ with spectroscopic

techniques such as UV-visible, FTIR, EPR, and Raman and the ability to monitor a new species. Besides its advantages, electrochemistry has the disadvantage that it cannot be used alone to characterize or identify electro-generated intermediates. It has to be supported by techniques like UV-visible, NMR, IR in order to have reliable conclusions for the studied process.

Table 1-1. Cyclic voltammetry data for selected porphinones and porphinediones

Compound	Ox2	Ox1	Red1	Red2	Red3	Ref.
H_2OEP		0.59	-1.80	-2.16		82
H_2MOEC		0.36	-1.83	-2.19		82
H_2OEPone		0.64	-1.66	-2.04		82
H_2(2,4-OEPdione)		0.61	-1.62	-1.99		82
H_2(2,4-DMOEiBC)	0.57	0.11	-2.12	-2.58		82
FeOEPCl		0.71	-0.91	-1.72	-2.29	82
FeOEPoneCl		0.56	-0.81	-1.69	-2.29	82
Fe(2,4-OEPdione)Cl		0.50	-0.62	-1.61	-2.01	82
Fe(2,4-DMOEiBC)Cl	0.57	0.10	-0.88	-2.08	-2.61	82

Solvent: tetrahydrofuran

3. Studies of porphyrin complexes by spectroscopical techniques

An important subject in the electrochemistry of metalloporphyrins is the assignment of the redox sites within porphyrins. The corroboration of the electrochemical experiments with spectroscopical analyses could be of a real importance to achieve this goal[81].

Electronic spectroscopy has been employed to identify the site of oxidation/reduction in metalloporphyrins. All metalloporphyrins have characteristic absorption bands in the ultraviolet-visible region. These bands are thought to arise mainly from the π-π^* transitions due to the π- electrons of the porphyrin ring[82].

Figure 1-2 shows the classical features of metalloporphyrin spectra: an intense B (Soret) band near 400 nm, and a pair of weaker bands Q (or α and β), between 500 and 600 nm; this is illustrated by the Gouterman's four-orbital model[82]. The LUMO is a degenerate π* (in the idealized D_{4h} point group), while the two HOMO have nearly the same energy. The two π-π* electronic transitions have similar energies and the same excited-state symmetry thus undergoing strong configuration interaction. The transition dipoles add up for the intense B transition and nearly cancel for the weaker Q transition. Some intensity (about 10%) is regained for the Q transition via vibronic mixing with the B transition, producing the Q sideband.

Abnormal electronic spectra are observed in Mn(III) porphyrins: the intense Soret band of the normal metalloporphyrin spectrum is split into two bands. It was suggested by Boucher that the anomalous behavior results from π-back bonding between the metal e_g orbitals and the antibonding π* orbitals of the porphyrin ligand[83].

The ring-centered oxidation and metal-centered oxidation usually give rise to distinctly different electronic spectral changes[84]. If the oxidation process is porphyrin ring- centered, the Soret band will usually blue shift, and its intensity will be reduced considerably. The Q-bands will usually red shift and decrease in intensity leading to a broad feature. If the oxidation process is metal-centered, there is no major loss of intensity of the Soret band, but the peak position will blue shift, while the two Q-bands are retained (with or without change in position)[85].

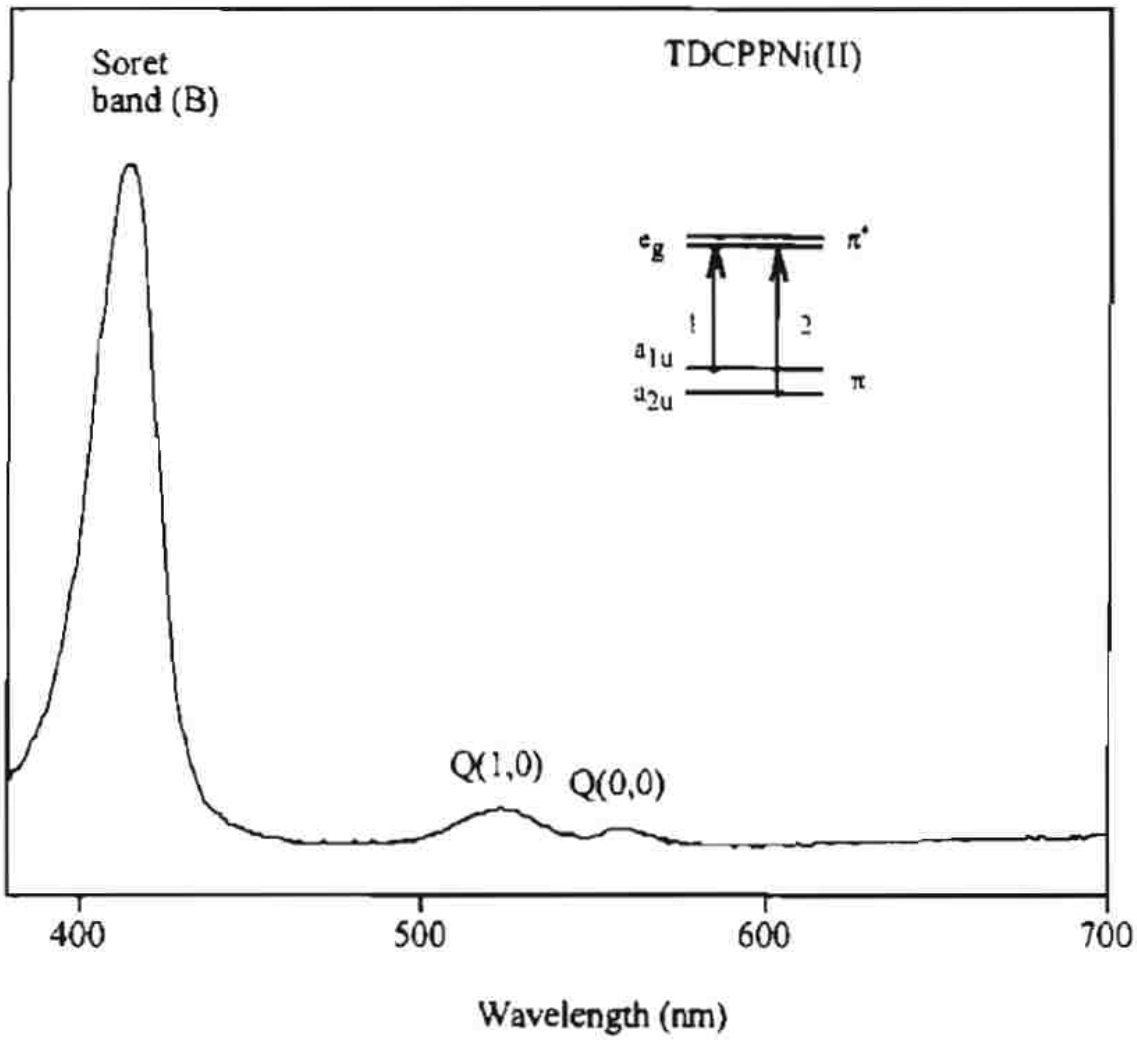

Figure 1-2. UV-Visible absorption spectrum of TDCPPNi(II) in CH_2Cl_2[85]

Spectroscopic methods of identification by UV-visible spectra can be used to distinguish a metal reaction from a ligand reaction. UV-visible absorption spectrum is explained with the aid of the Gouterman molecular orbital model of metalloporphyrins. For most of the studies, semiempirical correlations have been proposed[86] to rationalize the redox potentials:

1. Electronic spectra with two sharp bands between 500 and 600 nm indicate a metalloporphyrin with an uncharged porphyrin ring[87]. If a reduction step is

observed but the product still retained the characteristic metalloporphyrin spectrum, it means that only reduction of the central metal occurred.

2. If the visible spectrum is transformed from the characteristic two-banded spectrum to a broad band covering the whole visible range during oxidation, then a one-electron porphyrin-based oxidation could be observed[88].

3.1. Zinc porphyrin complexes

Spectroelectrochemistry of ZnTPP complex was first reported in 1963 by L. E. Closs[58], followed in 1972 by G. S. Wilson[89] and later on by Jean-Michel Saveant in 1994. The spectral data reported by all these three groups are comparable. Chemical reduction of ZnTPP by sodium or sodium benzophenone ketyl in THF or photochemical reduction with hydrazine affords stable mono- or dianions[90,91,92,93]. Pulse radiolysis of Zn(II)hematoporphyrin, with $(CH_3)_2CO^{-\cdot}$ as reductant, forms the anion radical with a rate constant of 10^9 M^{-1} s^{-1}. Thin-layer spectroelectrochemistry data of ZnTPP published by Wilson et al. is shown in Figure 1-3. It shows that ZnTPP reduction produces $ZnTPP^-$ radical anion and the anionic species can be reversibly reoxidized to the initial compound, ZnTPP.

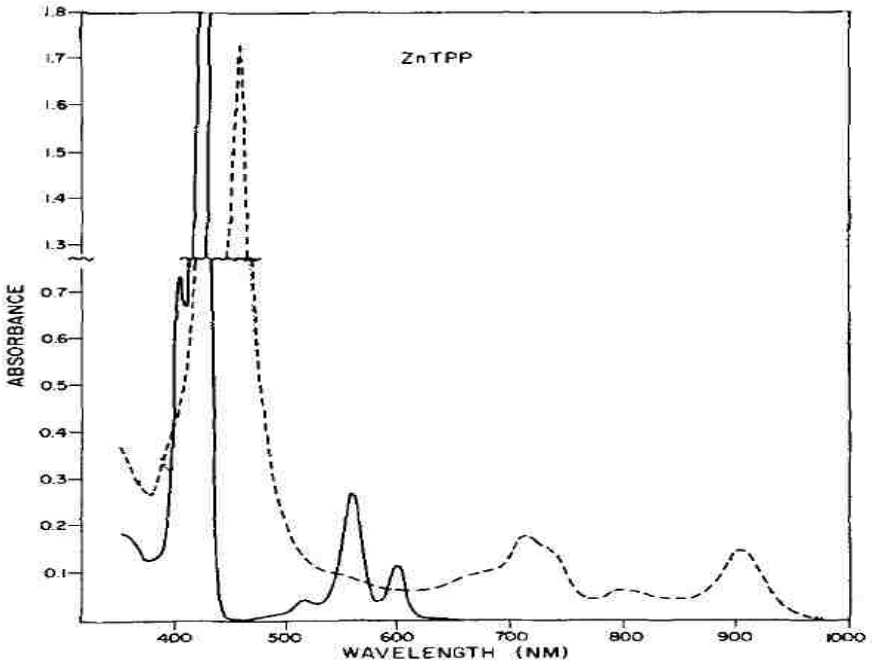

Figure 1-3. Thin-layer visible spectroelectrochemical reduction of ZnTPP:____ZnTPP, ----ZnTPP anion[58]

3.2. Manganese porphyrin complexes

The preparation and properties of some manganese porphyrins have been previously reported but manganese(III) porphyrin was first prepared by Zaleski [94,95] which was not fully investigated until Taylor examined its redox properties[96]. In the same study the electronic absorption spectra were given for the first time.

After Calvin and Loach[97], few years later Boucher[98] investigated physical and spectral properties and elemental analyses of manganese protoporphyrin IX dimethyl ester complexes of the halide ions (F^-, CI^-, Br^-, and I^-). Boucher also explained the UV-Visible absorption spectra rationalized with the Gouterman molecular orbital model of metalloporphyrins.

However, there are few studies on manganese metalloporphyrin reductions and most of them refer to the process that takes place at the metal. Little evidence is provided by Kadish[99] in 1973 who analyzed the redox potentials of 25 metalloporphyrins with different central metal ions and Neta[100] in 1984 that performed a study on redox reactions of manganese porphyrins in aqueous solutions by pulse radiolysis. Kadish's work revealed that when metal ions with an oxidation number of 3^+ or 4^+ are introduced into the porphyrin cavity the extra positive charge has a great influence on the porphyrin π system and its redox properties. The reduction potential values for Mn(III)/Mn(II) reduction is -0.42 V ($E_{1/2}$) and -1.61 V for Mn(II)/Mn(II)P^- reduction[99].

Guldi and Neta[100] provided additional information about Mn(II)P^- anion formation as shown by the study performed on redox reactions of manganese porphyrins in aqueous solutions by pulse radiolysis. The absorption spectra recorded upon radiolytic reduction of Mn(II)TPPS (tetrakis(4-sulfonato- phenyl)porphyrin) and Mn(II)TMPyP (tetrakis(N-methyl- 4-pyridyl)porphyrin) exhibit broad absorptions around 770 nm which are characteristic of the ligand π-radical anions.

Their studies also described a comparison between iron and manganese complexes in reactions with alkyl halides. The reaction of iron porphyrin with alkyl and fluoro-alkyl radicals form stable R-Fe(III)P complexes, which are consistent with previous interpretations. Another section of this study provided the experimental results of the reactions of Mn(III)P and Mn(II)P with various alkyl radicals by steady-state and pulse radiolysis (Figure 1-4). The starting point of these experimental determinations is that substituted alkyl radicals with reducing properties (such as $(CH_3)_2COH$) are able to reduce Mn(III)P to Mn(II)P. The author explained that although Mn(II) has a small size

so it could be accommodated very well within porphyrin ligand. Due to its high-spin d^5, Mn was found to be located outside the porphyrin plane (to lower the energy of the $d_{x^2-y^2}$ orbital). Consequently, when the Mn(II)P reacts with an alkyl radical along the z axis is expected to lead to a double occupancy of the d_{z^2} orbital. These radicals were also found to reduce M(II)P to the π-radical anion[101].

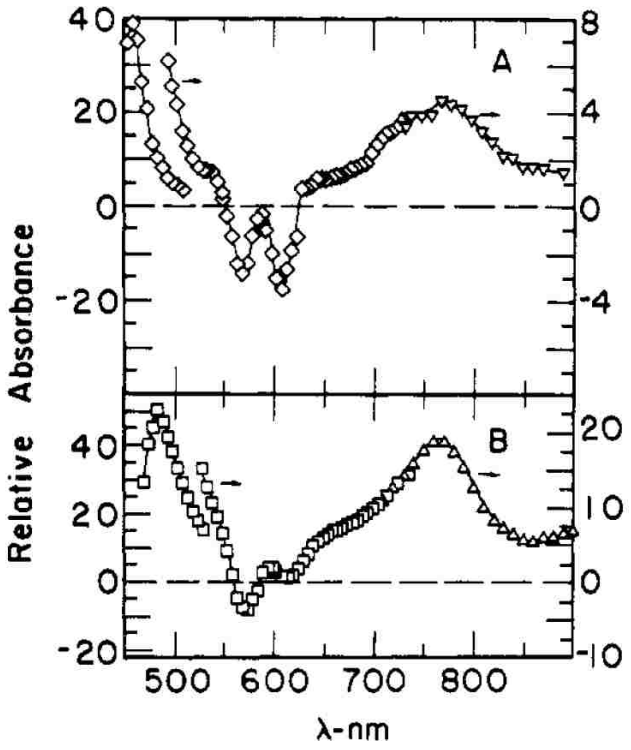

Figure 1-4. Differential absorption spectra observed upon one-electron reduction of Mn(II)P

Reduction of (TPP)MnCl in CH_2Cl_2, reported in literature by Kadish et al.[102], yielded a quasireversible one electron wave at $E_{1/2}$ = -0.33 V. The ratio of i_{pa}/i_{pc} was near unity, indicating the absence of coupled chemical reactions. The separation of the reduction peaks was around 0.10-0.20 V depending on scan rate. Figures 1-5 and 1-6

illustrates the spectroelectrochemical reduction of Mn(TPP)Cl in THF containing 0.1 M Bu_4NBF_4. The spectrum of the Mn(III) complex, shows the characteristic split Soret band and Q bands in visible region while the Mn(II) complex (Figure 1-6) displays a "normal" absorption spectrum.

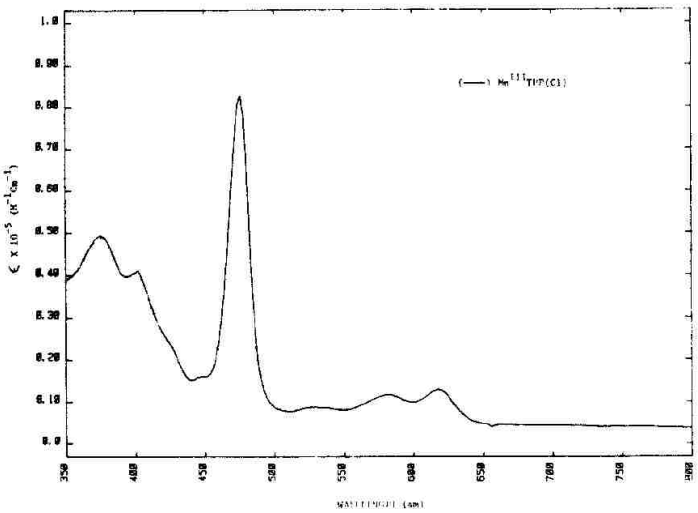

Figure 1-5. Thin-layer visible spectroelectrochemistry of Mn(III)TPPCl[103]

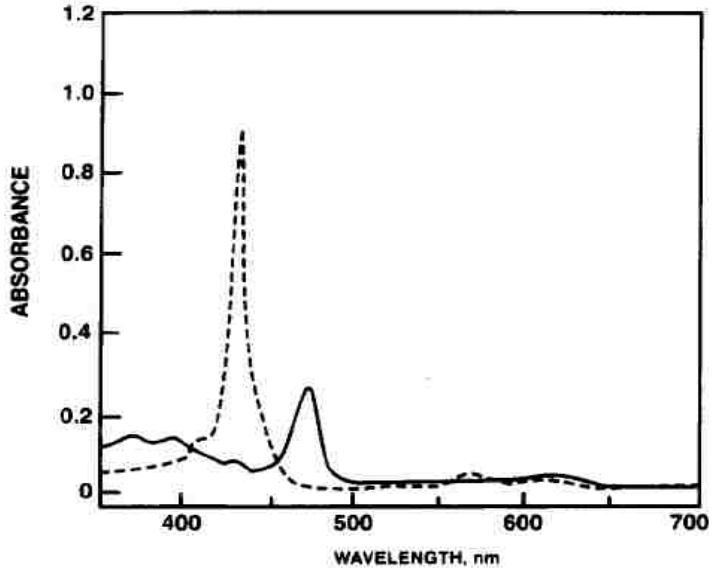

Figure 1-6. Thin-layer visible spectroelectrochemical reduction of Mn(III)/(II)TPP: Mn(II)---, Mn(III)___[103]

3.3. Cobalt porphyrin complexes

In 1971 Kobayashi and coworkers characterized for the first time Co(I)TPP. Based on spectral changes, magnetic susceptibility and NMR spectra, the authors concluded that CoTPP reduction leads to Co(I) species. The spectral changes during the reduction with Na in THF were monitored in time (Figure 1-7).

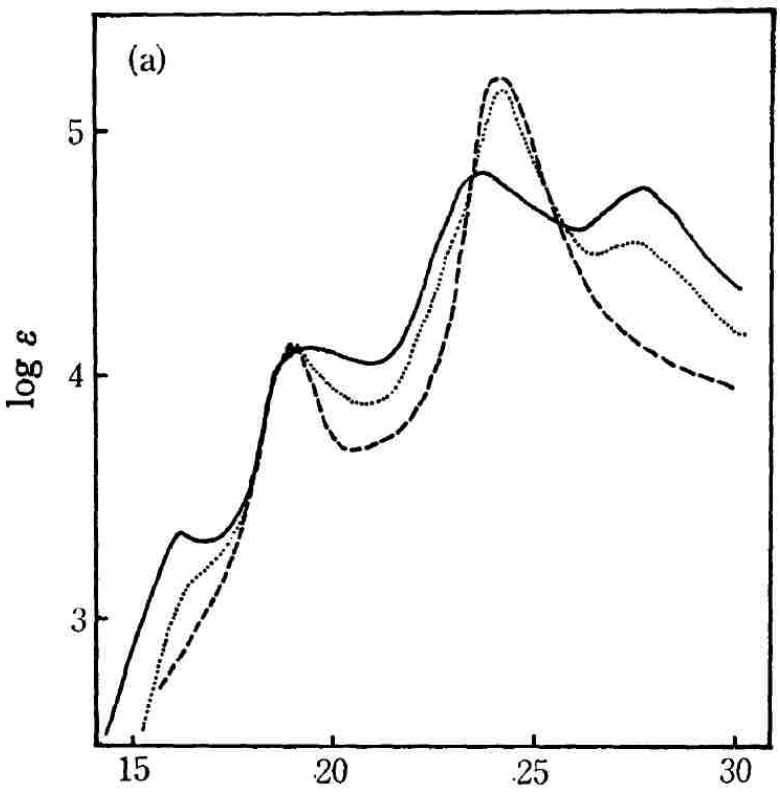

Figure 1-7. Spectral change for reduction process of CoTPP with sodium metal in THF. ---CoTPP, ····after ½ hour, —after one hour.[69]

The spectroelectrochemistry of CoTPP in toluene and benzene was examined by Kadish et al[63] and provided the first example of spectroelectrochemistry in low-dielectric constant solvents. Two-one electron reductions were observed at $E_{1/2}$= - 0.86 V and

-2.03 V vs SCE in toluene and benzene. D'Souza et al[61] examined the electrochemical and spectroelectrochemical behavior of Co(II) and Co(I) complexes of CoTPPBr in benzonitrile. The metal and ring centered reductions had $E_{1/2}$ values which were shifted positively with respect to the same electrode reactions of unsubstituted Co(TPP). The singly reduced products were stable on the cyclic voltammetry and thin layer electrochemistry however further reductions yield ultimately $[(TPP)Co^{I}]^{-}$ as a final product.

3.4. Iron porphyrin complexes

Spectroscopic studies of the reduction products of iron tetraphenylporphyrin with halogen or other anions as axial ligand (FeTPPX) were examined. Weak ligands such as ClO_4^- dissociate from the Fe(II) center after electron transfer. Stronger ligands, such as Cl^- and other strongly binding anions[104], may remain bound to Fe(II) and the probability of this reaction increases with addition of electron withdrawing substituents to the porphyrin macrocycle. For example Kadish et al.[105] have shown that $[(Br_xTPP)Fe(II)Cl]^-$ is the dominant Fe(II) species in solution after reduction of derivatives with six and eight Br groups. A dissociation of Cl^- anion occurs after reduction of $(Br_xTPP)FeCl$ for compounds having zero to four Br groups. Similar Fe(II)/Fe(I) half-wave potentials of -1.05 to -1.06 V were measured in $EtCl_2$ (ClO_4^-, Br^- or Cl^-), thus suggesting dissociation of the halide and identical coordination of the three complexes. Thin layer spectroelectrochemical techniques have been used to investigate the Fe(III)/Fe(II) reaction of TPPFe(II) as a function of the counterion[106].

Kadish et al. [107] analyzed spectroelectrochemically iron porphyrins substituted with electron withdrawing and electron donating substituents in non-aqueous media. The authors considered that the electron withdrawing substituents will lead to anion radical characteristics while electron donating substituents will show substantial electron density on the metal center.

Also previous studies from our laboratory on iron porphyrins and porphinones and isobacteriochlorins were performed. The results provided supplementary details regarding the formation of an iron(II) species after addition of one electron into the system and brought spectroelectrochemical arguments for the iron(I) species formation (Figure 1-8). Teraoka et al[108] performed resonance Raman, EPR and UV-visible analysis for highly reduced iron porphyrin complexes in THF. Their UV results showed spectral changes corresponding to $[Fe(OEP)]^-$ species structure (decrease in Soret band and also new bands formation at 373 and 455 nm). Their method (Na mirror reduction) provided pure species and the presence of isosbestic points upon conversion of Fe(II)OEP made them conclude that the species formed was $[Fe(I)OEP]^-$. Using resonance Raman spectroscopy they describe that the $[Fe(OEP)]^-$ spectrum was different from that of Fe(II)OEP an EPR study indicated the Fe(I) species formation. In previous report by Hickman et al[109], d-NMR, EPR and magnetic susceptibility measurements were performed to characterize the electronic structure of reduced iron porphyrins. Their NMR results favor a low spin iron(I) d^7 configuration.

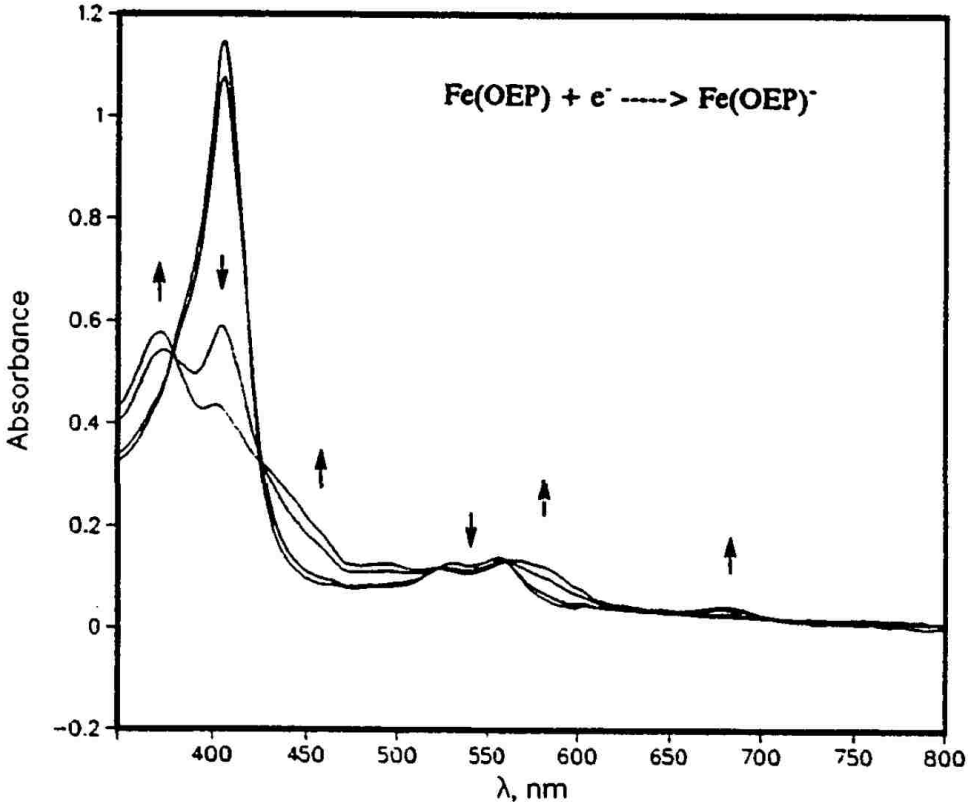

Figure 1-8. Visible spectra obtained during the reduction of FeOEPCl in THF by OTTLE spectroelectrochemistry[80]

As it can be seen besides UV-visible and FTIR analysis other spectroscopic methods have also been used to identify the site of the redox process in metal porphyrins. These methods include NMR[110], magnetic circular dichroism (MCD)[111], vibrational spectroscopy, and EPR spectroscopy[112].

4. Vibrational Spectroscopy of Porphyrins

Vibrational spectroscopy (IR and Raman spectroscopy) can provide ample information about the structure of porphyrins. A large amount of experimental data had been accumulated for metalloporphyrins in the past several decades, and some empirical rules of the IR and Raman spectral features regarding the coordination environment, the spin- and oxidation-states, and the core-size of the metalloporphyrins have been published in the literature[113,114].

FTIR spectroelectrochemistry is a well-known technique used to identify the oxidation site within metal complexes, and a great amount of work has been accomplished on tetraphenylporphyrins in comparison to octaethylporphyrins. FTIR spectroelectrochemical studies have been carried out for electro-oxidation of a series of selected metalloporphyrins. Analysis of the potential-dependant IR difference spectra of certain metalloporphyrins allowed assessment of the electrooxidation site on the molecule.

In 1981, Goff et al.[115] reported the IR spectra of some oxidized metalloporphyrins. They observed that the π-cation radicals of metallo-tetraphenylporphyrins and metallo-octaethylporphyrins displayed new strong IR bands near 1280 cm^{-1} and 1550 cm^{-1}, respectively. Consequently, the appearance of a new band at 1280 cm^{-1} in TPP^{+} complexes and a new band at 1550 cm^{-1} in OEP^{+} complexes have been suggested as a unique criterion for identifying the ring-centered oxidation processes. Hinman et al.[116] confirmed the presence of new bands in the electrochemically generated π-cation radicals of metallo- tetraphenylporphyrins and metallo- octaethylporphyrins by means of *in situ* FTIR

reflectance spectroelectrochemistry. They concluded that diagnostic bands can only be observed in the ring-centered oxidation products. Metal-centered oxidation causes much less perturbation to the porphyrin core vibrations than ring-centered oxidation. They compared the IR spectral changes between one-electron ring-oxidation and two-electron ring-oxidation for some TPP complexes and the difference spectra recorded in the di-cation formation process show characteristic bands similar to those observed for the π-cation radicals but shifted to higher frequencies.

IR spectroscopy has also been used to observe axial coordination changes accompanying the oxidation and to characterize the products of irreversible homogeneous reactions following the electron transfer such as isoporphyrin formation. Hinman et al[117] analyzed and compared the vibrational spectral changes of the complexes arising from metal-centered oxidation with those of the porphyrin centered oxidation and reported the comparison of metal vs ligand oxidations of silver and cobalt porphyrin complexes. It was also shown by Chang et al[14] that the first oxidation takes place at porphyrin ring to form the $OEP^{\cdot}Co(II)^{+}$ π-cation radical, while the second oxidation is metal centered and form $OEP^{\cdot}Co(III)^{2+}$ species[118,119].

An important topic discussed in the published literature is the electronic structure of low-valent metalloporphyrins. Addition of an electron to a four-coordinated iron(II) porphyrin, can be carried out in two ways: the electron will either reduce the iron(II) to iron(I) or the porphyrin to π-anion or a hybrid combination. When a second electron is added, structures such as iron(0), iron(I)-π-anion, and iron(II)-π-dianion can be formed. $[Fe(I)P]^{-}$ and $[Fe(I)P]^{2-}$ complexes have been investigated by spectroscopic techniques including UV-visible[120,121,122,123,124], Mossbauer[120], resonance Raman[124,125,126,127,128],

EPR[123,125,126], proton[123,129] and deuterium[130] NMR spectroscopy. The electronic structures of these highly reduced complexes are still controversial. When the porphyrin macrocycle was substituted by strong electron-withdrawing groups such as NO_2 and CN groups, Donohoe et al[126] observed that even though a small amount of unpaired density is shared with the metal ion through π-orbital interactions the unpaired electron is located on the porphyrin ring.

Two electron reduced iron porphyrins can assume several electronic structures upon the introduction of electron-withdrawing substituents on the porphyrin ring. Electron withdrawing substituents cause two effects: one is to lower the energy level of the porphyrin e_g orbital, the other effect is a weakening of the interaction between the iron and the porphyrin due to a decrease in the electron density at the porphyrin ring. According to these effects, the electronic structures of two electron reduced iron(III) porphyrin complexes can be roughly classified into four types: type I, four coordinated iron(I) low spin porphyrin; type II, five coordinated iron(I) low spin porphyrin; type III, four coordinated iron(II) low spin porphyrin anion radical; type IV, five coordinated iron(II) high spin porphyrin anion radical[123]. In general, choosing between metal or ligand oxidation/reduction has relied on combination of different techniques, particularly UV-visible spectroscopy, EPR spectroscopy, magnetic moment measurements, and electrochemical methods[131,132]. Such criteria are usually consistent for cases where metal oxidation/reduction is well separated in potential (> 0.3 V) from porphyrin ring oxidation/reduction but regularly lead to significant uncertainty in the most interesting cases (iron porphyrins).

Hinman et al[133] performed *in situ* infrared spectroelectrochemical work on some metalloporphyrin complexes among which manganese porphyrins were studied. One-electron oxidation of a Mn(III)OEP complex presented several features common to all metalloporphyrin complexes or at least the majority of compounds studied by this group. One notable feature is the presence of at least one strong new absorption band in the region 1537-1589 cm^{-1}. This result is similar to the value suggested by other research groups (1550 cm^{-1} marker band) for OEP π-cation radical formation. The same authors performed studies on MnTPPCl complex and their results indicated the appearance of absorption at 1280 cm^{-1} which was used as a diagnostic for ring oxidation.

5. Spectroelectrochemical studies of porphinones

Many improvements have been made in optically transparent thin-layer electrode (OTTLE) cell design which include the capability for monitoring in the ultraviolet[134] and infrared[135] spectral regions, the ability to perform precise[136] and cryogenic temperature studies, the flexibility of several working electrode materials[137,138] and special designed to allow deoxygenation[139].

Several thin-layer studies have been restricted to aqueous solutions[140,141,142] and to nonaqueous solvents like DMF or CH_3CN. In past cell designs, dissolution of one of the cell components restricted the use of particular solvents. This dissolution process either contaminated the solution of interest or caused severe leakage problems at one of the sealant junctions[143].

At the beginning of 1980's Kadish et al.[144] showed the improvements achieved in IR cell design which has proved useful in non-aqueous solvents: the body cell is made from Pyrex glass or quartz, and a rectangular thin-layer chamber is open to the bulk solution at all four edges allowing the electrolysis current to flow out of the chamber in all directions to minimize iR drop. The cell contains reference electrode (RE) –silver wire, the working electrode (WE) and the auxiliary electrode (AE) connected to the cell body by a cobalt-glass spot. The window (0.2 mm thickness) is positioned to let the light beam pass through the middle of the working electrode (100 mesh platinum gauze). It is assumed that the concentration of the oxidized and reduced species in the thin layer cavity is uniform. The thickness of the cavity should be as small as possible in order to minimize concentration gradients. There is always a trade off because the smaller the thickness of the cavity, the larger the iR drop, and the greater the potential gradient buildup across the surface of the working electrode. The platinum gauze thin-layer electrode shows a considerable advantage: almost 50% of the thin-layer chamber is occupied by the Pt metal. This reduces both the concentration gradient and the potential gradient developed in the thin-layer cell. The small ratio of solution volume to surface area is a feature of this cell. If the volume of the solution is kept small, the current flow will be decreased. This leads to a smaller iR drop, because the current will decrease faster than the current increases. Finally, the iR drop is significantly reduced in this design not only because of the small volume of the thin-layer solution, but also because the current flows out of the thin-layer chamber from both sides. However, the platinum metal that faces the bulk solution will introduce a certain amount of "background current" which must be taken into account. The size of the gauze electrode was chosen under the

assumption that the current contribution from the edges should be less than 5% of the current contribution from the thin-layer cell itself[145,146].

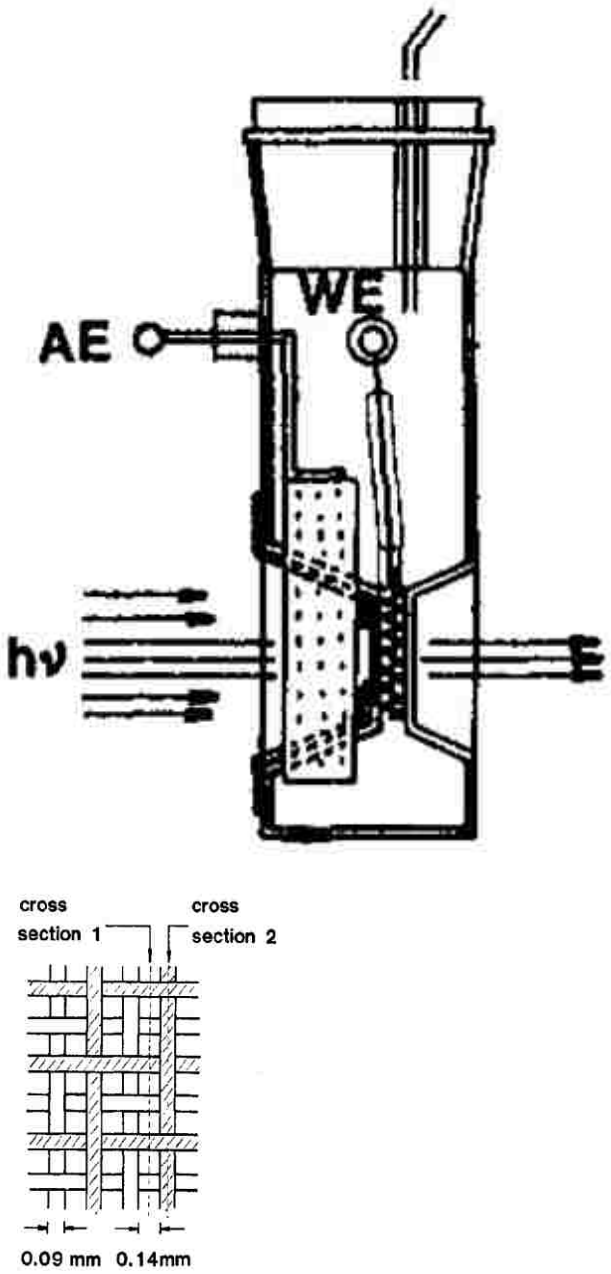

Figure 1-9. Vacuum-tight thin-layer spectroelectrochemical cell with a platinum gauze working electrode. Parts of the cell are: WE-working electrode; (c) thin-layer chamber; (d) thickness of the thin-layer chamber (f) window; (9) AE-auxiliary electrode [145]

Porphyrin complexes have been investigated by spectroscopic techniques like UV-Visible, resonance Raman, EPR, and NMR spectroscopy. Vibrational spectroscopy offers the advantage that it provides more detail regarding molecular structure of products, intermediates and reactants of the electrode process. It is also known that EPR, Mossbauer and NMR can provide structural information but it is complicated to perform these experiments on electrochemical systems.

The past decades have seen much progress in the development of infrared spectroscopy. The challenge was on the characterization of electrode surface by IR techniques[147,148], because surface phenomena are extremely important in electrochemistry.

There are only few applications of IR spectroscopy to electrochemical processes in solution when compared to surface studies. The main reason for that is the interference of the absorption of the solvent with the absorption of the redox species. Nevertheless, during last decade there has been an increase in IR studies of inorganic and organometallic complexes. The use of a thin layer enables bulk electrolysis of reactant species on the experimental time scale. The spectra collected at the stepped potential are the result of the product[149].

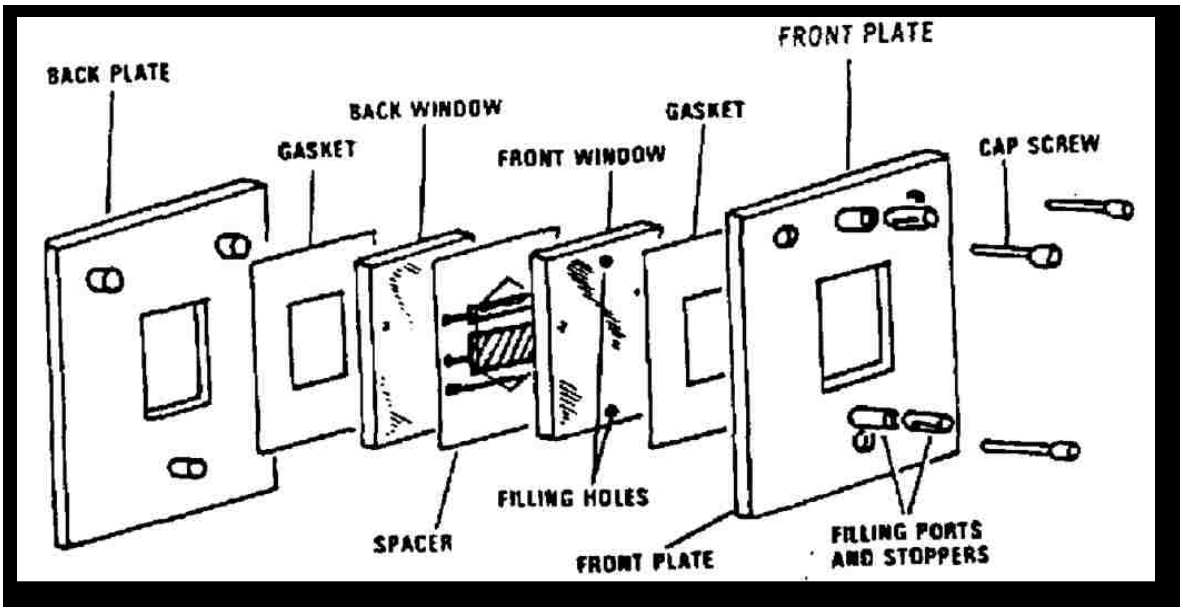

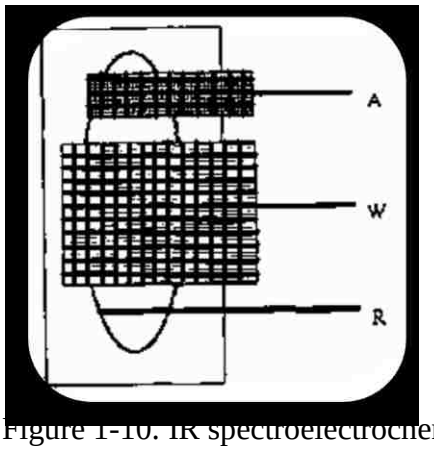

Figure 1-10. IR spectroelectrochemical cell[149]

In contrast to several papers discussing metalloporphyrins, there are few studies characterizing the primary redox products of chlorins, bacteriochlorins or porphinones. Among these the oxidation process was most extensively studied.

Reduction potentials of both cobalt(II) and iron(II) complex of OEiBC appeared at almost same potentials with those metal complexes of OEP and OEC because of the d-electron configurations among these metals. For Co(II) and Fe(II) which have d^7 and d^6 electron configurations either metal or porphyrin macrocycle can be reduced. In contrast

reduction of zinc porphyrins should be centered at porphyrin macrocycle because the d-electron configuration of zinc is completely filled.

The spectroelectrochemical published literature on ZnOEP and ZnOEP anion is provided by Spiro[150] and Blackwood (Figure 1-11)and the results are similar to most of the previous reports for metalloporphyrin[151,152] and metallochlorin[153] but different from what Bocian[154]. The spectral change reported by former authors recorded a red shift in the Soret band up to 452 nm while the Q band was bleached while in the published report by Bocian the Soret band has at 417 nm.

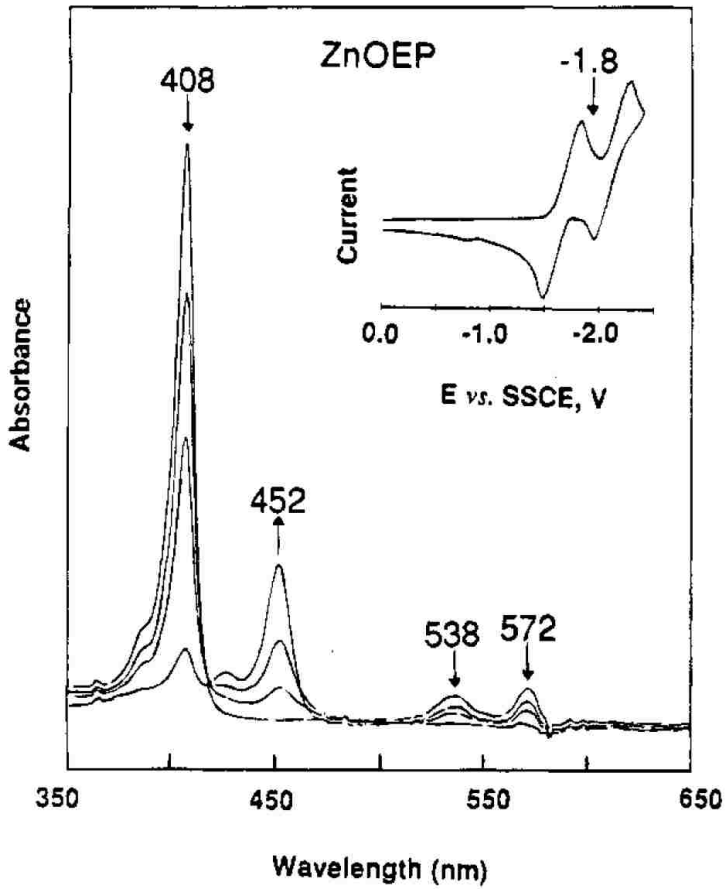

Figure 1-11. Electronic absorption spectra of ZnOEP and its radical anion in THF[150]

Literature studies have shown that metal-centered redox processes have little dependence on the nature of the macrocycle in ferric complexes of octaethylporphyrin (FeOEP), octaethylchlorin (FeOEC), and octaethylisobacteriochlorin (FeOEiBC) being all reduced to the ferrous species at about the same potentia1[155,156,157,158,159,160,161,162,163].

The structural characterization of the metal complexes of isobacteriochlorin, porphinedione and their intermediates in the enzyme systems was carried out by spectroscopic studies. The effects of five- and six-coordination on high-spin ferric isobacteriochlorins were examined by Sullivan et al[160], while the characterization of the molecular structure and NMR spectra of an iron(III) porphinedione was completed by Barkigia et a1[161].

Several papers were published on iron porphyrin complexes with various techniques including resonance Raman, NMR spectroscopy, and X-ray crystallography in comparison to the amount of work that has been done for the iron chlorin and iron isobacteriochlorin complexes. Fe(OEP), Fe(OEC) and Fe(OEiBC) have been synthesized and the physicochemical properties of these complexes have been examined. The cyclic voltammetric results showed that OEiBC macrocycle had not have any advantage for the reduction. Spectroelectrochemistry of porphyrins, hydroporphyrins and porphinones was intensively studied in our laboratory in the past. The spectral changes observed for FeOEP, FeOEPone, FeOEPdione were a red shift and an increase in absorbance of the Soret bands after the addition of the first electron into the system. Also a sharp decrease and broadening of the Soret bands together with a red shift of the bands in the visible region was noted. The results for Fe (2,4- DMOEiBC) and Fe(2,4-OEPdione) were

slightly different in the sense that the reduction cause a smaller decrease in Soret bands and a smaller shift for the bands in the visible region[80].

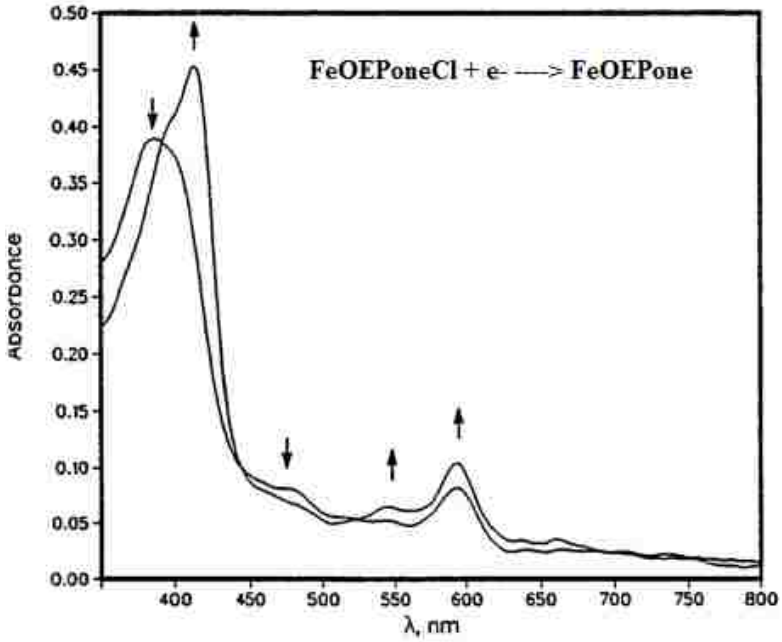

Figure 1-12. Visible spectra obtained during the reduction of FeOEPdione in THF by OTTLE spectroelectrochemistry [80].

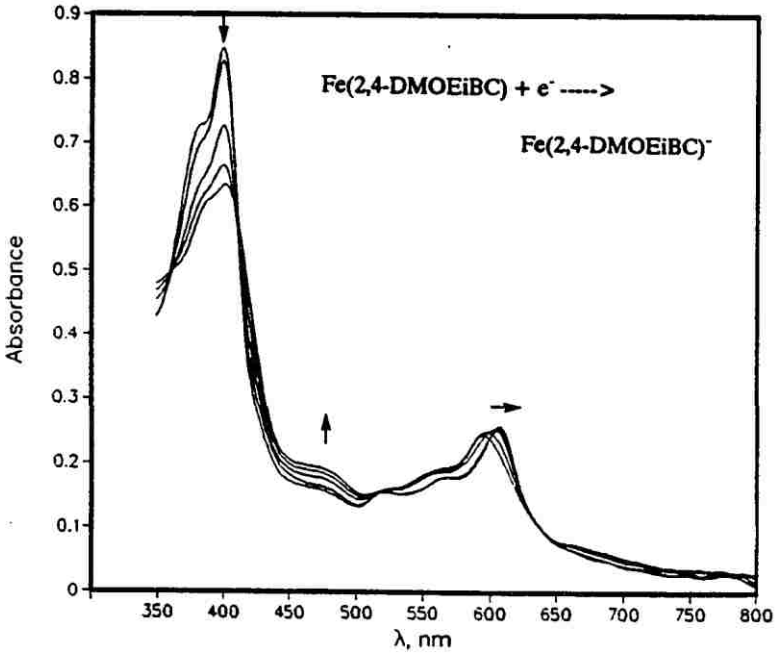

Figure 1-13. Visible spectra obtained during the reduction of Fe(2,4-dioxoOEiBC)Cl in THF by OTTLE spectroelectrochemistry [80].

Data obtained from visible spectroelectrochemistry of iron complexes still confer an ambiguous situation. In order to clarify the oxidation state of $Fe(P)^{-}$, more work on porphyrin systems was performed in this work. For this purpose porphyrins, porphinones and porphinedione of different metals were analyzed by electrochemistry, spectroelectrochemistry and infrared techniques. Metals were chosen as a function of their known oxidation state: zinc does not reduce in our potential range, cobalt reduction is well known[122] to be metal centered, manganese which upon one electron addition changes its oxidation state from 3^{+} to 2^{+} while after a second addition of an electron a porphyrin ring process takes place[100].

The IR spectroelectrochemical study of iron porphinones and porphinediones and their free base complexes published recently from this lab completes the characterization of these compounds. In this report the porphinones structure was easily investigated due to the presence of the C=O group in the molecule which display a strong absorption in 1700 cm^{-1} region. It was shown that the first reduction decreased the νC=O by 16 cm^{-1} and it was ascribed to an increase of back bonding from the metal to the porphyrin. The addition of a second electron to the system showed a shift in the νC=O band of 32 cm^{-1} indicating further weakening of the carbonyl. In case of the porphinediones similar spectral changes as with porphinones were reported: a first small shift in carbonyl band 14 cm^{-1} which was attributed to a metal centered process followed by a second process which shifted the carbonyl band with 32 cm^{-1}. In addition it was found that the carbonyl vibration was split into two bands for this complex.

A comparison with free base porphinones and porphindiones (from the thesis of Z.-C. Wei[164]) was also made which showed the IR shifts when the free bases were

reduced. The shift in the carbonyl band for the reduction of Fe(II)OEPone (31 cm^{-1}) was smaller that the shift for the reduction of H_2OEPone (38 cm^{-1}) indicating that the reduction of $FeOEPone^-$ product had considerable delocalization to the ring. On the other hand, new bands are observed at 1551 and 1529 cm^{-1} for H_2OEPone and only one band at 1576 cm^{-1} for Fe(II)OEPone. For Fe(II)OEPdione the shift is 42 cm^{-1} which is similar to the one of H_2OEPdione (44 cm^{-1}). New bands in the porphyrin region 1569 cm^{-1} and 1523 cm^{-1} were seen for H_2OEPdione, and at 1595 cm^{-1} and 1564 cm^{-1} for $FeOEPdione^-$. The shifts observed for $FeOEPone^-$ and $FeOEPdione^-$ were consistent with DFT calculations which indicated a delocalized Fe(I) species.

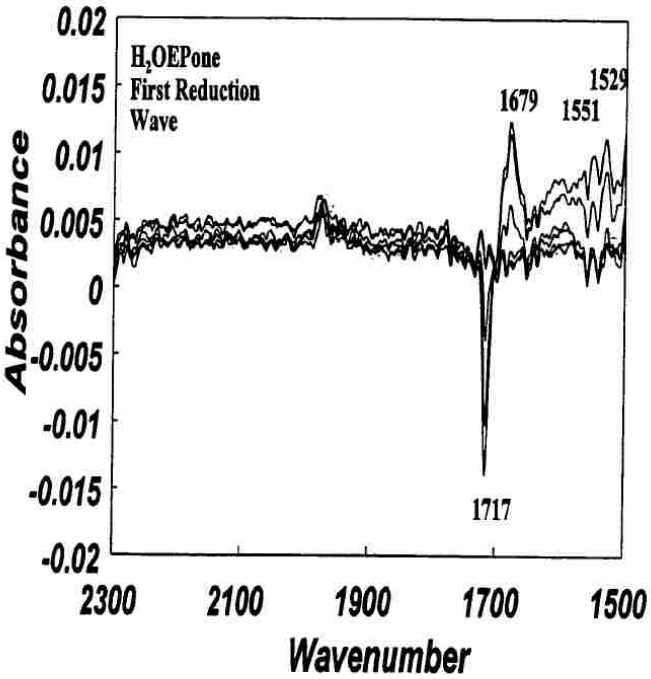

Figure 1-14.FTIR difference spectra for controlled potential reduction of H_2OEPone in THF, first reduction[165]

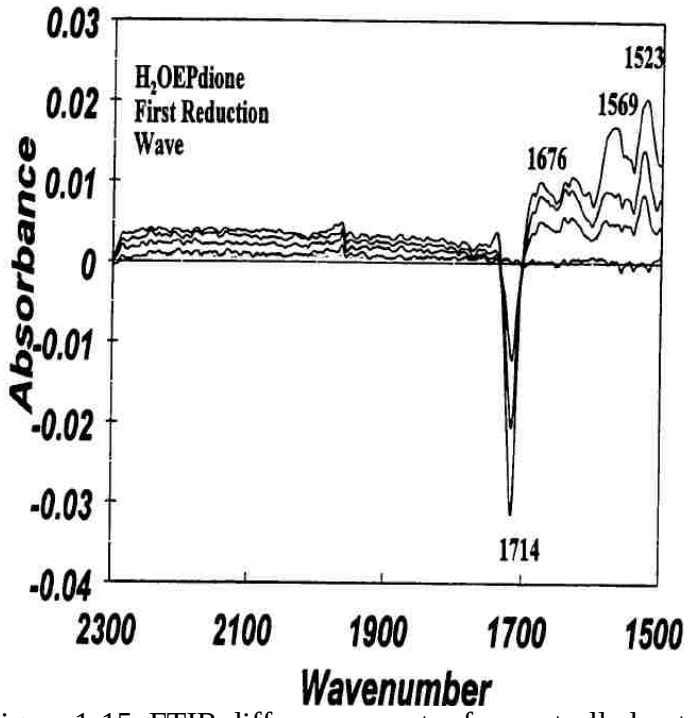

Figure 1-15. FTIR difference spectra for controlled potential reduction of H_2OEPdione in THF, first reduction[165]

To complete the study, DFT calculations were performed on these compounds which revealed that few IR bands in the porphyrin region at 1562 cm^{-1} and 1550 cm^{-1} are due to Cm-Cα and Cβ-Cβ vibrations. The results of the DFT calculations performed on methylated porphinones showed comparable results with the experimental spectrum of FeOEPdione. Upon second reduction the carbonyl band gave rise to more peaks as the electron density becomes predominant on the porphyrin ring. The study has shown how the carbonyl vibration was sensitive to the interaction between the metal and the porphinone and a further objective was to observe these effects on different transition metals.

6. Objectives

Although there are a large number of studies on metalloporphyrins, the UV-visible spectral changes of some compounds have not been studied. Most spectroelectrochemical work reported in the literature cover the porphyrins and metalloporphyrins complexes studies known to be useful in biological systems. Besides the extensive work completed in this laboratory, only a few studies have been found on porphinones or porphinediones.

The FT-IR spectroelectrochemical analysis of porphinones is straightforward because the carbonyl has a strong absorbance peak in IR spectrum in a region well separated from porphyrin bands, so it can be easily distinguishable and its vibrations can be correlated with the electroreduction process that the complex undergoes. When reduction process occurs, the carbonyl bond is weakened due to an electron density increase in the porphyrin ring consequently carbonyl peak shifts toward a lower frequency. This spectral change makes the FTIR an important tool in the process of structure determination of metalloporphyrins. This way the carbonyl group shift can be correlated with the metal oxidation state. It was observed from previously published studies that a higher metal oxidation state move the carbonyl band at a higher frequency while a lower oxidation state will shift the carbonyl vibration to a lower frequency. Based on this information, our studies will be focused on the mentioned correlation and bring additional evidences for the problem addressed by researchers in the last 25 years concerning the oxidation state of iron(II) upon reduction.

The electrochemical reduction of iron porphyrins is intriguing because the metal and porphyrin are capable of accepting electrons. Both the Fe(I) and Fe(II) porphyrin

radical anion have been proposed as products in the reduction of the ferrous complex. Neither structure represents the actual electronic structure because of electron delocalization. Unfortunately, there are few correlations available to relate the degree a reduction of the porphyrin ring to shifts in the carbonyl band.

Based on the reviewed literature electrochemistry and spectroelectrochemistry of different porphyrin and metallo-porphyrins has been intensively studied. The electronic studies of the reduced Fe(II) porphyrin shows that the complex is not well characterized, a good reason for us to establish as a first goal of this work the identification of spectroscopic features for metal vs ring reduction. The aim is to characterize complexes in which the structure of the reduced complex is well known from previous literature studies. In order to have a complete comparison, different metal porphinone complexes will be prepared and analyzed using same methods and the results will be presented in next chapter. Another goal will be to perform a similar comparison for compounds that resemble heme d_1, previously established by Chang et al to be a porphinedione. For this reason we will synthesize free base porphinones, porphinediones and incorporate into the porphyrin cavity certain transition metals (Zn, Mn, Co) in order to analyze by spectroelectrochemistry and observe the IR shift during electroreduction process.

Chapter 2 EXPERIMENTAL STUDY OF PORPHINONES

2.1. Chemicals: Reagents, supporting electrolyte and solvents

H_2OEP was purchased from Aldrich and used as received. Tetrabutylammonium perchlorate (TBAP) was purchased from Alfa Aesar and dried at 90° C in a vacuum oven overnight before use. Anhydrous tetrahydrofuran THF was refluxed in the presence of sodium and benzophenone under nitrogen until the solution was blue and deoxygenated by at least three freeze-pump-thaw cycles before being used in the glove-box. Ocasionally, THF was purified and dried using a Vacuum Atmospheres solvent purification system. All other solvents were spectrophotometric grade and were used without further purification.

Metallo porphinones

ZnOEPone synthesis

The ZnOEPone was prepared by a two step reaction via OsO_4 oxidation and acid catalyzed pinacolic rearrangement using the literature method published by Chang et al[165,166,167]. This reaction gives a mixture of unreacted H_2OEP, ZnOEPone and 2,6-OEPdione.

In order to synthesize zinc complexes, the above mixture was reacted with zinc acetate dihydrate in $CHCl_3$/MeOH (20/10 mL) at reflux for one hour. The reaction completion was verified by TLC (the solution color turns from purple to blue). TLC

plates (H x W 20 x 20 cm) with alumina back plate were used. Plates were immersed in hexane:CH_2Cl_2 (1:1) solvent mixture. The resulting solution was cooled at room temperature and washed 3 times with 300 mL of water. After removing the solvent, the mixture of zinc complexes were purified using alumina column and elution was initiated with chloroform. A small violet band containing free base 2,6 porphinedione, H_2(2,6-OEPdione), which did not react with zinc acetate, was eluted first. The second band containing ZnOEP (pink) from unoxidized starting material was eluted with $CHCl_3$ containing 0.5% methanol. The third band (blue) was eluted with $CHCl_3$ containing 5% methanol, which contained ZnOEPone. The product was characterized by UV-Visible, IR and ^{l}H NMR and the results correspond to the ones published in literature[168,169,170].

Mn(III)OEPone synthesis

Manganese insertion was performed according to the procedure: 25 mg of H_2OEPone, 50 mg of manganese acetate tetrahydrate, 40 mg sodium acetate and 25 mg sodium chloride were added to 15 mL of glacial acetic acid and refluxed for 24 h. At that point, fresh amounts of manganese acetate tetrahydrate were added to the reaction mixture and the reaction was allowed to proceed for another 24 hours.

The reaction completion was monitored by disappearance of fluorescence under UV lamp and also by UV-visible spectra. The resulting solution was cooled at room temperature, reduced to a volume of less than 5 mL, and washed 3 times with 100 mL of water, 5%$NaHCO_3$ solution (2x100mL), then once more 3 times with 100 mL of water.

The crude manganese complex was purified using an alumina column. Elution started with chloroform to remove the unreacted material and continued with chloroform

containing 1% methanol. The Mn(III)OEPoneCl product was characterized by UV-visible (THF), λ_{max}, nm: 364, 478 and 642.

Co(II)OEPone synthesis

The free base H_2OEPone was allowed to react with cobalt acetate tetrahydrate in $CHCl_3$/MeOH at reflux for 24 hours. The reaction completion was checked using thin layer chromatography TLC plates. The resulting solution was cooled at room temperature and washed 3 times with 300 mL of water. The product was characterized by UV-visible (THF), λ_{max}, nm: 374, 412, 606.

Metal-2,4-octaethylporphinedione M(2,4-OEPdione) (M=Zn, Mn, Co)

The H_2(2,4-OEPdione) compound [167,171] was prepared according to a procedure described in previously published papers and it was characterized by UV-visible and ^{1}H-NMR. The product characterization results were according to literature[169,172].

To obtain zinc, manganese and cobalt porphinediones, the H_2(2,4-OEPdione) compound was allowed to react with the corresponding metal acetates in $CHCl_3$/MeOH (20/10mL) at reflux for one hour, in case of zinc, and 24 hours for cobalt and manganese. The reaction completion was checked using thin layer chromatography techniques. Silica gel TLC plates were immersed in a solvent mixture of hexane:dichloromethane (1:1 ratio). The resulting solution was cooled at room temperature and washed 3 times with 300 mL of water. After removing the solvent, the crude metal complex was purified on silica gel column. Elution was initiated with chloroform. The products were

characterized by UV-visible (THF), λ_{max}, nm: Co(2,4-OEPdione) 384, 432, 620; Zn(2,4-OEPdione) 390, 414, 440, 482, 624, 688; Mn(2,4-OEPdione) 402(sh), 436(sh), 464, 628.

^{18}O-OEPone labelling procedure

Trifluoroacetic acid (TFA, 15 µL) and $H_2{}^{18}O$ (97% ^{18}O atom, 0.18 mL) was added to toluene (6 mL) solution of H_2OEPone (20 mg). The solution color turned from purple to blue. The solution mixture was stirred at 70 ºC under an inert atmosphere for 4 days using a condenser. After opening the flask, the reaction mixture was neutralized with an aqueous 4% $NaHCO_3$, stirring for five minutes (red color solution). The mixture was transferred in a separatory funnel and the organic phase was washed with distilled water (three times), filtered and evaporated to give the ^{18}O-labelled porphyrin. Before choosing toluene as solvent, the reaction was performed in $CHCl_3$, CH_2Cl_2 and THF, varying the reaction conditions (acid amounts, time and temperature). Toluene heated at 70 ºC gave the highest yield of labeled product without decomposition. During the work-up a problem was encountered with the incomplete removal of $NaHCO_3$, which could be detected in IR spectrum (1732 cm^{-1}). For this reason the work-up was done in toluene, checking the pH after each wash in order to ensure a slightly acidic media. The labeled product was characterized by FTIR and NMR. The ^{1}H-NMR showed same spectrum as unlabeled H_2OEPone. The yield of labeled porphinone was 87% as calculated from IR spectrum. The ratio of the intensities of carbonyl peaks was used to estimate the conversion.

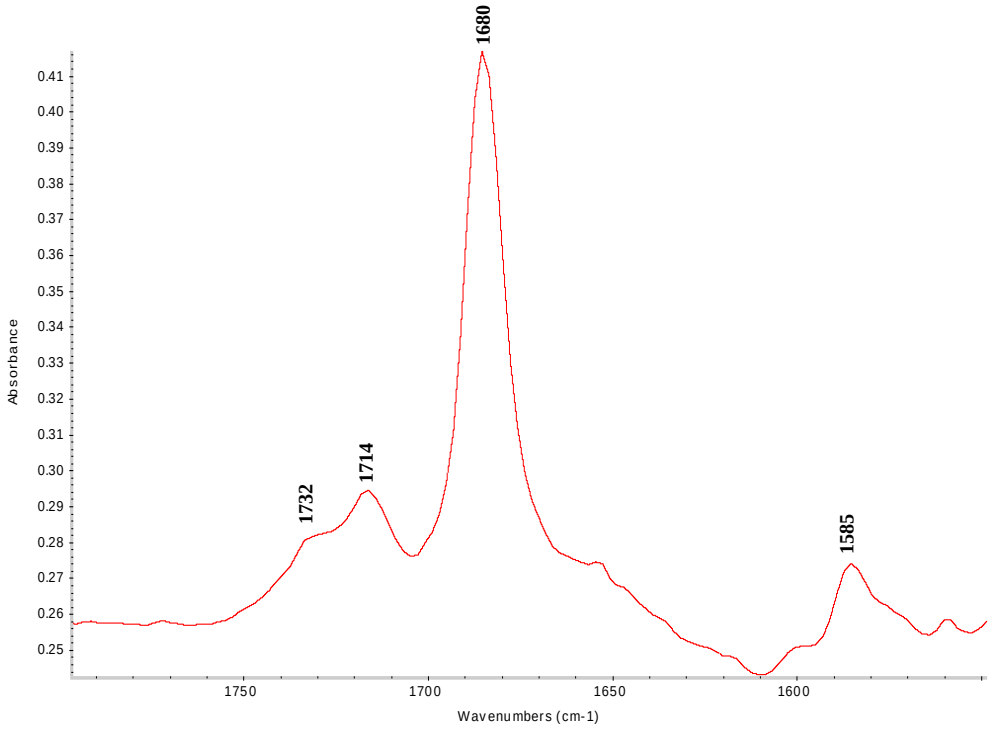

Figure 2-1.FTIR of ^{18}O-CoOEPone with bound $NaHCO_3$

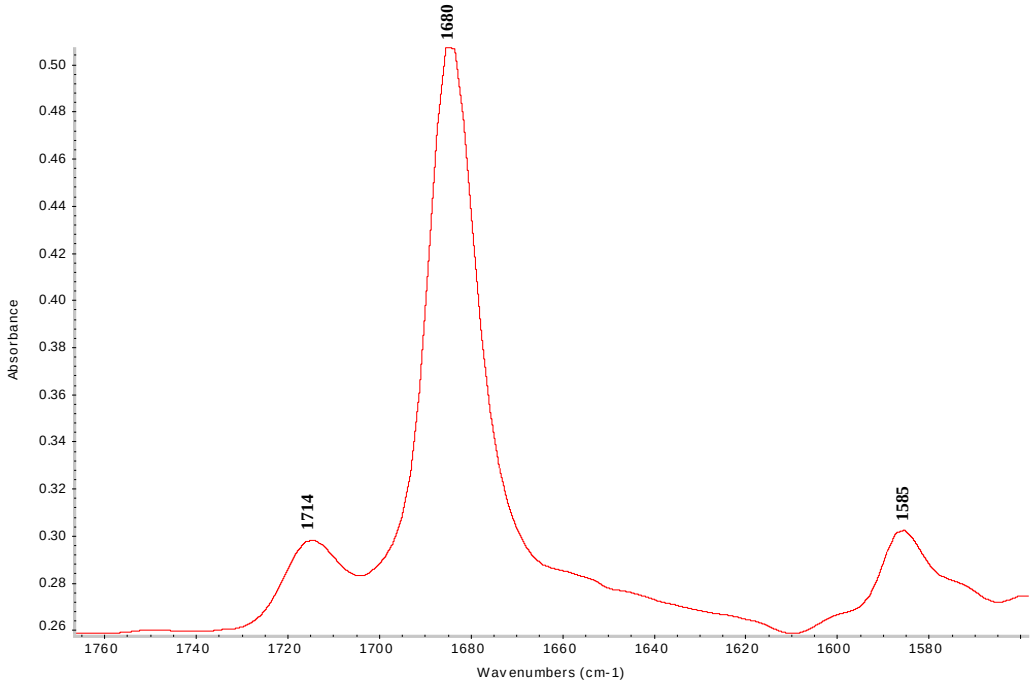

Figure 2-2. FTIR of ^{18}O-CoOEPone without $NaHCO_3$

2.2. Equipment

The voltammetric analyses were performed using an Omnic-101 microprocessor-controlled potentiostat system (software Aquire-101 for Windows, Cypress Systems Inc., Lawrence KS). The step-potential experiment was processed with a model 410 potentiostat controller system (Electrosynthesis Corp, New York). The voltammetric cell was bought from Pine Instruments as well as the patterned electrodes used for analysis. The working electrode was platinum or gold and the reference electrode Ag/AgCl. Cyclic voltammetry was performed in a glove box. A known volume of solvent (6 mL anhydrous THF) containing electrolyte (tetrabutyl ammonium perchlorate - TBAP) was added to the voltammetric cell. A known amount of metalloporphyrin was added to the solution and a patterned platinum electrode was immersed in the solution.

The UV-visible spectra were recorded on a Hewlett-Packard 8452A Diode Array spectrophotometer with an OLIS data acquisition program. An optically transparent thin layer electrochemical (OTTLE) cell was used for visible spectroelectrochemical experiments. The cell assembly was based on the design of Li and Kadish[173] (Figure 1-9). A silver wire was used as reference electrode and 0.1 M TBAP was used as supporting electrolyte. For spectroelectrochemical measurements all samples were prepared and filled into OTTLE cell in the glove box. A solution of 0.8 mM of corresponding metallocomplex was prepared in the glove box by dissolving the compound in anhydrous THF to which the electrolyte was added. Spectra were obtained by scanning the potential.

The infrared spectra were produced with a Thermo Nicolet –IR Spectrometer Model 670 Nexus with a MCT detector. Infrared spectra were collected in KBr pellets or

in solution using OTTLE cell (Figure 1-10). The range of the IR measurements was between 400 and 4000 cm^{-1}. IR measurements were recorded using 32 scans with resolution 1 cm^{-1} and 2 cm^{-1}, in absorbance mode, unless specified on the spectra.

Spectrochemical cell design

A modified infrared (OTTLE - Optically Transparent Thin-Layer Electrochemical) cell was used to acquire in situ IR spectra during electrochemical reduction procedure. It is based on a "sandwich cell" design holding three optically transparent electrodes: working electrode (WE), auxiliary electrode (AE), and reference electrode (RE) positioned between two IR-transparent windows [130](Figure 1-10).

The KBr salt plates were purchased from Wilmad Co. NJ. The working electrode and auxiliary electrode are manufactured from different size platinum gauze (100 mesh, Aldrich Co.). A silver wire (0.05 mm diameter) was used as a pseudo reference electrode. The electrodes were cleaned by flushing the cell with THF. The cell was filled using a 1.0 mL gas-tight Hamilton syringe in the glove box.

Single crystals of Mn(III)OEPoneCl and Mn(III)OEPdioneCl were crystallized from chloroform/pentane (1:3 ratio), mounted in inert oil and transferred to the cold gas stream of the diffractometer. The experiment was done with Oxford SuperNova diffractometer using Cu(Kα) radiation.

Chapter 3 SPECTROELECTROCHEMICAL STUDIES OF COBALT PORPHINONE COMPLEXES

Iron porphinedione complexes are present in certain classes of dissimilatory nitrite reductases (heme d_1). These complexes have been much less intensively studied than their heme counterparts. The structure of octaethylporphinone (OEPone) and octaethylporphinedione (OEPdione) are shown in Scheme 3-1. One interesting aspect of these complexes is the presence of the carbonyl group on the porphyrin ring. The carbonyl band absorbs strongly in the infrared region. As a result, the interaction between the central metal and the porphyrin ring, as well as reduction in the ring can be monitored by the shift in the carbonyl band.

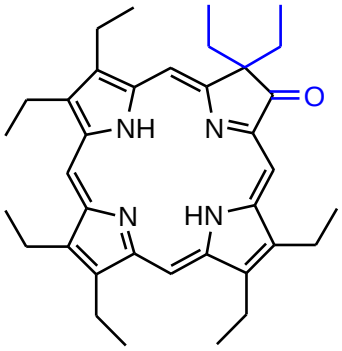

Octaethylporphinone (OEPone)

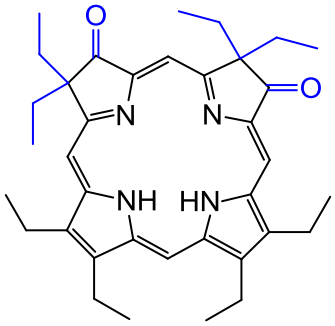

octaethylporphinedione (OEPdione)

Scheme 3-1.

Recent work in our laboratory has examined shifts in the carbonyl band as the iron atom is reduced to iron(II) and the formal iron(I) oxidation state[174]. Unfortunately,

there are few correlations available to relate the degree a reduction of the porphyrin ring to shifts in the carbonyl band. Cobalt porphinone complexes should provide considerable additional information on the carbonyl shifts. This is because the reduction of cobalt tetraphenylporphyrin complexes has indicated that cobalt(III) complexes are reduced to cobalt(II), and then to cobalt(I)[175,176]. In addition, cobalt(III) complexes can be oxidized to cobalt(IV) and/or cobalt(III) radical cations[116,177]. D'Souza et al have reported on the electrochemistry of cobalt-TPP complexes with electron withdrawing groups[65].

3.1. Voltammetry of Cobalt porphinone complexes

The electrochemistry of Co^{II}-OEPone and Co^{II}-OEPdione was investigated by both cyclic voltammetry and UV-visible spectroelectrochemistry. The redox process of each complex was carried out on a gold electrode in tetrahydrofuran containing 0.10 M TBAP. A typical voltammetric wave is shown in Figure 3-1. The cobalt complexes undergo one electron transfer process with an $E_{1/2}$ of -1.36 V in the case of Co(II)-OEPone (Figure 3-1) and -1.15 V for Co(II)-OEPdione (Figure 3-3). The reduction wave is reversible as indicated by the anodic/cathodic waves at the scan rates investigated (0.05 – 0.2 V/s). The peak current ratio, i_a/i_c is close to unity indicating diffusion controlled one-electron transfer. The voltammetric data are summarized in Tables 3-1 and 3-2.

A comparison of the reduction potential of Co(II)OEP with Co(II)OEPone shows that the carbonyl group significantly decreases the reduction potential (240 mV). This shift was much larger than that observed for Fe(II)OEP versus Fe(II)OEPone, where a much smaller 30 mV shift was observed[164]. The addition of a second carbonyl group on

the ring (Co(II)OEPdione) had a much smaller effect (a decrease of 80 mV compared to Co(II)OEPone). This was similar to the shift observed between Fe(II)OEPone and Fe(II)OEPdione (80 mV decrease)[165].

The oxidation of Co(II)OEPone and Co(II)OEPdione showed two successive one-electron transfer processes that occur in the potential range of 0 to 1.8 V and the results for Co(II)-OEPone are illustrated in Figure 3-2. The first electron oxidation of the cobalt complex occurred within a peak potential of +0.90 V. The wave was quite irreversible, probably due to the fact that the oxidized product was probably coordinated to an anion such as perchlorate[179], while the Co(II) complex was uncoordinated. Similar with the case of CoTPP [66], the first oxidation is irreversible and displays non coupled anodic and cathodic peaks, while the second process appears to be reversible. In the absence of ligand exchange, the Co(III)/Co(II) wave is generally reversible[64].

Some differences in the redox potentials were observed in the oxidation process of Co(II)OEPone (Figure 3-2) and Co(II)OEPdione (Figure 3-4) complexes. The oxidation peak potentials were shifted to a more positive value for porphinedione (+1.09 V) complex as compared to the porphinone macrocycle (+0.90 V). This is expected due to the presence of the two electron withdrawing groups in the molecule. The electron subtraction becames more difficult as the second carbonyl was present in the system.

The peak currents for the first oxidation processes of Co(II)OEPone and Co(II)OEPdione were higher when compared with the corresponding second oxidation processes. Therefore the question addressed was if the process is one electron or two electron transfer process. To answer the question, the UV-visible spectra were carefully

analyzed as shown in the next section and the presence of the isosbestic points confirmed that the first oxidation process in both cases was one electron transfer.

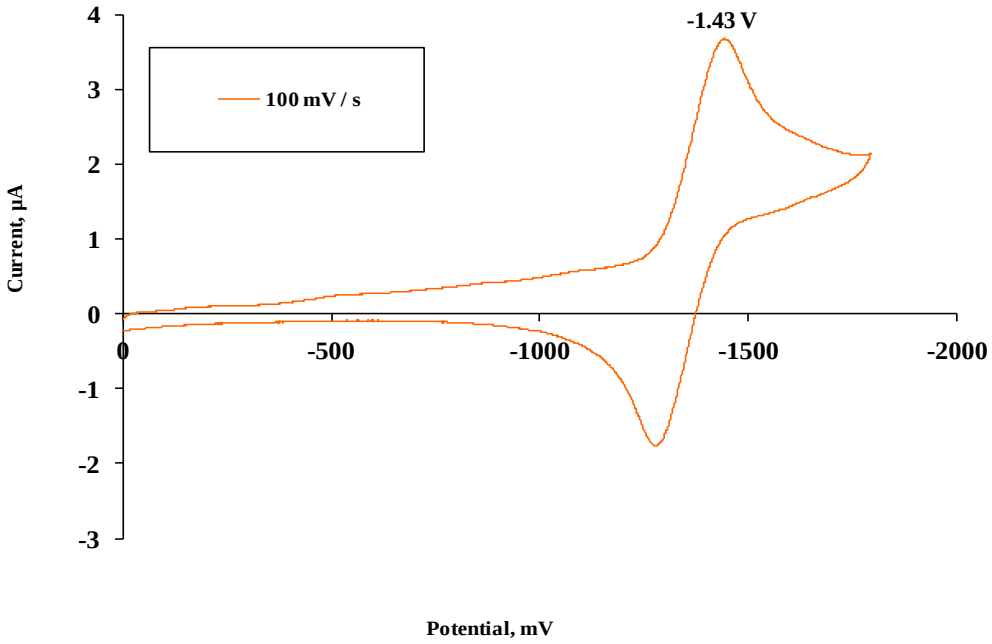

Figure 3-1. Cyclic voltammogram for the reduction of Co(II)-OEPone. Solution conditions: 0.80 mM in THF, with 0.10 M TBAP electrolyte, WE: Au, RE: Ag/AgCl

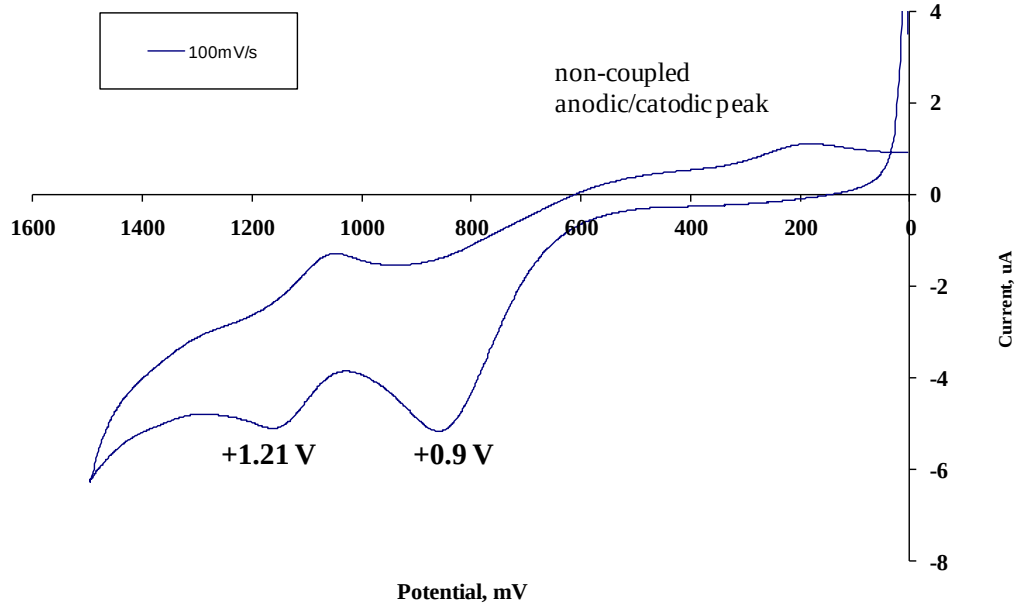

Figure 3-2. Cyclic voltammogram for the oxidation of Co(II)-OEPone. Solution conditions: 0.80 mM in THF, with 0.10 M TBAP electrolyte, WE: Pt, RE: Ag/AgCl

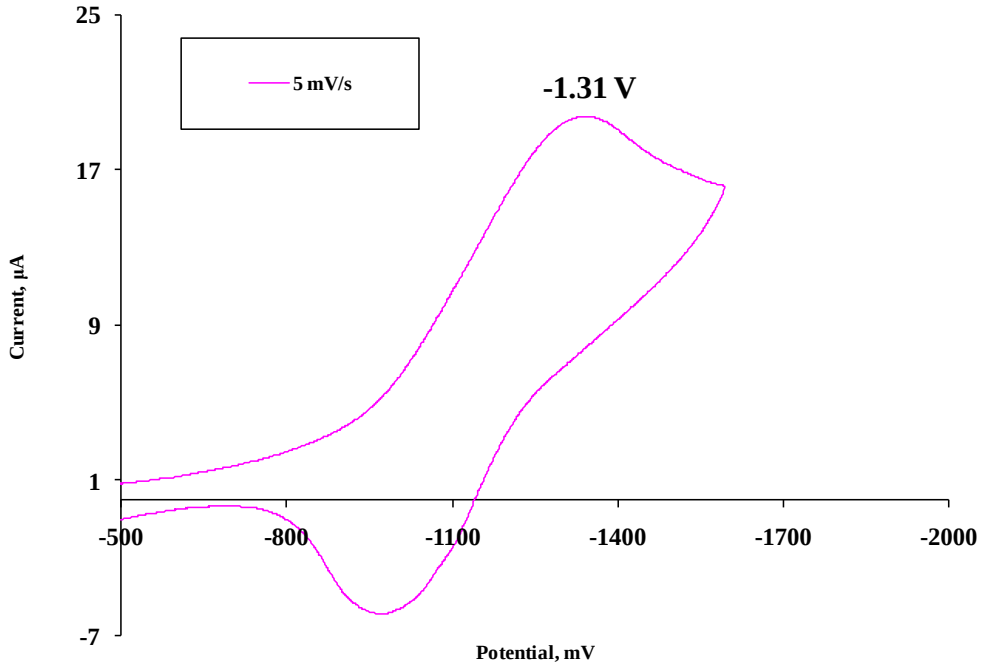

Figure 3-3. Cyclic voltammogram for the reduction of Co(II)-OEPdione. Solution conditions: 0.80 mM in THF, with 0.10 M TBAP electrolyte, WE: Pt, RE: Ag/AgCl

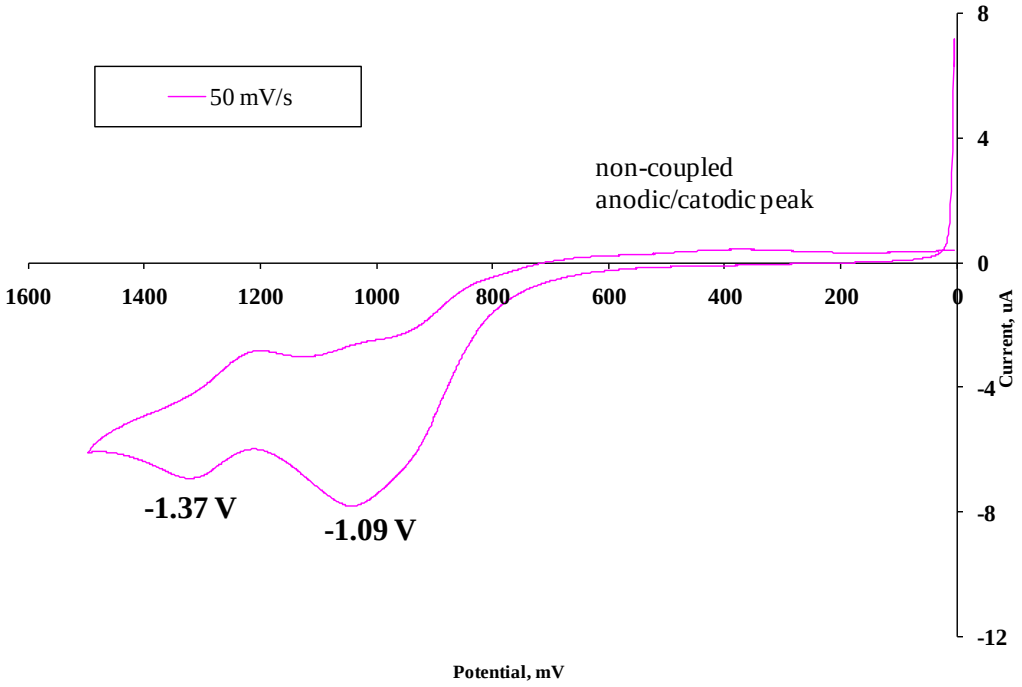

Figure 3-4. Cyclic voltammogram for the oxidation of Co(II)-OEPdione. Solution conditions: 0.8 mM in THF, with 0.10 M TBAP electrolyte, WE: Pt, RE: Ag/AgCl

3.2. UV-Visible of Cobalt porphinone complexes

The electroreduction of Co(II)OEPone and Co(II)OEP was analyzed by spectroelectrochemistry in order to characterize their reduced products (Figure 3-5 and 3-6). The electro-reduction process was performed in an OTTLE cell in THF containing 0.10 M TBAP and the changes in the visible spectra were recorded by controlled potential electrolysis. The reduction of Co(II)OEPone (Figure 3-5) resulted in a decrease in absorbance for Soret band. The Q band and the peak at 374 nm are blue shifted. The isosbestic points at 382, 426, 624 nm indicated that no intermediates were formed during the electrolysis. The UV-visible spectra typical for the Co complexes were obtained following the reoxidation of respective reduced species, confirming the stability of the compounds within the experimental time frame. Similar spectral changes have been reported for CoTPP [66,73]. The lack of band broadening in the 450-550 and 700-900 nm regions suggests that the reduction process occurs at the metal center[178]. Further confirmation using vibrational studies are needed.

Figure 3-7 shows the UV-visible spectral changes for the reduction of Co(II)-OEPdione in THF and the spectroelectrochemical data are summarized in Table 3-3. The Soret and the Q bands decreased in absorbance and were blue shifted. As with the Co(II)OEPone reduction, isosbestic points were observed and the original spectrum was obtained upon re-oxidation. No broad bands were observed between 700-900 nm which might indicate a radical anion species. The band at 575 nm observed in the UV spectrum is due to light scattering, by the grid electrode of the source emission bands.

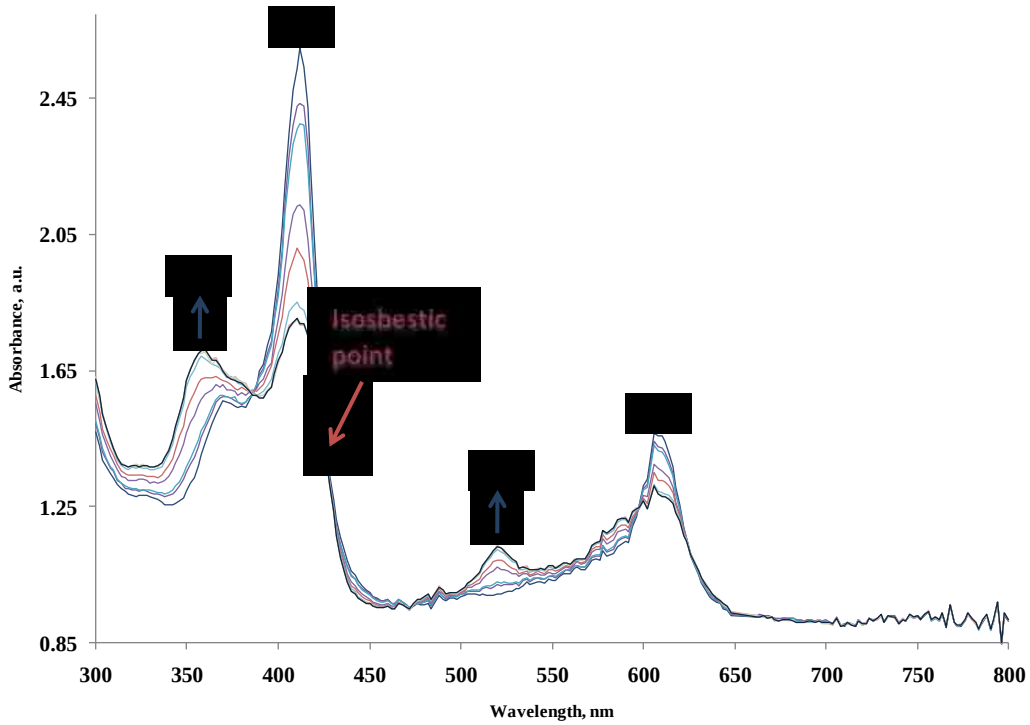

Figure 3-5. Thin-layer visible spectroelectrochemistry obtained during the reduction of Co(II)-OEPone 0.80 mM in THF, with 0.10 M TBAP, potential range 0 to -1.8 V

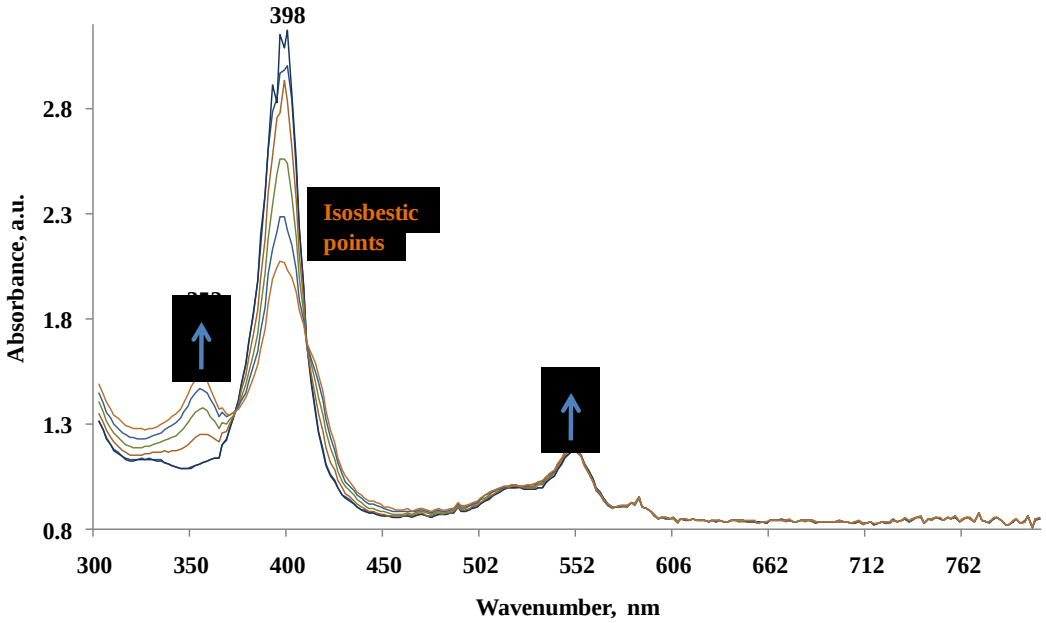

Figure 3-6. Thin-layer visible spectroelectrochemistry obtained during the reduction of Co(II)OEP 0.80 mM in THF, with 0.10 M TBAP

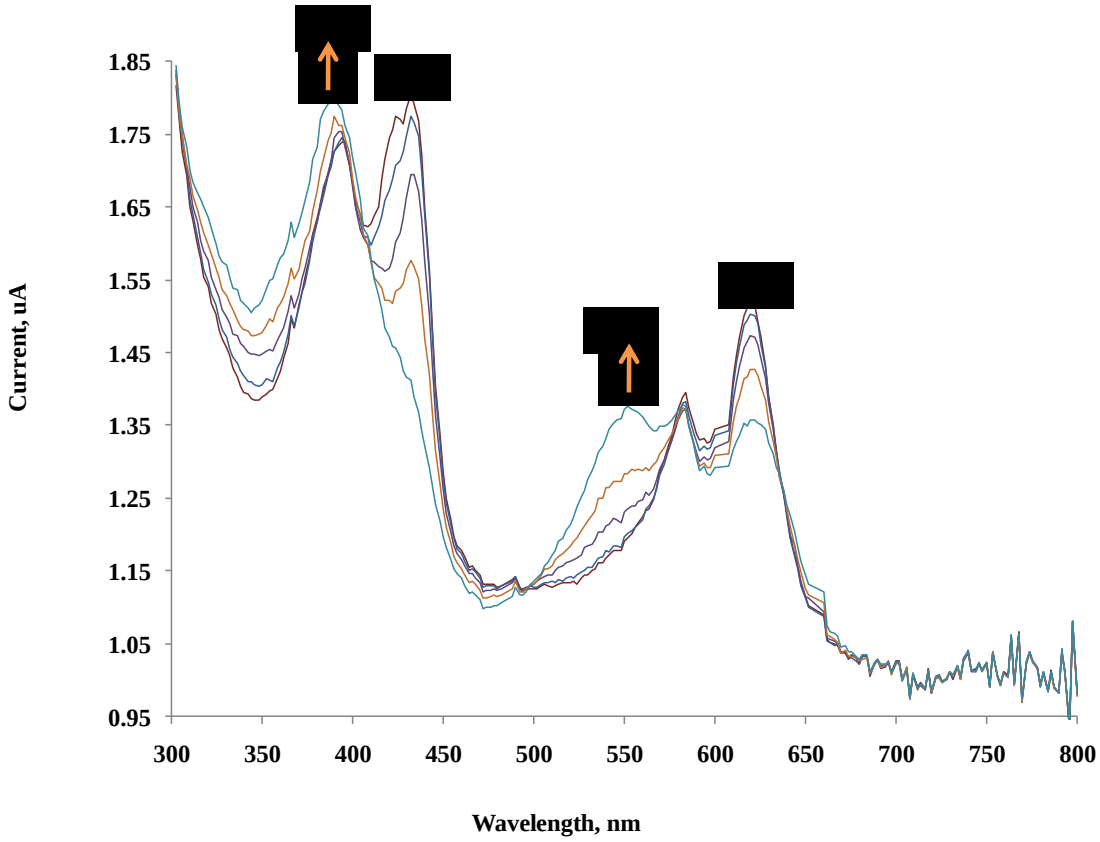

Figure 3-7. Thin-layer visible spectroelectrochemistry obtained during the reduction of Co(II)-OEPdione 0.80 mM in THF, with 0.10 M TBAP, potential range 0 to -1.6 V

For the first oxidation of Co(II)-OEPone, the Soret and Q band maintain their shape and intensity recording a small red shift in position (Figure 3-8). These spectral changes are similar to the features used to assign the oxidation in porphyrin complexes as metal centered[87]. It was stated previously in the literature that when the oxidation process is metal centered the Soret band will shift while the absorbance is preserved. At the same time the Q bands might change position or not but the peak absorbance is retained. This feature was used to assign oxidation in porphyrin complexes as metal centered [11] and the resulting species is $[Co(III)]^{+}$.

Further one electron oxidation revealed that the Soret band decreased in absorbance and was blue shifted while the Q band became featureless (Figure 3-9).

Generally, the bleaching of the Q band coupled with a decrease in absorbance in the B band suggests that the electron is lost from the macrocycle forming a π cation radical [11,87].

The oxidation of Co(II)-OEPdione reveals one reversible and one irreversible process as shown by cyclic voltammetry (Figure 3-4). For the first process the potential wave is scanned up to 1.2 V and the Soret band recorded a red shift from 432 nm to 470 nm while the Q band from visible region had a slight shift from 620 nm to 624 nm (Figure 3-10). The shape and absorbance of the B band and the absence of band broadening at 700-900 nm is an indication of a metal centered process as previously assigned in literature [11,87]. Isosbestic point at 440 nm during the first oxidation suggests that intermediates were not formed. Reduction of the oxidized species resulted in the formation of Co(II)-OEPdione, demonstrating the stability of the compound . The removal of a second electron from the system occurs in the potential region 1.2 V - 1.5 V and the UV-visible spectrum changes are presented in Figure 3-11. During the second oxidation process, a decrease and a blue shift in 470 nm band was observed and also the Q band diminished in intensity. UV-Visible spectrum (Figure 3-11) shows an incomplete second electron oxidation. The analysis performed illustrates that only 75% conversion occurred. Generally, the featureless Q band suggests a ring centered process[87] and also previous studies on cobalt porphyrins indicate the second oxidation is porphyrin centered.

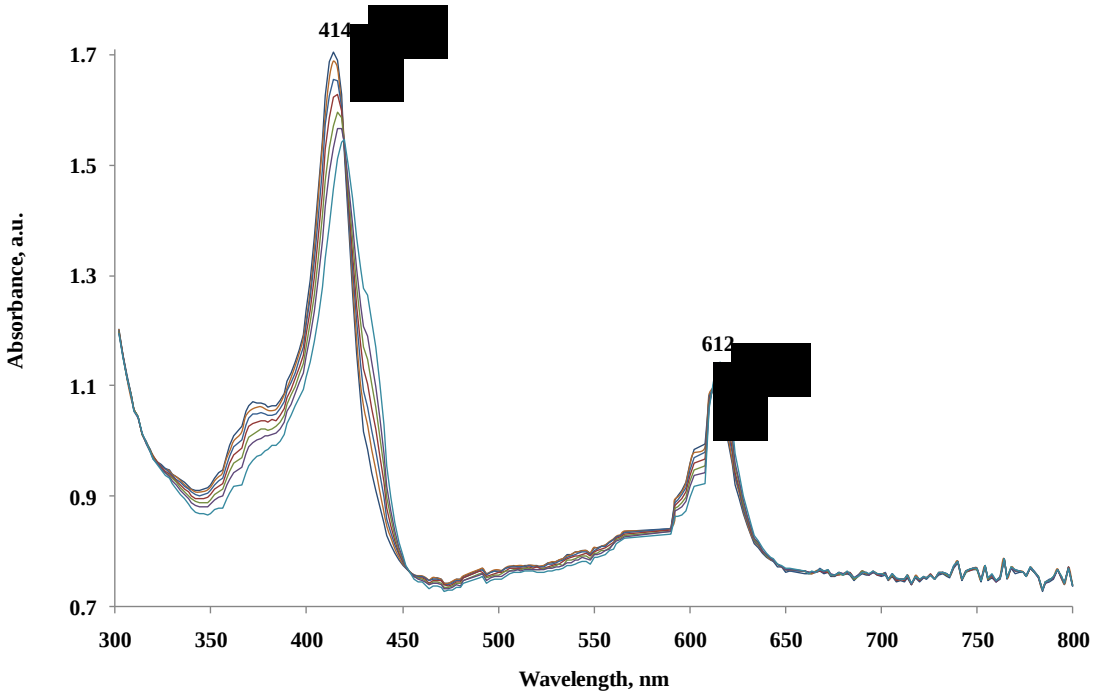

Figure 3-8. Thin-layer visible spectroelectrochemistry obtained during the first oxidation of Co(II)-OEPone 0.80 mM in THF, with 0.10 M TBAP, potential range 0 to 1.2 V

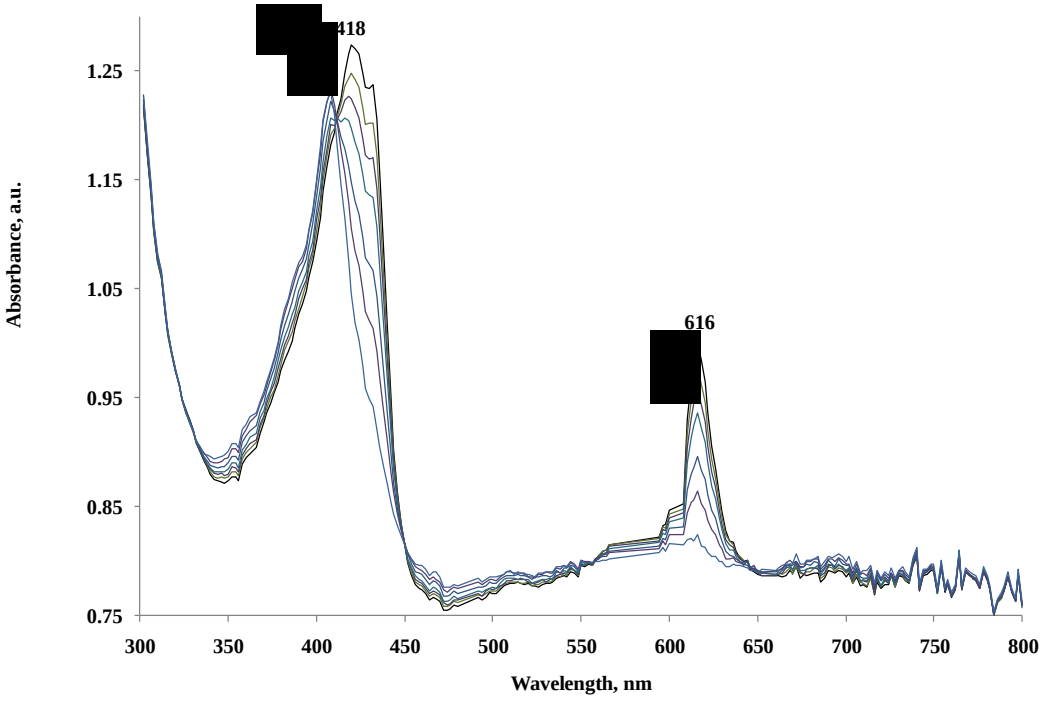

Figure 3-9. Thin-layer visible spectroelectrochemistry obtained during the second oxidation of Co(II)-OEPone 0.80 mM in THF, with 0.10 M TBAP, potential range 1.2 V to 1.8 V

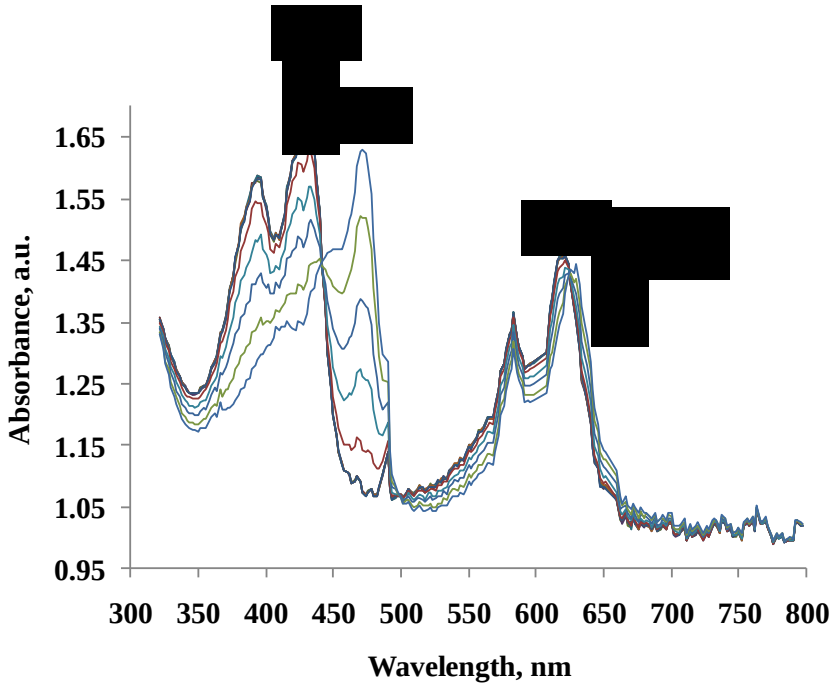

Figure 3-10. Thin-layer visible spectroelectrochemistry obtained during the first oxidation of Co(II)-OEPdione 0.80 mM in THF, with 0.10 M TBAP, potential range 0 to 1.2 V

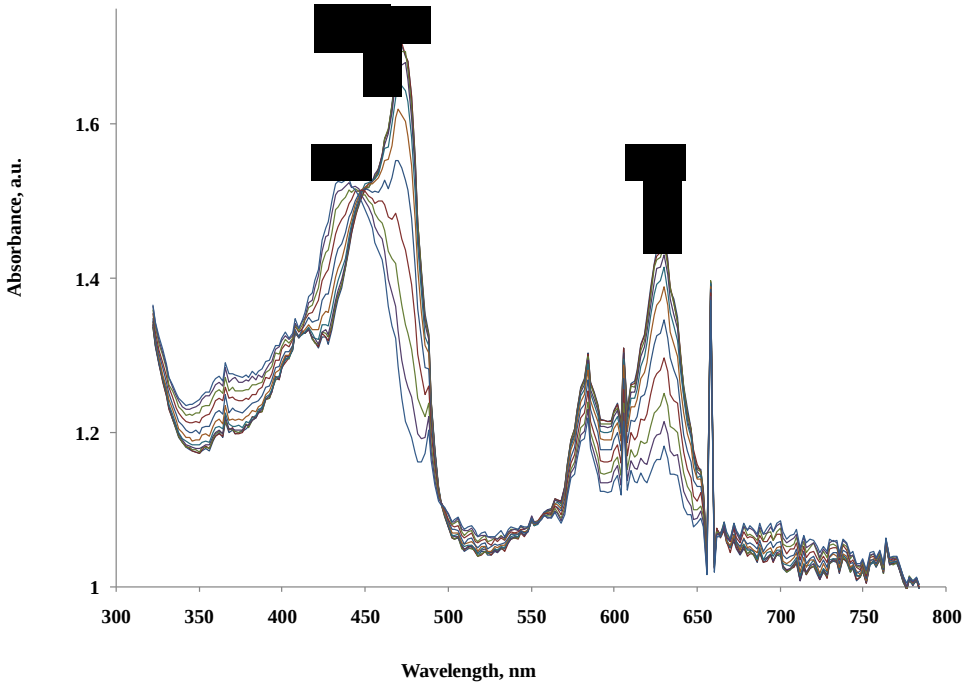

Figure 3-11. Thin-layer visible spectroelectrochemistry obtained during the second oxidation of Co(II)-OEPdione 0.80 mM in THF, with 0.10 M TBAP, potential range 1.2 V to1.8 V

3.3. Thin layer FTIR of Cobalt porphinone complexes

The infrared thin layer spectroelectrochemistry utilizes the advantage of vibrational spectra to understand the electronic structure of reduced porphinones. Because the d_π-orbitals of the central metal can interact with the porphinone π-system, the energy of the carbonyl vibration will be affected depending on these interactions. More significant shifts in the band should be observed if the reduction is centered on the porphinone.

The IR spectrum of Co(II)-OEPone was obtained using spectroelectrochemistry and the IR data are summarized in Table 3-4 and Table 3-5. The carbonyl band for Co(II)-OEPone was observed at 1709 cm^{-1} (Figure 3-12). Upon reduction, the band shifted to 1676 cm^{-1}, a decrease of 33 cm^{-1}. In addition to the band at 1676 cm^{-1}, bands at 1616, 1593, 1580 and 1556 cm^{-1} were observed. The band at 1646 cm^{-1} is due to a solvent-electrolyte species. Upon reoxidation the original spectrum of Co(II)OEPone was obtained (Figure 3-13). The carbonyl shift in Co(II)OEPone (33 cm^{-1})was similar to the shift observed for the Fe(II)OEPone reduction (32 cm^{-1})[174]. This suggests that the carbonyl vibration is weakened due to the electron density on the porphyrin ring caused by back-bonding from metal to porphyrin ring. According to previous studies from our laboratory[174] on iron porphinones and porphinediones, the 1566 cm^{-1} band shifted to 1556 cm^{-1} as similar result was observed in the 1562 cm^{-1} band for the reduction of Fe(II)OEPone, which corresponds to C_m-C_α and C_β-C_β vibrations according to DFT calculations. The Co(II)OEPone reduction results are similar to the previous data obtained on Fe(II)OEPone reduction which illustrate ring delocalization as shown by IR

results where the carbonyl band shifts to a lower frequency. Taking into account all these spectral changes, the Co(I)OEPone$^-$ species is quite similar to Fe(I)OEPone$^-$, for which the DFT calculations have indicated considerable Fe(I) character, with significant d_π back bonding to the ring.

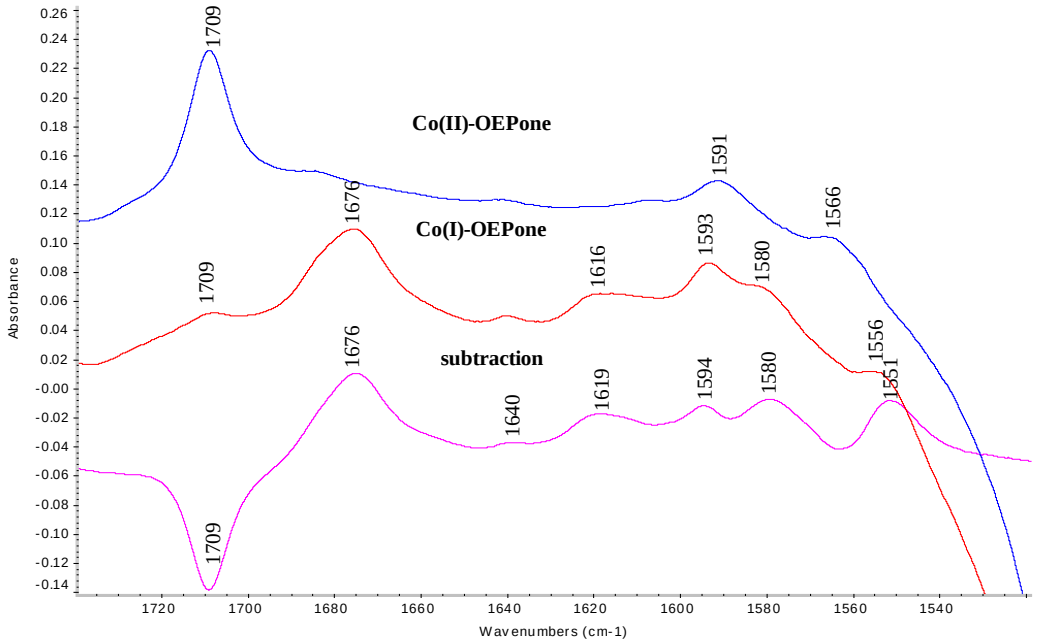

Figure 3-12. FTIR spectra of Co(II)-OEPone reduction 3.0 mM, in THF, 0.10 M TBAP, at -1.5 V by OTTLE spectroelectrochemistry, 32 scans

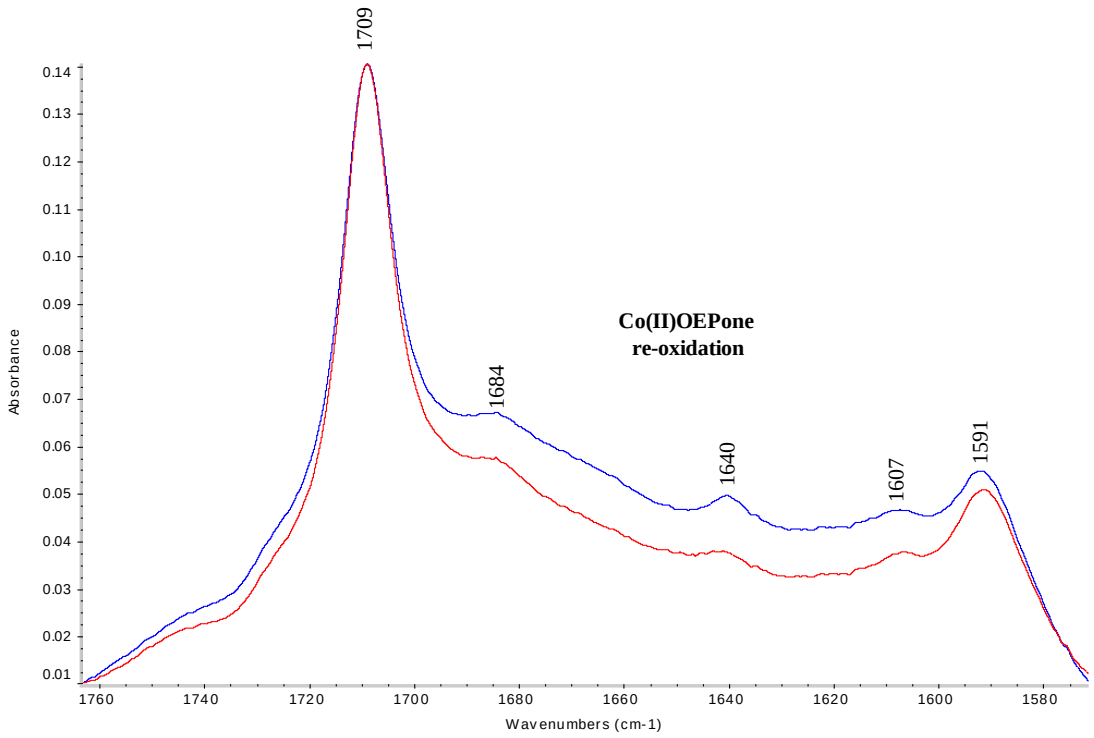

Figure 3-13. FTIR spectra of Co(II)-OEPone reoxidation 3.0 mM, in THF, 0.10 M TBAP by OTTLE spectroelectrochemistry

Figure 3-14 illustrates the IR spectra of Co(II)-OEPone ^{16}O vs Co(II)-OEPone ^{18}O and their difference spectrum. The carbonyl band in isotopically labeled porphyrin was observed at 1680 cm^{-1}, 29 cm^{-1} decrease when compared with the unlabeled porphyrin. The band in the porphyrin region at 1591 cm^{-1} was unchanged when the porphyrin was labeled indicating that it was not sensitive to isotopic labeling. The second peak at 1566 cm^{-1} for the unlabeled porphyrin shows a small shift to 1564 cm^{-1} which means that it was sensitive to the labeling and had weak C=O coupling.

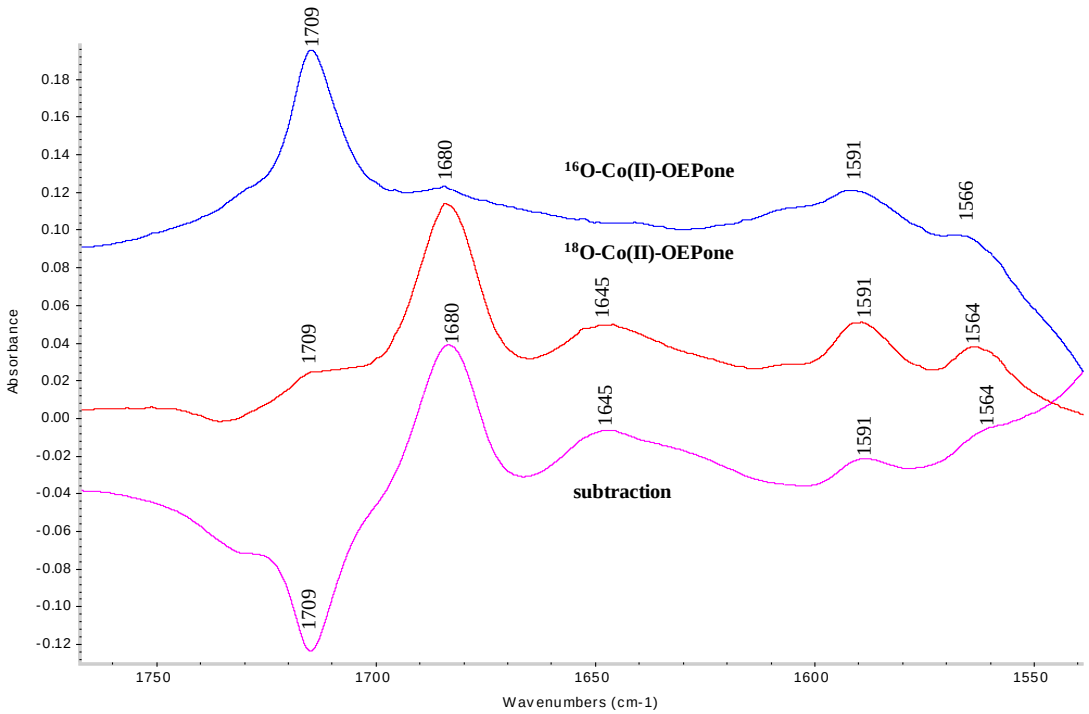

Figure 3-14. FTIR spectra of Co(II)-OEPone ^{16}O vs Co(II)-OEPone ^{18}O 3.0 mM, in THF, 0.10 M TBAP by OTTLE spectroelectrochemistry, 32 scans

Infrared spectroelectrochemisty of labeled Co(II)-OEPone with ^{18}O facilitates the identification of vibrational bands within the 1600-1500 cm^{-1} region. The carbonyl band decreased from 1709 cm^{-1} to 1680 cm^{-1} with ^{18}O substitution, a 29 cm^{-1} shift. Assuming a localized C=O vibration, a shift of 41 cm^{-1} is expected. Therefore, a 29 cm^{-1} is reasonable because of the coupling between the carbonyl and the porphinone ring. Figure 3-15 shows the ^{18}O labeled carbonyl band at 1680 cm^{-1} which shifts to 1654 cm^{-1} (26 cm^{-1}) during electrolysis. This compares with 1676 cm^{-1} in normal abundance porphinone, a shift of 22 cm^{-1}. In the porphyrin region the addition of one electron into the system produces a peak shift from 1564 cm^{-1} to 1552 cm^{-1} (12 cm^{-1}) and also new vibrational peaks are observed at 1616 cm^{-1} and 1579 cm^{-1}. The Co(II)OEPone spectrum was

observed upon oxidation of the reduced species indicating that the product was stable on the time scale of the experiment.

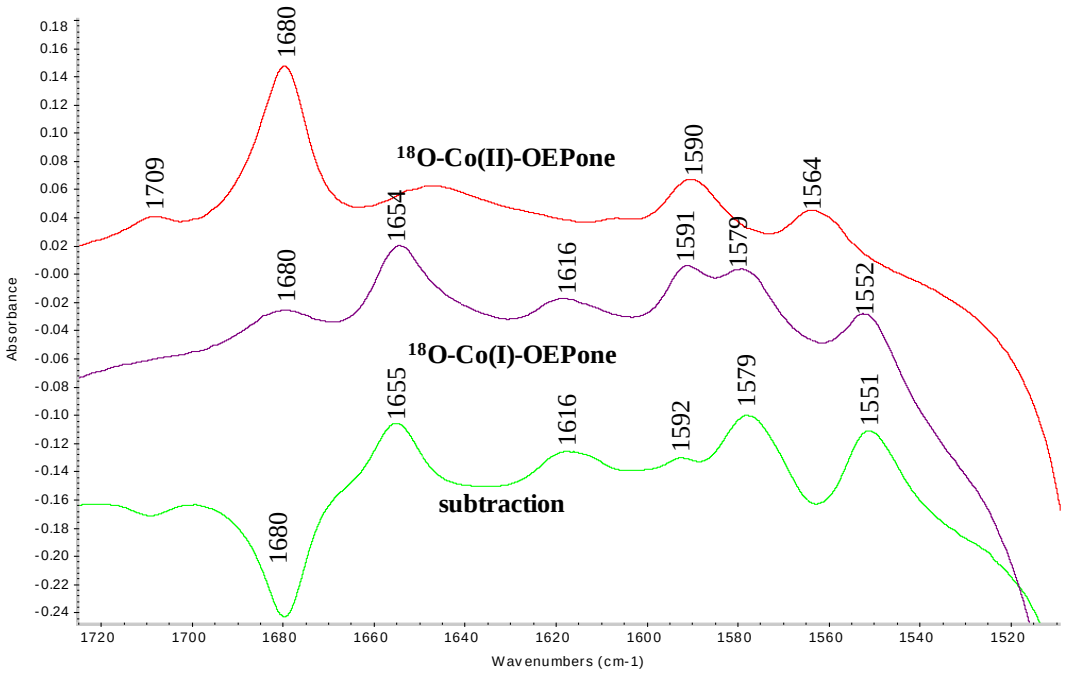

Figure 3-15. FTIR spectra of Co(II)-OEPone ^{18}O reduction 3.0 m<u>M</u>, in THF, 0.10 <u>M</u> TBAP, at -1.5 V by OTTLE spectroelectrochemistry, 32 scans

Figure 3-16 illustrates the difference IR spectra during the addition of one electron to ^{16}O Co(I)OEPone and ^{18}O Co(I)OEPone. For the former complex, one electron reduction shifted the carbonyl band by 33 cm^{-1} (1709 cm^{-1} to 1676 cm^{-1}), and the band in the porphyrin region shifted 2 cm^{-1} (1591 cm^{-1} to 1593 cm^{-1}). Furthermore another 10 cm^{-1} shift wave is observed from 1566 cm^{-1} to 1556 cm^{-1}. The labelled compound showed a 26 cm^{-1} shift in carbonyl peak and 1 cm^{-1} for the 1552 cm^{-1} porphyrin peak upon reduction. Besides vC=O vibration, the band at 1566 cm^{-1} showed a significant shift which indicates that it is isotopically sensitive. Reoxidation of the

electrolyzed species regenerates the original spectrum indicating that reduced species was stable (Figure 3-17).

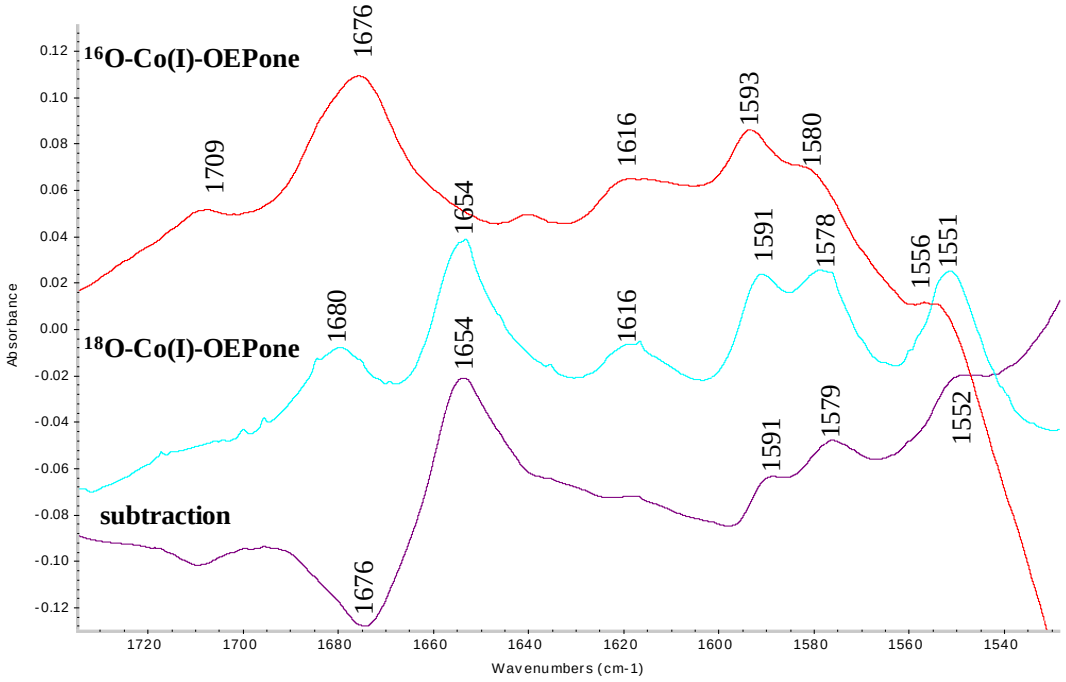

Figure 3-16. FTIR difference spectra of Co(II)-OEPone ^{18}O/ Co(II)-OEPone ^{16}O reduction 3.0 mM, in THF, 0.10 M TBAP, at -1.5 V by OTTLE spectroelectrochemistry, 32 scans

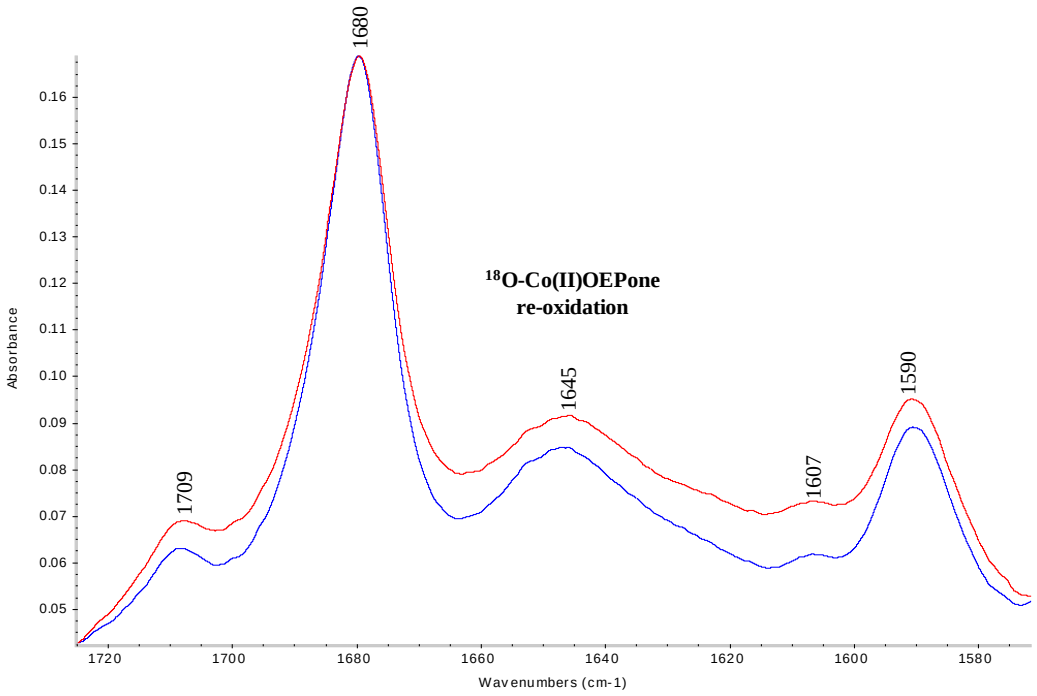

Figure 3-17. FTIR spectra of Co(II)-OEPone ^{18}O re-oxidation 3.0 mM, in THF, 0.10 M TBAP by OTTLE spectroelectrochemistry

Similar results were observed for Co-OEPdione (Figures 3-18, 3-19). The IR spectrum of the Co(II)-OEPdione complex in THF exhibits the carbonyl peak at 1709 cm $^{-1}$ and additional bands at 1606 cm^{-1} and 1583 cm^{-1}. During electrolysis the carbonyl peak shifted and split into two bands at 1681 and 1667 cm^{-1} as can be seen from the difference spectrum. The additional bands at 1583 and 1605 cm^{-1} record a small shift and also a new vibration at 1620 cm^{-1} is observed. These spectral changes are similar with the ones seen in porphinone complex and also in iron porphinones and porphinediones: the carbonyl band splits in two peaks with same absorbance although slightly higher wavenumber than the iron porphinedione case. The porphyrin region peak shifted from 1583 cm^{-1} to 1579 cm^{-1}. A small difference is noted for the carbonyl band of porphinedione in comparison with porphinone. The carbonyl band of porphinedione is split in two bands due to the presence of the two non-equvalent carbonyls in the molecule

while the porphinone carbonyl band display one peak in 1700 cm^{-1} region. According to previous studies from this laboratory, the source of these shifts is due to increased electron density on the porphyrin ring caused by back bonding of d_π electron from the metal to the lowest vacant π molecular orbitals of porphyrin.

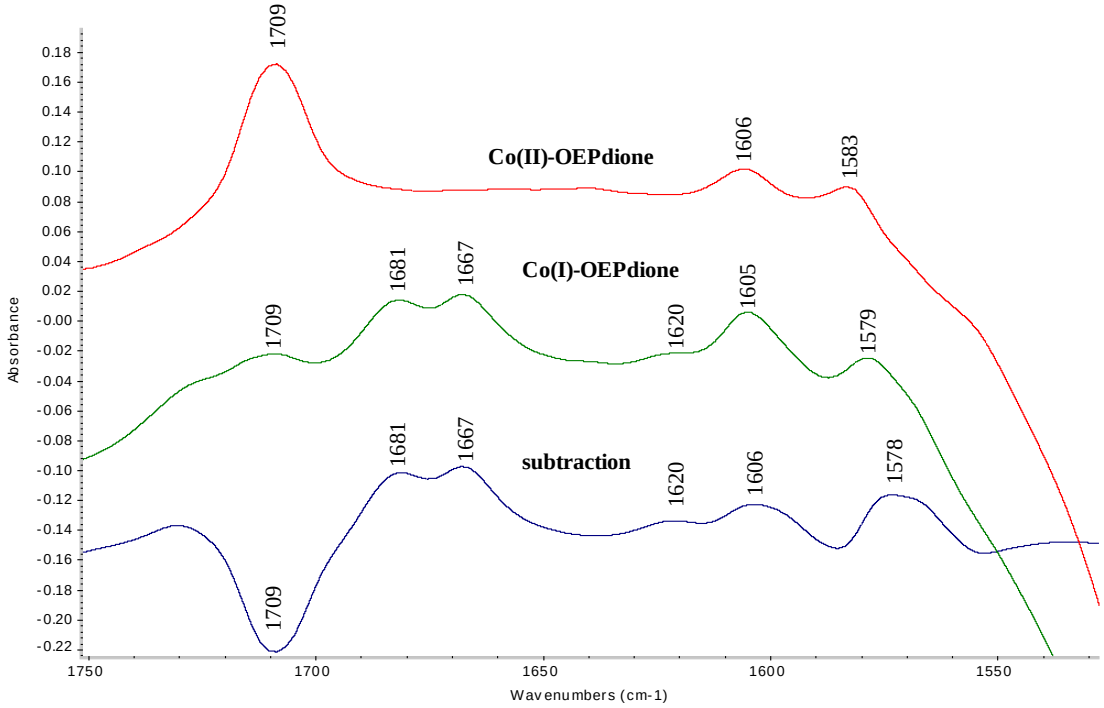

Figure 3-18. FTIR spectra of Co(II)-OEPdione reduction 3.0 m<u>M</u>, in THF, 0.10 <u>M</u> TBAP, at -1.5 V by OTTLE spectroelectrochemistry, 32 scans

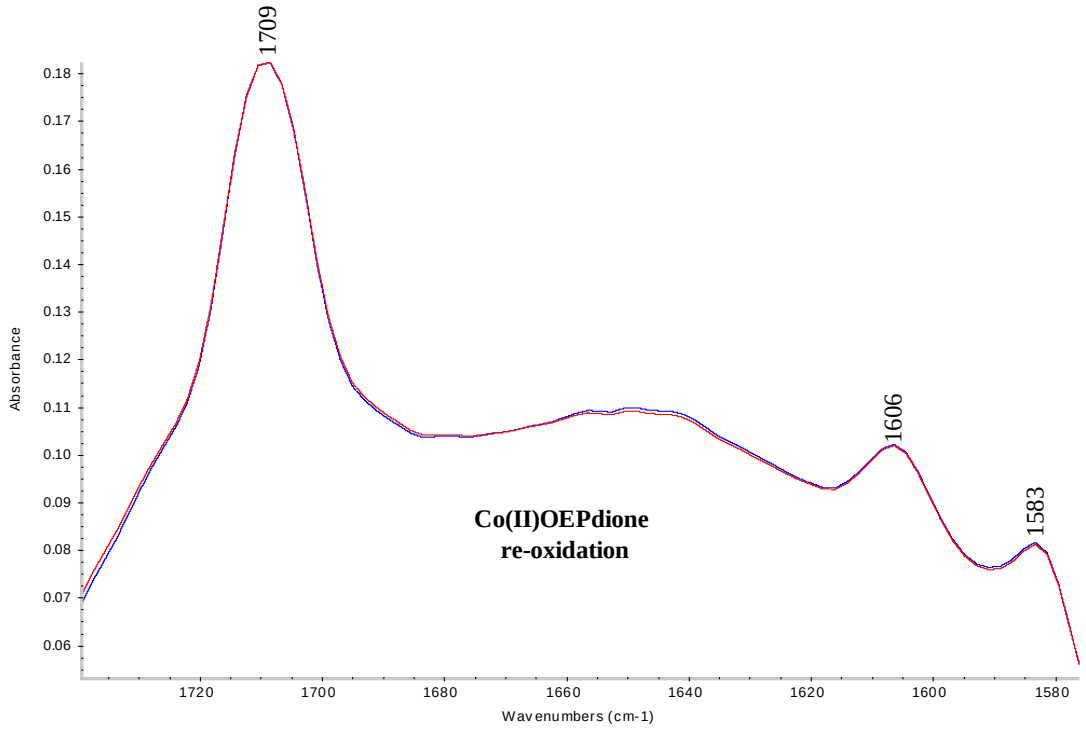

Figure 3-19. FTIR spectra of Co(II)-OEPdione reoxidation 3.0 mM, in THF, 0.10 M TBAP by OTTLE spectroelectrochemistry

Cyclic voltammetry and spectroelectrochemistry results of Co(II)-OEPone oxidation indicate two one electron transfers. As a consequence the FT-IR data were performed as a function of oxidation potential of each process.

Upon the first oxidation, the carbonyl peak recorded a shift from 1709 cm^{-1} to 1714 cm^{-1} and the bands from 1591 cm^{-1} and 1565 cm^{-1} decreased in absorbance (Figure 3-20). Based on previous studies, it is known that cobalt(II) unpaired spin is localized in d_{z2} orbital which has a weak orbital interaction with the porphyrin[179]. Therefore the removal of an electron from the system produces a carbonyl shift to a higher frequency, because the carbonyl bond strengthens due to less back-bonding from the cobalt complex. Generally removal of one electron from the central metal causes less perturbation to the porphyrin vibrations than removal of one electron from the ring; in addition, it results in a

decrease in the absorbance of the band at 1557 cm^{-1}[187]. The removal of the second electron from the system shifted the carbonyl bond from 1715 cm^{-1} to 1736 cm^{-1} strengthening the carbonyl bond (Figure 3-22). Re-reduction of the oxidized species returns the carbonyl band to the original position (Figure 3-23). This indicates that the compound was stable in the time scale of the experiment.

Removal of one electron from the labeled porphyrin system shifted the C=O band from 1680 cm^{-1} to 1684 cm^{-1} (4 cm^{-1}) while the peaks at 1590 cm^{-1} and 1563 cm^{-1} region are unchanged (Figure 3-24). Reoxidation of the electrolyzed species regenerates the original spectra indication that the oxidation product is stable on the time scale of the experiment (Figure 3-25). The difference IR spectra for the oxidation of ^{16}O Co(III)OEPone and ^{18}O Co(III)OEPone is illustrated in Figure 3-26. One electron oxidation produces a shift in carbonyl peak for both labeled and unlabeled porphyrin of 4 cm^{-1} while there is no change in the 1600 cm^{-1} region peaks. A small shift in the 1566 cm^{-1} band to 1563 cm^{-1} upon ^{18}O substitution was observed. Unfortunately, in was not possible to oxidize the labeled compound at the second oxidation potential. Higher potential are sometimes not attainable due to the exact placement of the auxiliary electrode.

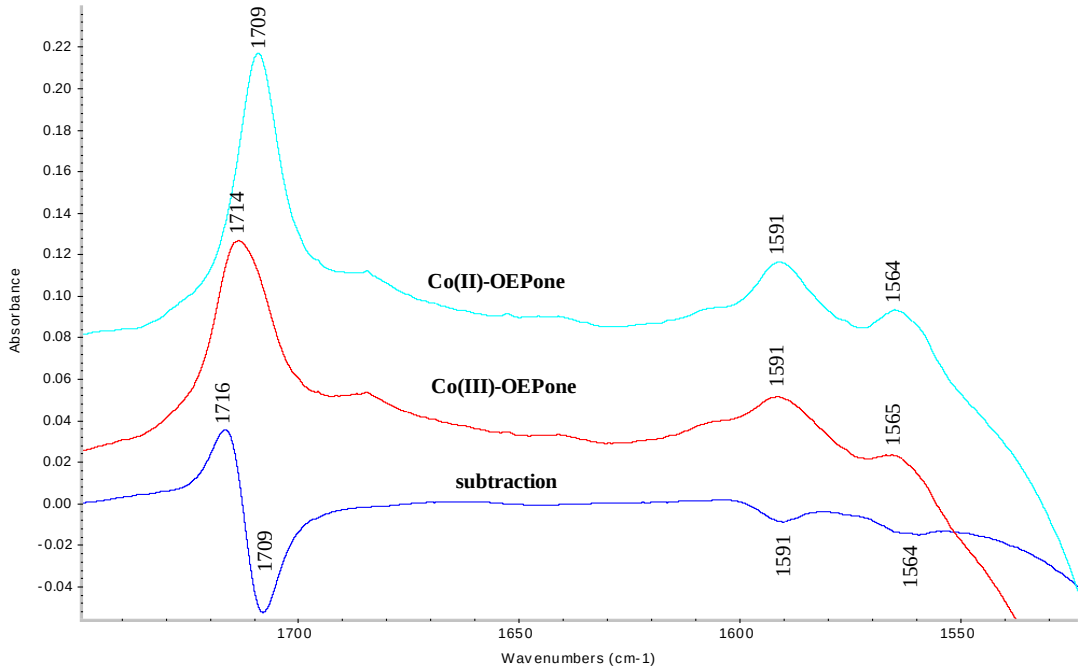

Figure 3-20. FTIR spectra of Co-OEPone oxidation 3.0 mM, in THF, 0.10 M TBAP, at 1 V and 1.5 V by OTTLE spectroelectrochemistry, 32 scans

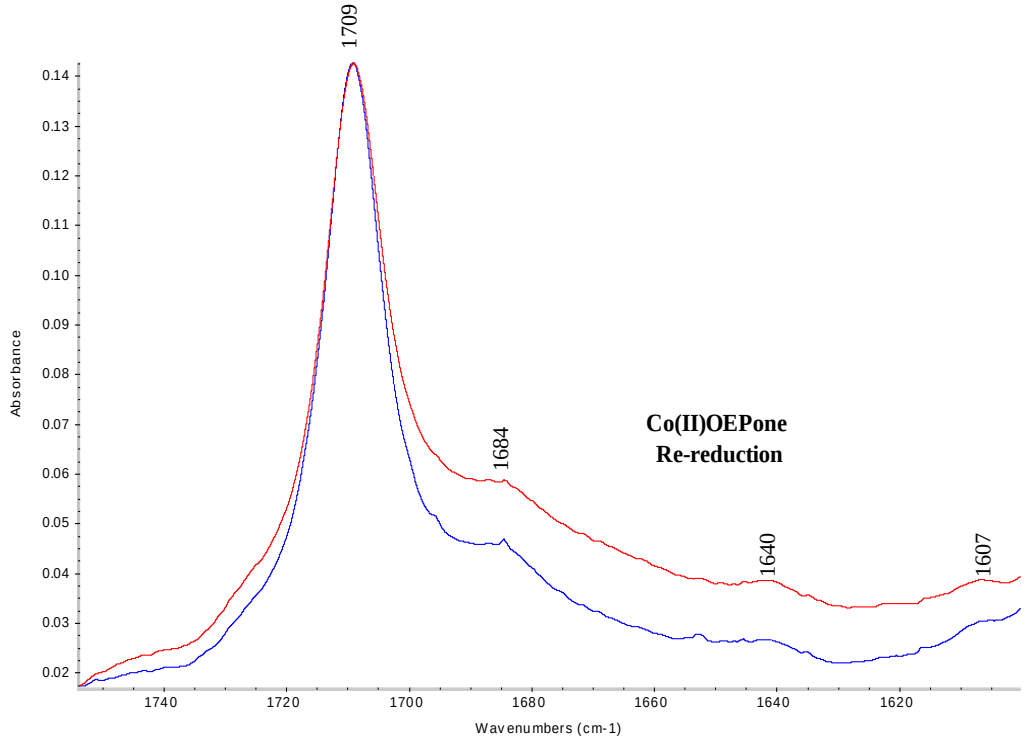

Figure 3-21. FTIR spectra of Co-OEPone re-reduction 3.0 mM, in THF, 0.10 M TBAP by OTTLE spectroelectrochemistry

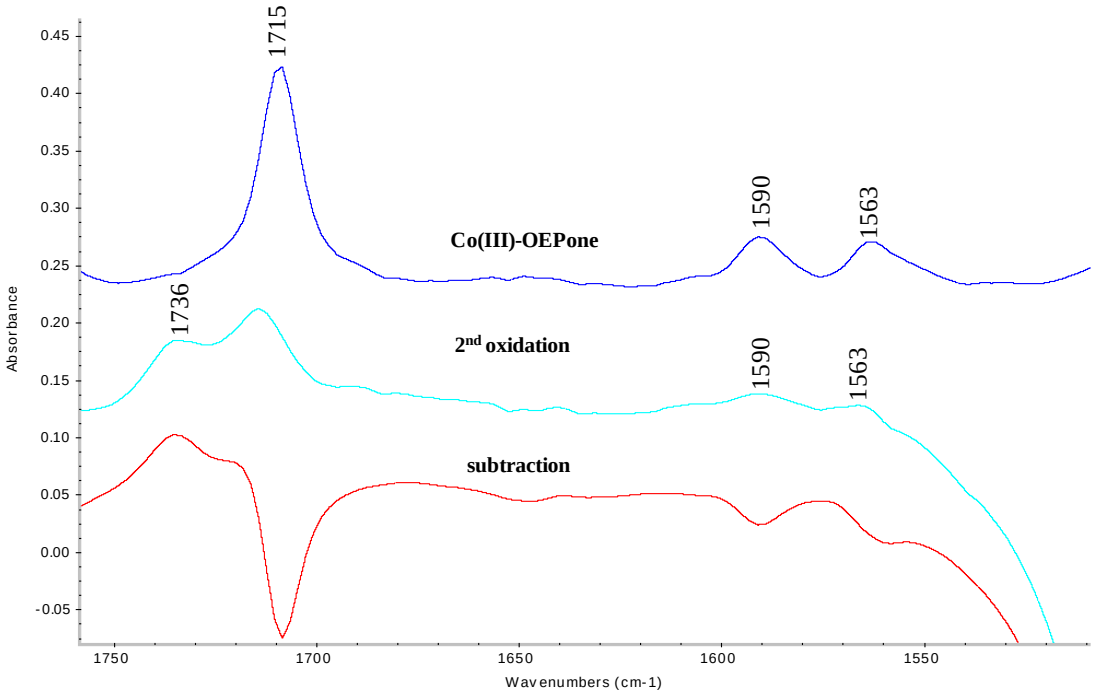

Figure 3-22. FTIR spectra of Co-OEPone oxidation 3.0 mM, in THF, 0.10 M TBAP by OTTLE spectroelectrochemistry, 32 scans

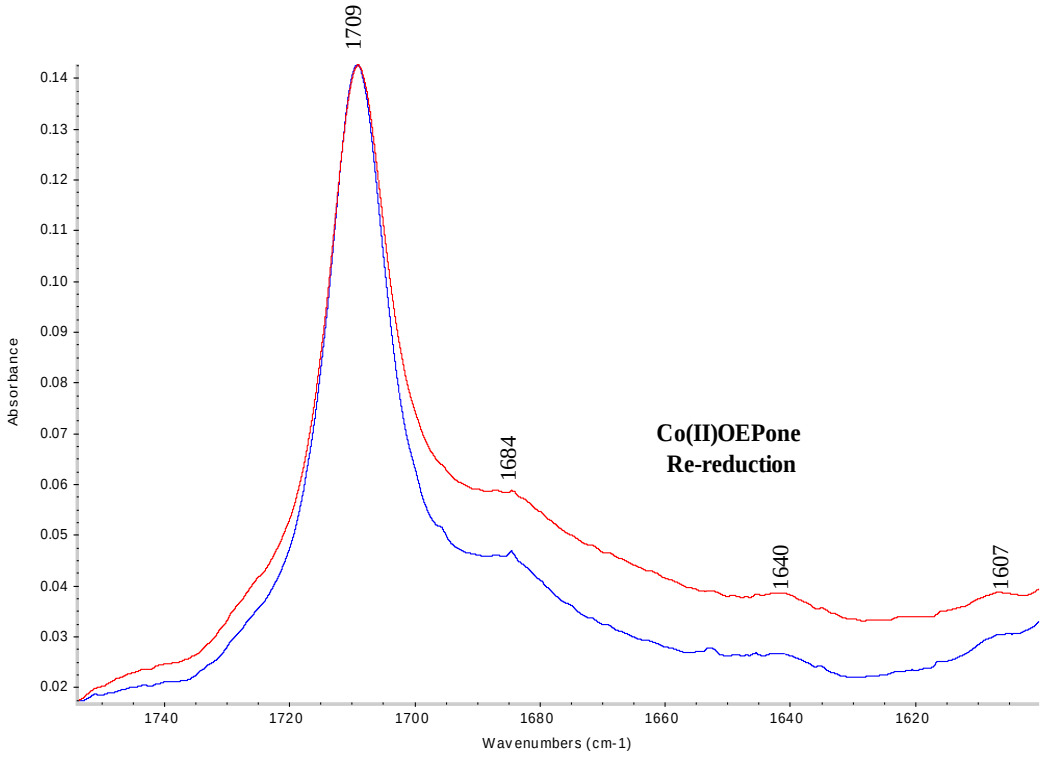

Figure 3-23. FTIR spectra of Co-OEPone re-reduction 3.0 mM, in THF, 0.10 M TBAP by OTTLE spectroelectrochemistry

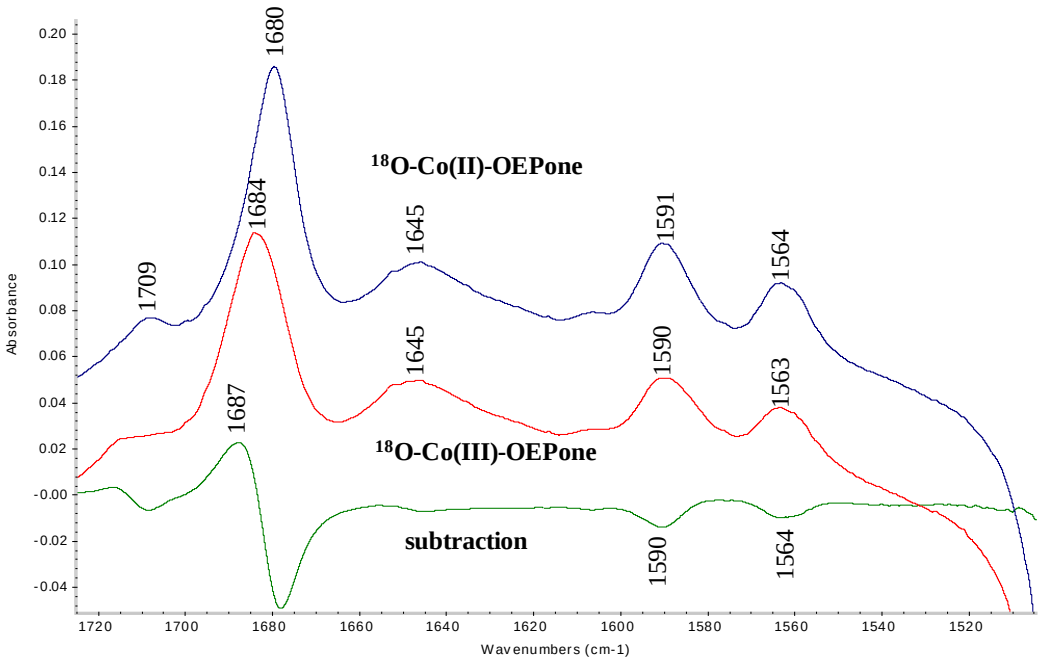

Figure 3-24. FTIR spectra of ^{18}O Co(II)-OEPone oxidation 3.0 mM, in THF, 0.10 M TBAP, at 1.0 V by OTTLE spectroelectrochemistry, 32 scans

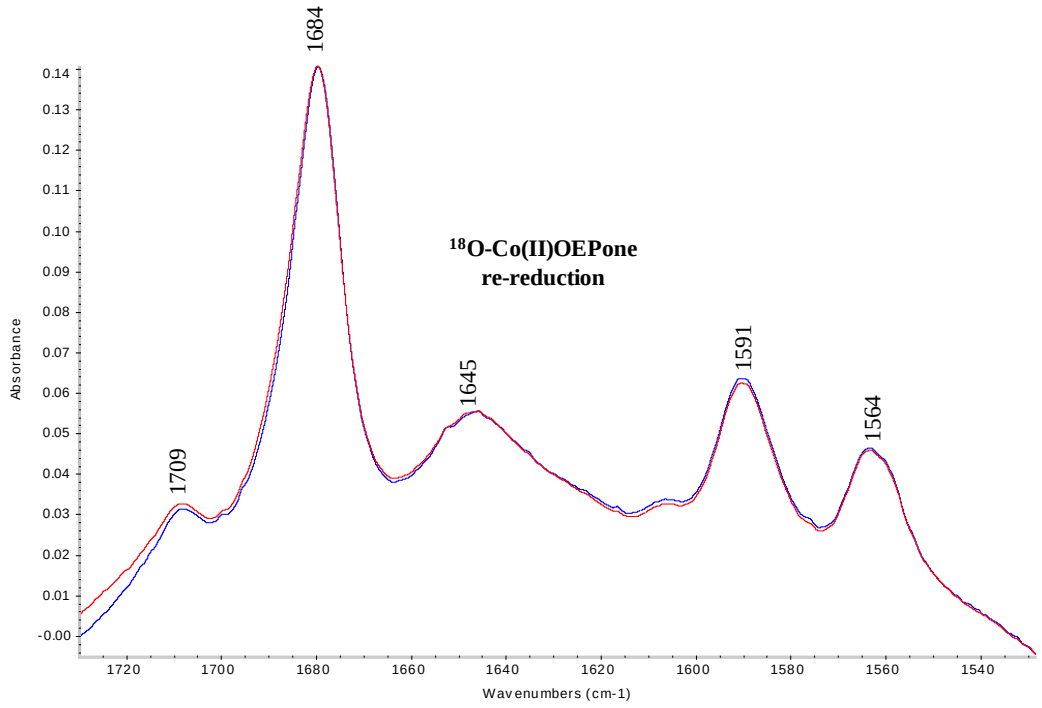

Figure 3-25. FTIR spectra of ^{18}O Co(II)-OEPone re-redaction 3.0 mM, in THF, 0.10 M TBAP by OTTLE spectroelectrochemistry

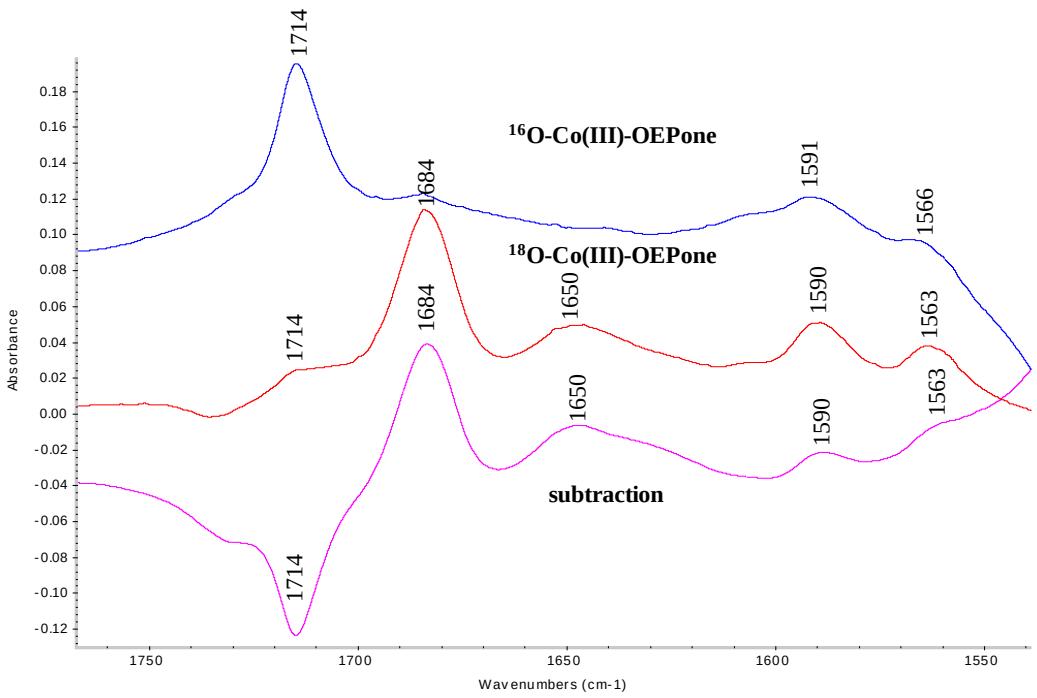

Figure 3-26. FTIR difference spectra of Co(II)-OEPone ^{18}O/ Co(II)-OEPone ^{16}O oxidation 3.0 mM, in THF, 0.10 M TBAP, at 1.0 V by OTTLE spectroelectrochemistry, 32 scans

Following the cyclic voltammetry and UV-Visible results which indicated that a metal centered process occur, the first oxidation of Co-OEPdione complex was also evaluated by controlled potential FT-IR (Figure 3-27). Scanning of the potential to 1.2 V, it is observed that the carbonyl peak shifted to a higher wave number (1712 cm^{-1}). Similar to Co-OEPone, the first oxidation led to a small shift in the carbonyl band (1709 to 1712 cm^{-1}), strengthening the C=O bond and suggesting less back-bonding from the metal to porphyrin. In the region close to 1600 cm^{-1}, the peaks initially present at 1605 cm^{-1} and 1582 cm^{-1} lost absorbance. With the removal of the second electron, the carbonyl band shifted from 1712 cm^{-1} to 1734 cm^{-1} resulting in a further strength of the carbonyl bond (Figure 3-28).

Comparison of the two electrooxidation results of Co-OEPone (4 cm^{-1}) and Co-OEPdione (3 cm^{-1}) upon electrolysis shows that the carbonyl band shifts are comparable

and smaller in contrast with the Fe(III)/Fe(II) shift of the respective porphyrins (16 cm^{-1}, 14 cm^{-1}). The source might be that the cobalt has more electrons in the d-π orbitals than iron. As a result, even with the removal of one electron, there is still considerable back bonding in the cobalt(III) complex. This might explain the larger shift in carbonyl for the iron complex compared to cobalt compound. Further electrooxidation reveals a shift in carbonyl of 22 cm^{-1} for both cobalt complexes. Based on the cyclic voltammetry and UV-visible results, it matches a porphyrin centered process. After the electrolysis of the second electrolytic process the carbonyl peak returns to 1709 cm^{-1} which means that the compound is stable (Figure 3-29).

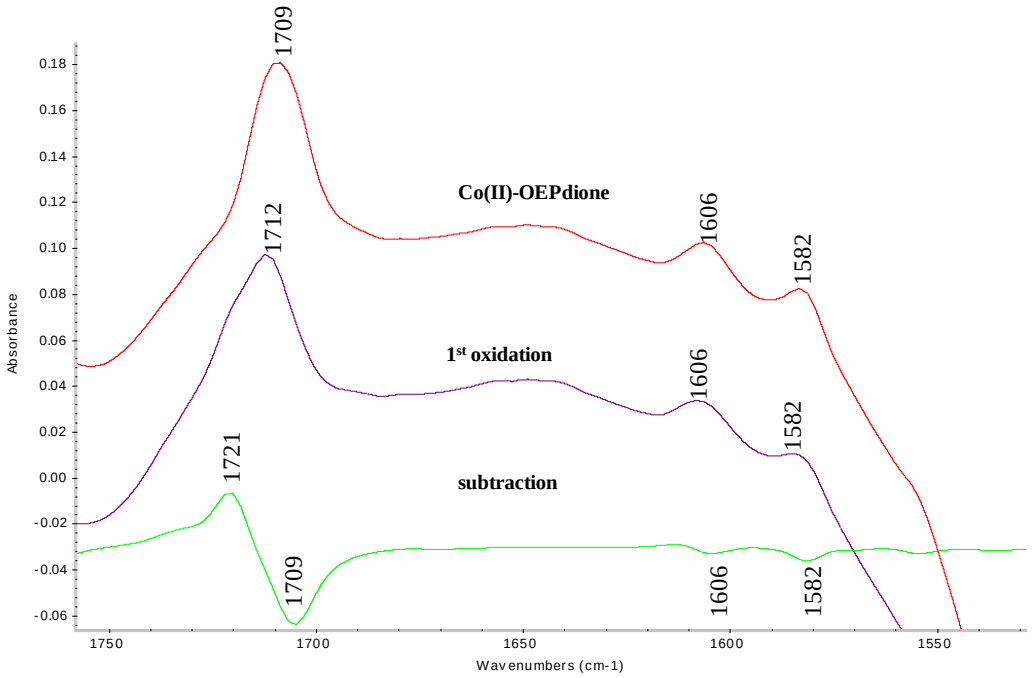

Figure 3-27. FTIR spectra of Co-OEPdione oxidation 3.0 mM, in THF, 0.10 M TBAP by OTTLE spectroelectrochemistry, 32 scans

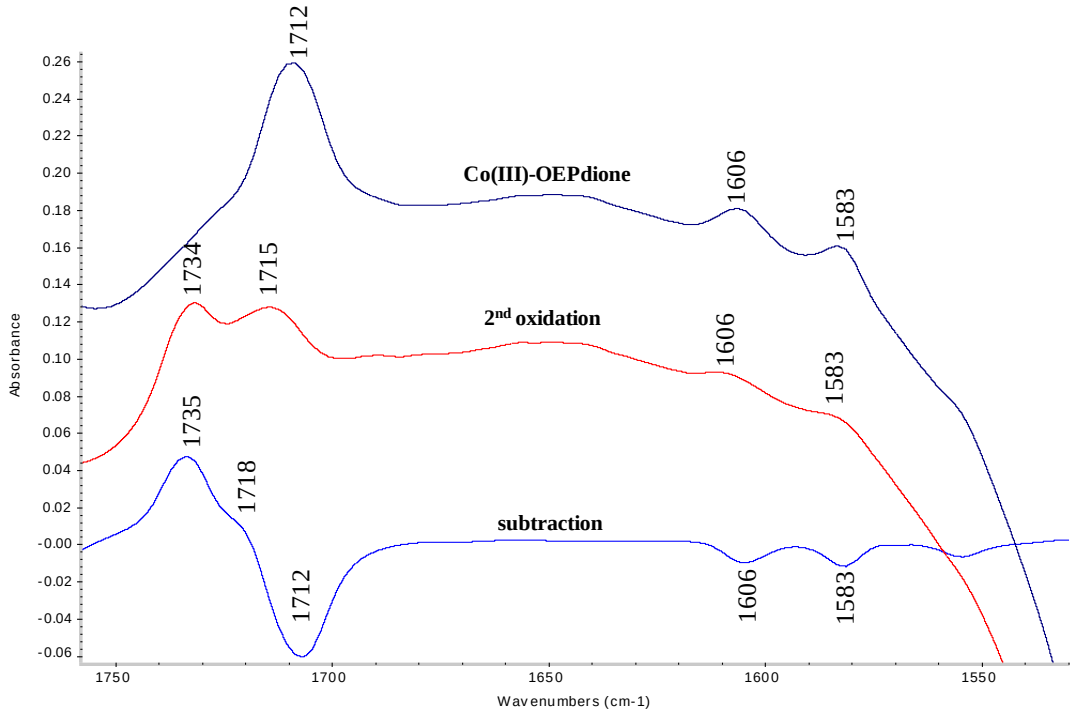

Figure 3-28. FTIR spectra of Co-OEPdione oxidation 3.0 mM, in THF, 0.1 M TBAP by OTTLE spectroelectrochemistry, 32 scans

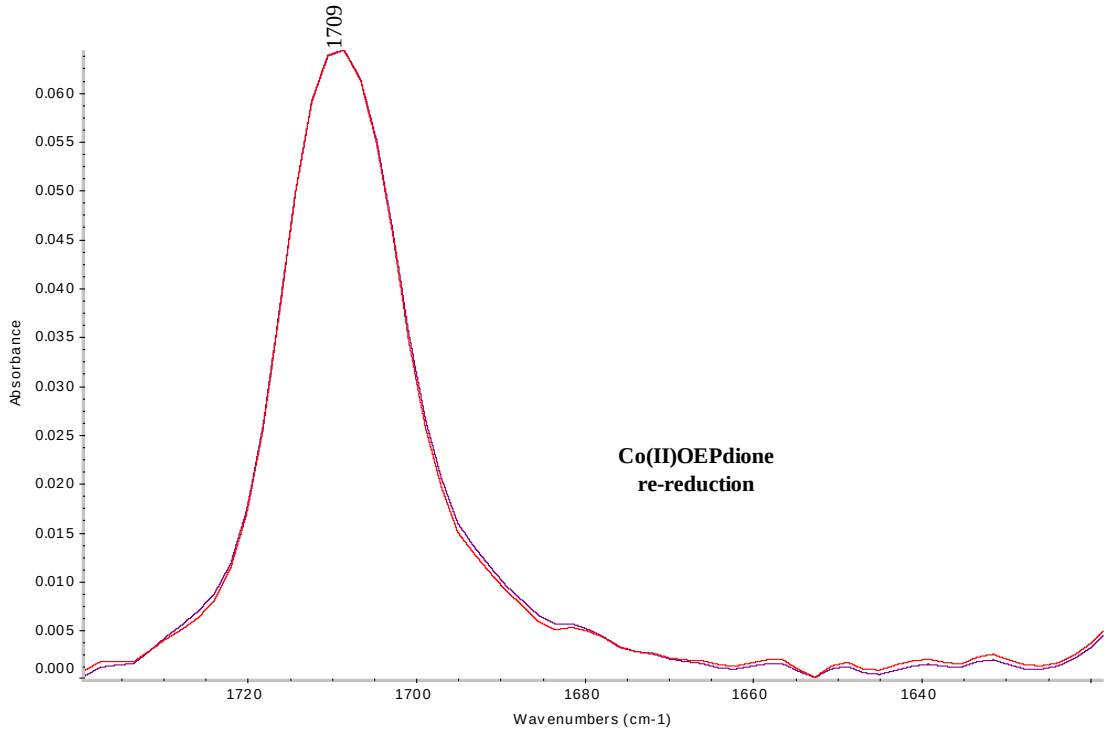

Figure 3-29. FTIR spectra of Co-OEPdione oxidation 3.0 mM, in THF, 0.10 M TBAP by OTTLE spectroelectrochemistry

Table 3-1.Comparison of the reduction/oxidation potentials of Cobalt Porphyrin Complexes

Compounds	**Reduction** $E_{p,1}$	**Oxidation** $E_{p,1}$	$E_{p,2}$	**References**
Co(II)-TPP	-1.38	+1.01	+1.38	this work
Co(II)-OEP	-1.63	+0.98	+1.32	this work
Co(II)-OEPone	-1.43	+0.90	+1.21	this work
Co(II)-OEPdione	-1.31	+1.09	+1.37	this work

Solution conditions: Au electrode, 0.80 mM in THF, with 0.10 M TBAP

Table 3-2.Cyclic voltammetry data for Cobalt porphinone and Cobalt porphindione

Compound		**Ipf, µA**	**Ipr, µA**	**Ipr/ipf**	**Epf, V**	**Epr, V**	**E1/2, V**
Co-OEPone	reduction	3.094	3.057	0.982	-1.43	-1.29	-1.36
Co-OEPdione	reduction	23.828	23.361	0.98	-1.42	-0.91	-1.16
Co-OEPone	oxidation	1.223	1.279	0.96	+1.21	+1.12	+1.17
Co-OEPdione	oxidation	0.908	1.434	0.63	+1.24	+1.19	+1.22

Table 3-3.Thin-layer visible spectroelectrochemistry obtained during the reduction of Co-OEPone, Co-OEPdione 0.80 mM in THF, with 0.10 M TBAP

Compounds	**Solvent**	**UV-visible spectra (nm)**	**Reference**
Co(I)-OEP	THF	352, 398, 510(sh), 546	this work
Co(II)-OEPone	THF	374, 412, 606	this work
Co(I)-OEPone	THF	354, 412, 510, 606	this work
Co(III)-OEPone^{+}	THF	414, 612	this work
Co(III)-OEPone^{2+}	THF	418, 612	this work
Co(I)TPP	THF	365, 424, 509	73
Co(II)-OEPdione	THF	384, 432, 620	this work
Co(I)-OEPdione	THF	382, 544, 620	this work
Co(III)-OEPdione^{+}	THF	470, 624	this work
Co(III)-OEPdione^{2+}	THF	432, 624	this work

Table 3-4.Infrared spectroelectrochemistry of metal porphinones

Compounds	**IR wavelength (cm^{-1})**	**Reference**
CoOEPone – ^{16}O	1709, 1591, 1566	this work
Co(I)(OEPone) $^{-}$ ^{16}O	1676, 1616, 1593, 1580, 1556	this work
CoOEPone – ^{18}O	1680, 1591, 1564	this work
Co(I)(OEPone)$^{-}$ ^{18}O	1654, 1618, 1591, 1579, 1552	this work
Fe(III)-OEPoneCl	1719, 1563, 1536	174
Fe(II)-OEPone	1703, 1550, 1530	174
Fe(OEPone)$^{-}$	1672, 1609, 1578, 1548	174

Table 3-5.Infrared spectroelectrochemistry of metal porphinediones

Compounds	**IR wavelength (cm^{-1})**	**Reference**
Co-OEPdione	1709, 1605, 1583	This work
Co(I)(OEPdione)$^{-}$	1681, 1667, 1605, 1579	This work
Fe(III)(OEPdione)Cl	1717, 1580, 1560, 1543,1526	174
Fe(II)(OEPdione)$^{-}$	1703, 1547, 1524	174
Fe(OEPdione)$^{-}$	1671, 1655, 1648, 1640, 1593, 1562, 1535	174

3.4. Conclusions

Several conclusions can be drawn from the spectroelectrochemical analysis of Co(II)OEPone and Co(II)OEPdione regarding the oxidation /reduction process of these complexes. The experiments performed for the reduction of cobalt complexes resulted in a collection of data that would suggest a metal centered process. Compared to $Co^{II}OEP$ reduction potential (-1.63 V), the cobalt(II) porphinone and porphinedione $E_{1/2}$ are -1.39 V and -1.31 V respectively which parallel previous observations from literature for OEP>OEPone>OEPdione series. These values are expected because the compounds contain one and two carbonyl groups. The effect of these electron withdrawing groups is the decrease in reduction potential.

The spectroelectrochemical results for the reduction of cobalt(II) porphinone and porphinedione are in agreement with the empirical rules for a metal centered process. A small decrease and the shift in the Soret band, coupled with the absence of band broadening in the UV and visible region, are consistent with a metal centered process. The fact that the Soret band has a significant decrease accounts for a ring contribution to the electrolytic process. The presence of the isosbestic points during the process is an indication that no intermediates were formed.

The IR spectroelectrochemistry of Co-OEPone shows a red shift in carbonyl band of 33 cm^{-1} which was similar to the carbonyl shift recorded for Fe(II)OEPone (32 cm^{-1}). These shifts are thought to be metal centered. Therefore the carbonyl vibration is weakened due to increased electron density on the porphyrin ring caused by back-bonding from metal to porphyrin. Furthermore some shifts and new bands were observed

in 1600-1500 cm^{-1} region which were identified using ^{18}O-Co(II)OEPone labeling. Comparison of the peaks in the porphyrin region for the labeled-unlabelled Co(II)OEPone illustrates that only 1566 cm^{-1} (2 cm^{-1}) vibration is sensitive to isotopic labeling which indicates a weak C=O coupling. In the case of Co(I)OEPone besides the C=O vibration, the 1556 cm^{-1} band is isotopically sensitive. IR data for CoOEPdione show a shift in the carbonyl band of 28 cm^{-1} upon reduction which compares with the shift of 32 cm^{-1} for the reduction of FeOEPdione. The latter reduction is thought to be metal centered.

Cobalt complexes displayed two one-electron oxidations, first is considered to be metal centered, while second is suspected to be a porphyrin centered process. The oxidation potentials of CoOEPone are +0.90 V and +1.17 V while for CoOEPdione are in the range of +1.09 V and +1.22 V. As expected, the oxidation potentials were shifted to a more positive value for porphinedione because removal of electrons is more difficult from a system containing two electron withdrawing groups. The spectral changes for the first oxidation of cobalt porphinone and porphinedione are similar to the features used to assign the oxidation in porphyrin complexes as metal centered. The Soret band shifted but the intensity was preserved. No band broadening was observed in the UV and visible region. The second oxidation process showed a shift in the Soret band while the Q band became featureless with the appearance of a band broadening in the visible region. All these changes indicated a porphyrin centered process according to previous literature. The IR spectroelectrochemistry of Co-OEPone shows a shift in carbonyl band of 5 cm^{-1} for the first oxidation which was in the range of a metal centered process and a shift of 21 cm^{-1} for the second oxidation process which is thought to occur at the porphyrin

center. The shifts in the porphyrin region for the labeled porphinone show no sensitivity to isotopic labeling, but isotope shifts of 4 cm^{-1} were observed for the carbonyl band.

Chapter 4 SPECTROELECTROCHEMICAL STUDIES OF ZINC PORPHINONE COMPLEXES

4.1. Voltammetry of Zinc porphinone complexes

The electrochemistry of ZnOEP, ZnOEPone and ZnOEPdione was investigated by both cyclic voltammetry and UV-visible spectroelectrochemistry. The redox process of each complex was carried out on a platinum electrode in tetrahydrofuran containing 0.10 M TBAP. The voltammetric data are presented in Table 4-1 after adjusting for the difference in reference electrodes (-0.11 V).

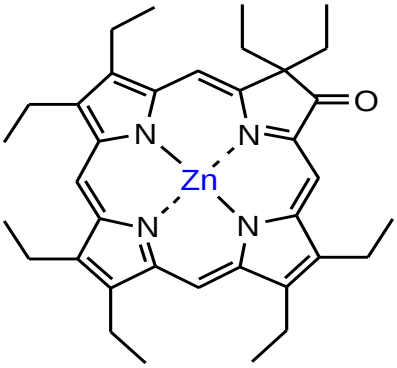

Zn-porphinone (ZnOEPone)

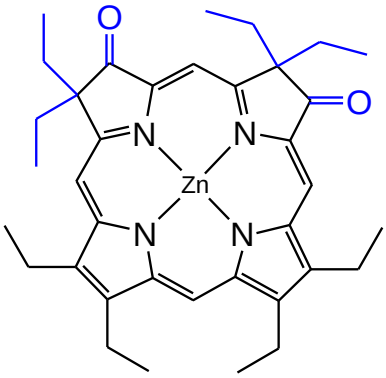

Zn-porphinedione (ZnOEPdione)

Scheme II

The electrochemistry of ZnOEP was studied previously[53-60]. Cyclic voltammetry and UV-visible analysis was performed for comparison. The reduction potentials reported by Spiro for the reduction of ZnOEP to radical anion is -1.8 V vs SCE in well purified THF solution containing 0.10 M TBAP supporting electrolyte.[151] The results from our laboratory show that zinc octaethylporphyrin complex (ZnOEP) undergoes a one electron transfer process with a half wave potential of -1.69 V vs Ag/AgCl in THF (Figure 4-1).

The reduction process is reversible as indicated by the peak current ratio, i_{pa}/i_{pc} which is close to unity at the scan rates investigated (0.05 – 0.2 V/s).

Zinc porphinones and zinc porphinediones complexes undergo one-electron quasireversible reduction as indicated by the peak current ratio (i_{pa}/i_{pc}) with the $E_{1/2}$ value of -1.28 V in the case of Zn(II)OEPone and -1.09 V for Zn(II)OEPdione. The peak separation between the anodic and cathodic peak potentials, E_{pa} -E_{pc}, should be close to 0.059 V (one electron transfer) for a reversible electron transfer. Some broadening occurred due to uncompensated resistance. Typical voltammetric waves are shown in Figure 4-2 and Figure 4-3.

A comparison of the reduction potential of Zn(II)OEP with Zn(II)OEPone shows that the carbonyl group significantly decreases the reduction potential (410 mV). The addition of a second carbonyl group on the ring (Zn(II)OEPdione) had a smaller effect (190 mV) compared to Zn(II)OEPone. These shifts were much larger than the shifts in the reduction potentials observed between Fe(II)OEP vs Fe(II)OEPone (30 mV)and Fe(II)OEPone vs Fe(II)OEPdione (80 mV).

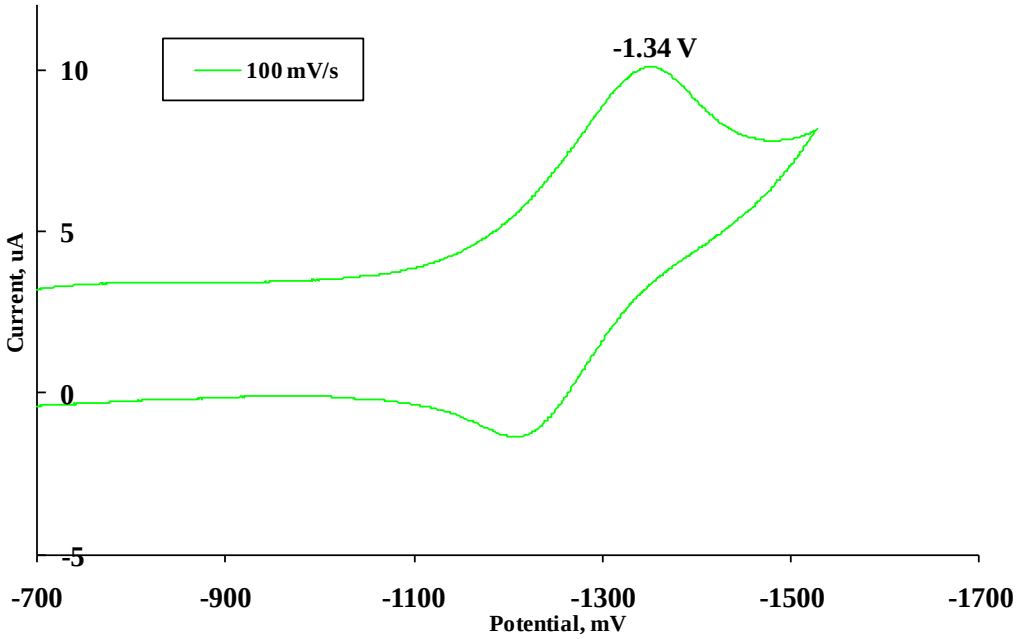

Figure 4-1. Cyclic voltammogram of Zn-OEPone reduction. Solution conditions: 0.80 mM in THF, with 0.10 M TBAP electrolyte, WE: platinum, RE: Ag/AgCl

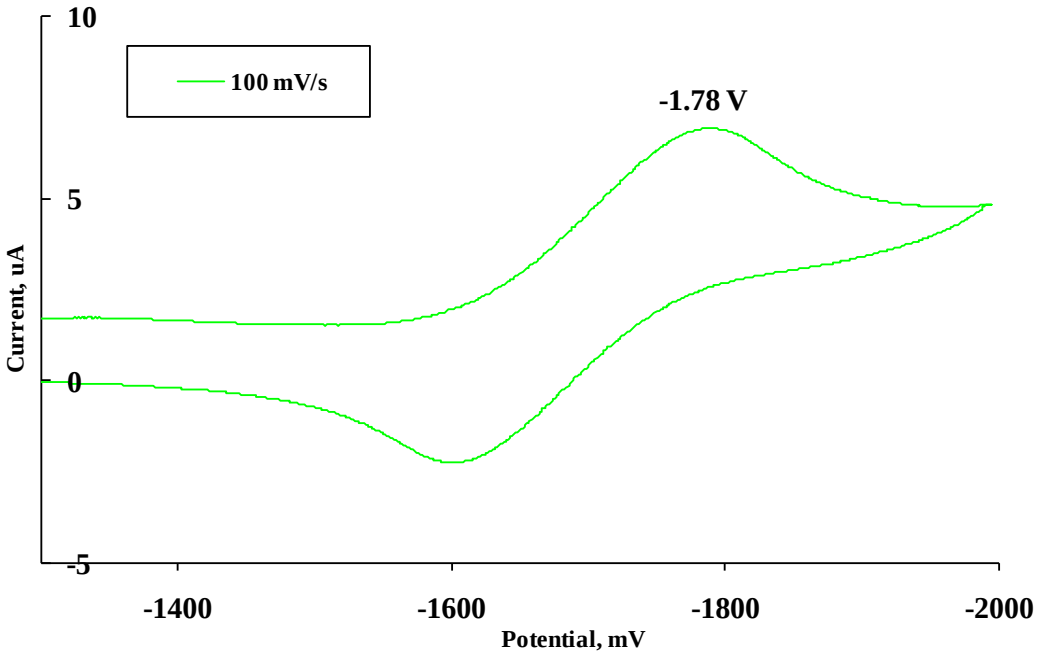

Figure 4-2. Cyclic voltammogram of ZnOEP reduction. Solution conditions: 0.80 mM in THF, with 0.10 M TBAP electrolyte, WE: platinum, RE: Ag/AgCl

The $E_{1/2}$ values of free base porphyrin and free base porphinones reveal that H_2OEP is reduced at a potential more negative than H_2OEPone and H_2TPP. Earlier studies[180] indicated that porphinone complexes are weaker bases than porphyrin. Similar to the free base porphyrins, the carbonyl group on the pyrrolic ring and phenyl rings attached to the porphyrin ring makes Zn-OEPone and ZnTPP easier to reduce. The ring reduction of ZnTPP occurs at considerable lower potential than ZnOEP complex at around 370 mV more positive and at more negative potential when compared with Zn-OEPone (Table 4-2). Carbonyls as well as phenyls are electron withdrawing groups. Consequently this weakens the interaction between the metal and porphyrin.

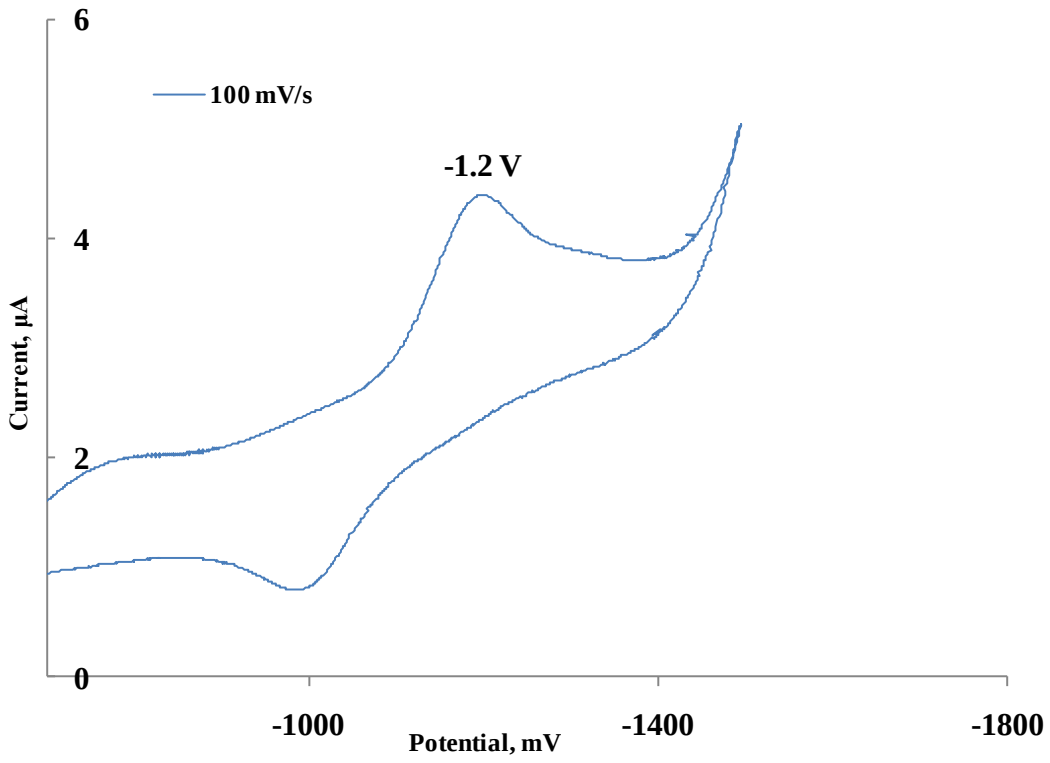

Figure 4-3. Cyclic voltammogram of ZnOEPdione reduction. Solution conditions: 0.80 mM in THF, with 0.10 M TBAP electrolyte, WE: platinum, RE: Ag/AgCl

4.2. Spectroelectrochemistry of Zinc porphinone complexes

UV-visible spectroelectrochemical technique was used to further study the electronic structure of the reduction product. The visible spectroelectrochemical analysis of zinc complexes was performed in THF using OTTLE cell containing 0.10 M TBAP and the changes in the visible spectra were recorded by controlled potential electrolysis in order to provide spectral characterization of reduced products. The UV-visible data are summarized in Table 4-3.

The UV-visible spectral changes during electrolysis of ZnOEP to $ZnOEP^-$ showed the Soret band shifted toward longer wavelength (408 to 451nm) while the Q bands decreased sharply in absorbance (Figure 4-4). No isosbestic point was observed at 420 nm, suggesting the formation of other species. A comparison of Figure 4-5 with Figure 1-11 shows that the spectra are essentially the same, but there was a broadening of the band around 430 nm, which was sharper in Spiro's data[151]. This could be due to instrumental issues or solution effects caused by solute concentration or electrolyte. As ZnOEP was not a focus of our work, these issues were not investigated further, as good isosbestic points were observed for the zinc porphinone complexes. Our spectrum and Spiro's differed from the one reported by Bocian[154]. In the Bocian[154] report, the Soret band records a small shift at 418 nm which is explained by Spiro group[151] as being due to the presence of impurity. Spiro's group also observed the 420 nm band shift in the VO(OEP) complex analysis when the solvent was not carefully purified. On the other hand, the porphyrin anion radical spectra are reported by Bocian to be sensitive to

changes in solvent and electrolyte[181]. In our work, re-oxidation of $ZnOEP^-$ regenerated the original spectrum.

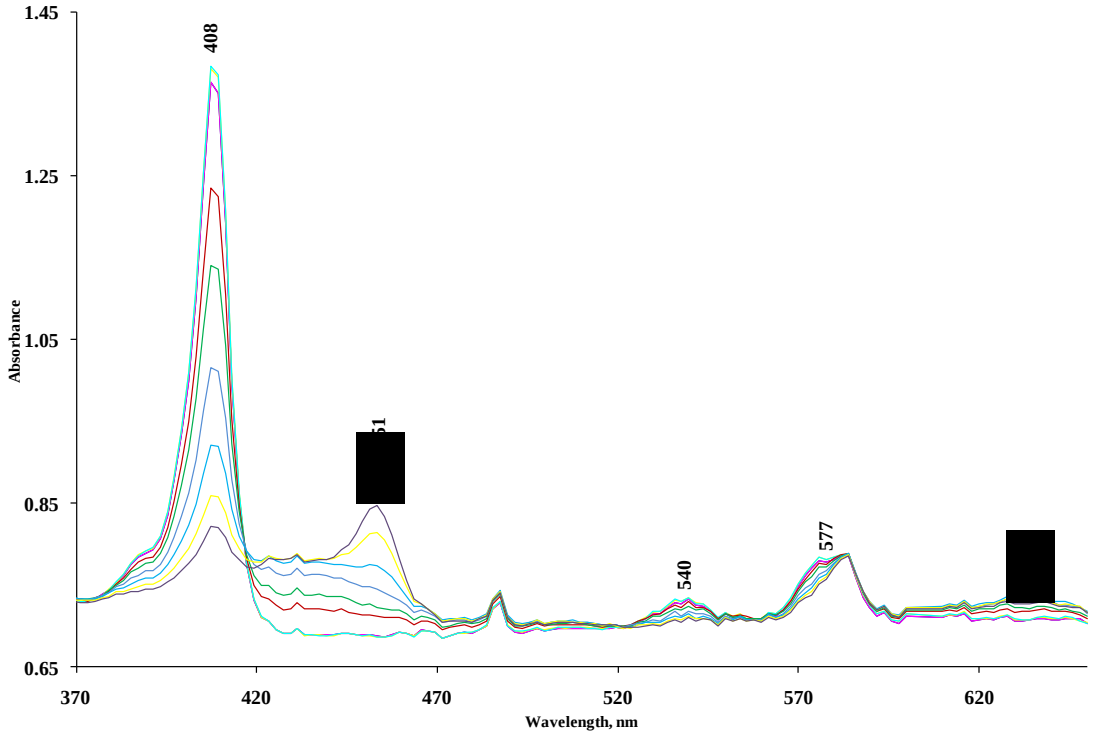

Figure 4-4. Thin-layer visible spectroelectrochemistry obtained during the reduction of ZnOEP 0.80 mM in THF, with 0.10 M TBAP, potential range 0 V to -1.9 V

The reduction of Zn(II)OEPone displayed a significant decrease in Soret band and shifted towards longer wavelength (420 to 450 nm) while Q band at 620 nm was bleached. Isosbestic points were observed at 360 and 430 nm, indicating only two spectral species present (Figure 4-5). According to empirical rules[88,89,90] and previous reports, a significant decrease in Soret and Q bands with formation of broad bands indicates π anion radical formation. The initial ZnOEPone spectrum was regenerated by

reoxidation, indicating that the one-electron reduction product was stable on the time scale of this experiment. Similar spectral changes have been reported for ZnTPP[62].

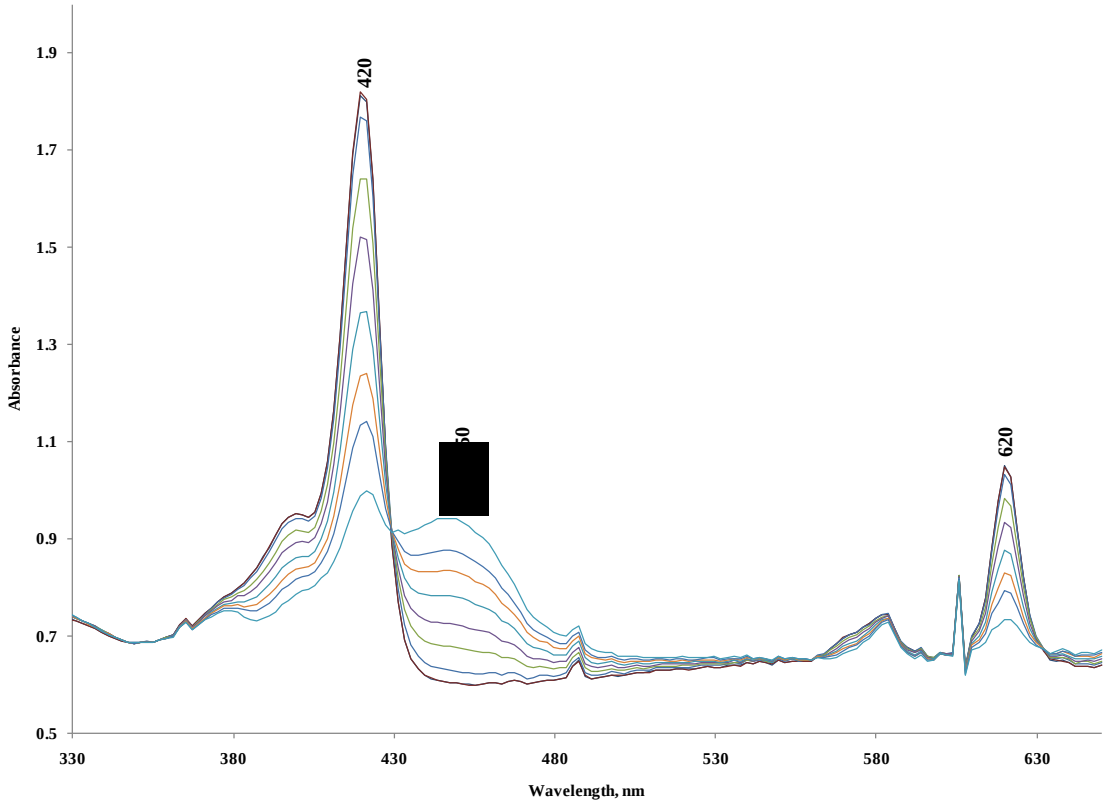

Figure 4-5. Thin-layer visible spectroelectrochemistry obtained during the reduction of Zn-OEPone 0.80 mM in THF, with 0.10 M TBAP, potential range 0 V to -1.6 V

The UV-visible spectrum of Zn(II)OEPdione is characterized by a Soret band at 390 (sh), 414 (sh), 490 nm and a Q band in the visible region at 624 nm (Figure 4-6). Controlled potential reduction of the complex at -1.69 V in a thin-layer spectroelectrochemical cell led to a significant decrease in the Soret band while the Q band is almost bleached. Band broadening in the UV (458-550 nm) and in the visible region (650-730 nm) coupled with the sharp decrease in intensity of Soret band suggests a π anion radical formation. The isosbestic points at 436 nm and 450 nm indicate that

intermediates were not formed. The reoxidation of the singly reduced species led to complete recovery of the initial UV-visible spectrum. The reduction behavior is similar with the one observed previously in ZnOEPone complex and previously reported in literature[62], corresponding to a ring-centered process.

A comparison of the zinc porphyrin, porphinones, porphinediones complexes reveals that the spectral changes during electroreduction occur in the same UV region and follow the empirical rules stated in literature for π anion formation[86]. The addition of one electron into the system leads to significant decrease in the Soret band and to the appearance of broad bands in visible region which is characteristic for the formation of a π anion species.

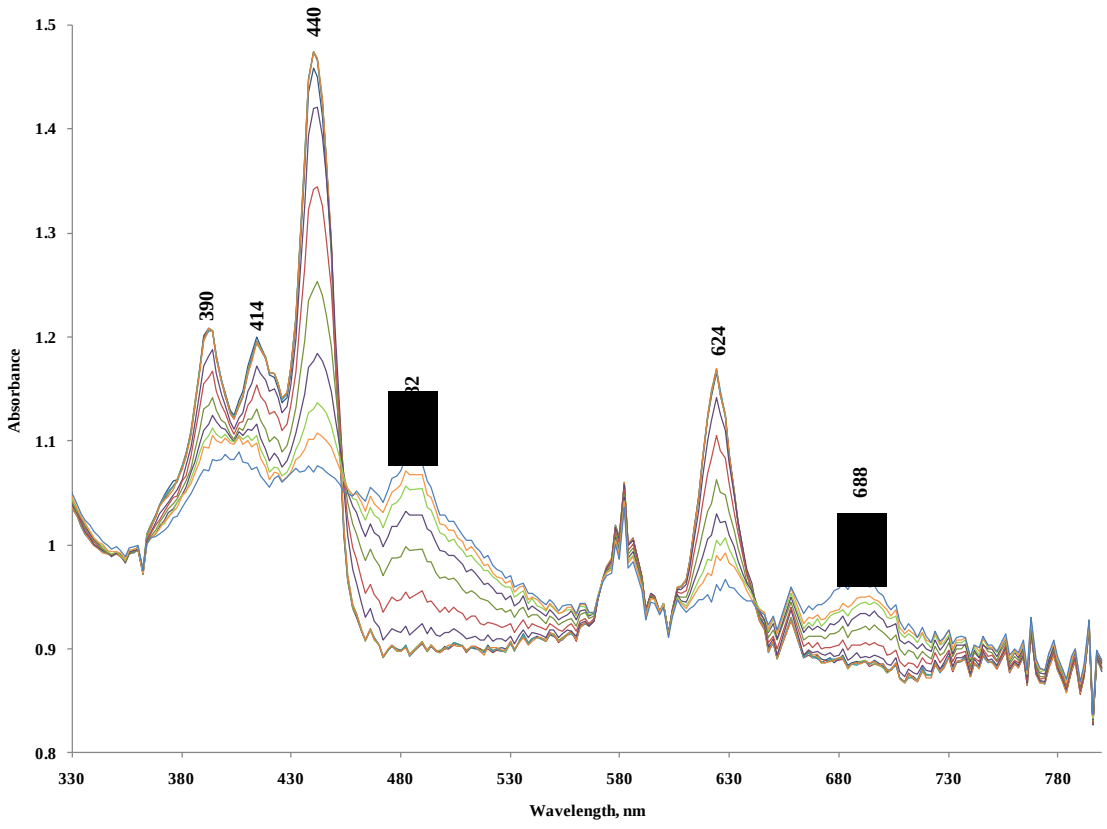

Figure 4-6. Thin-layer visible spectroelectrochemistry obtained during the reduction of Zn-OEPdione 0.80 mM in THF, with 0.10 M TBAP, potential range 0 V to -1.6 V

4.3. Thin-layer FTIR of Zinc porphinone complexes

According to cyclic voltammetry and UV-visible data, reduction of zinc complexes is porphyrin based. Further IR studies were performed to characterize these species and the data are summarized in Table 4-4.

Thin-layer FTIR spectroscopic data were collected during the electroreduction of ZnOEPone and the result is presented in Figure 4-7. The IR spectrum of Zn(II)OEPone illustrates a carbonyl band at 1709 cm^{-1} and an additional band at 1560 cm^{-1}. Upon reduction the carbonyl band shifted from 1709 cm^{-1} to 1662 cm^{-1} (47 cm^{-1}), new peaks were observed at 1550 cm^{-1} and 1540 cm^{-1}. The carbonyl band was regenerated upon reoxidation but complete recovery of the peak did not occur. The difference may be due to shifts in the background or some small amount of decomposition. In any case, the effect was small with over 97% recovery based on the absorbance of the carbonyl band at 1709 cm^{-1} (Figure 4-8). The presence of the isosbestic points indicated that no intermediates were observed.

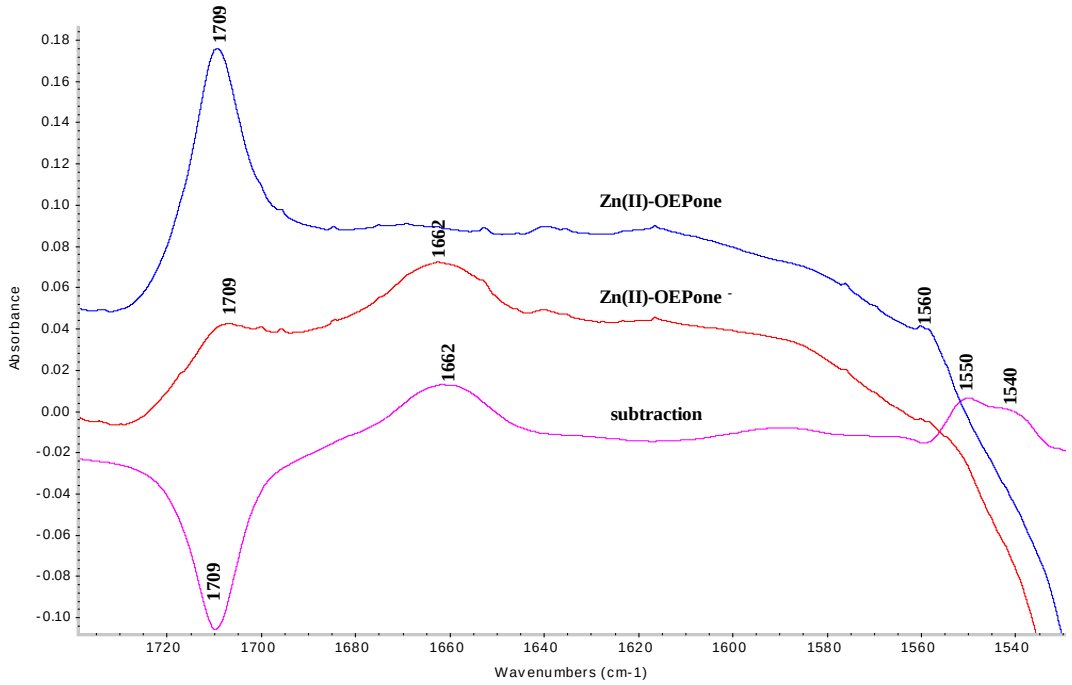

Figure 4-7. FTIR difference spectra of Zn-OEPone with THF as reference 3.0 mM, in THF, 0.10 M TBAP by OTTLE spectroelectrochemistry, 32 scans

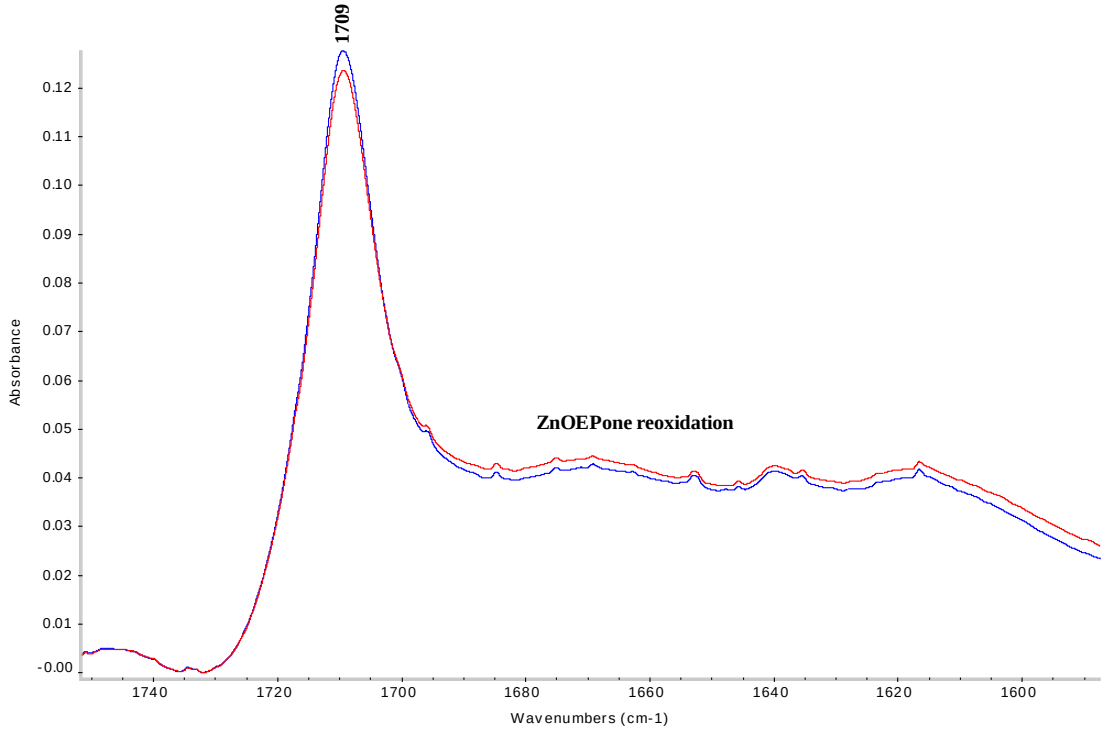

Figure 4-8. FTIR difference spectra of Zn-OEPone reoxidation with THF as reference 3.0 mM, in THF, 0.10 M TBAP by OTTLE spectroelectrochemistry, 32 scans

The reduction of ZnOEPdione was examined by infrared spectroelectrochemistry and similar to ZnOEPone, the metal complex displays bands in 1700 cm^{-1} region corresponding to the carbonyl groups (Figure 4-9). In this case the absorbance matching the carbonyl group appears as a broad band with two peaks at 1713 cm^{-1} and 1709 cm^{-1} in comparison with the Zn porphinone complex which displays a single absorption at 1709 cm^{-1} as expected. Upon reduction of porphinedione complex, the carbonyl peak shifts to a lower wavenumber at 1690 cm^{-1} (Figure 4-9). In the region 1500-1600 cm^{-1} the band at 1583 cm^{-1} shifted to 1585 cm^{-1}, while 1560 cm^{-1} increased intensity. The presence of the isosbestic points during the reduction indicates that no intermediates or significant decomposition of product occurred. Further investigation by computational calculation method or porphyrin labeling would be necessary for an accurate assignment of this band.

A comparison of the FTIR results obtained upon reduction of the zinc porphinone and porphinedione is given in the Table 4-4. A large carbonyl shift for ZnOEPone complex (47 cm^{-1}) was observed, while ZnOEPdione was smaller (23 cm^{-1}). It can be also observed that the carbonyl peak of porphinedione is broad due to the presence of two C=O groups in the molecule and for this reason there are two peaks at 1713 cm^{-1} and 1709 cm^{-1}. The IR peaks analysis of both zinc complexes in the porphyrin region reveals new peak formation for porphinone complex and only an increase in intensity and a small shift for porphinedione complex. In depth analysis of these peaks like porphyrin labeling or theoretical calculations could provide supplementary details about the coupling of carbonyl vibrations with the porphyrin vibrations. Upon reoxidation the carbonyl band was regenerated but not completely recovered due to the short electrolysis time

(Figure 4-10). Isosbestic points were also observed during the reoxidation indicating only two species (ZnOEPdione/ZnOEPdione^{-}) were present.

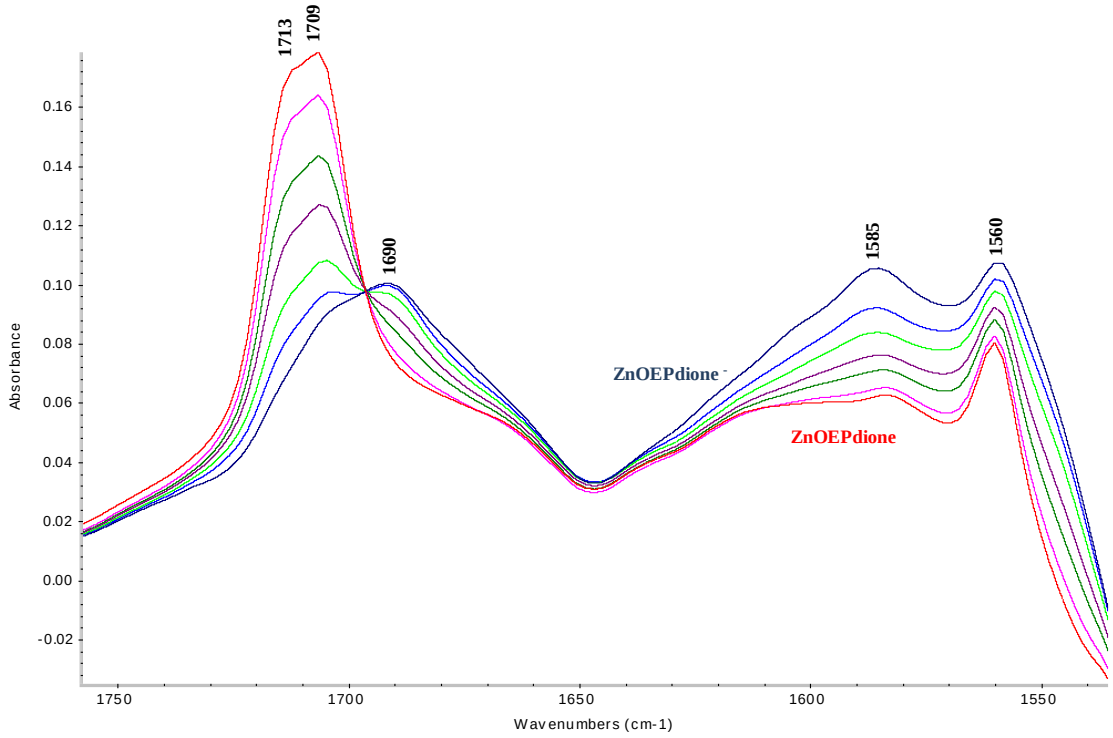

Figure 4-9.FTIR spectra of Zn-OEPdione with THF as reference 3.0 mM, in THF, 0.10 M TBAP by OTTLE spectroelectrochemistry, 32 scans

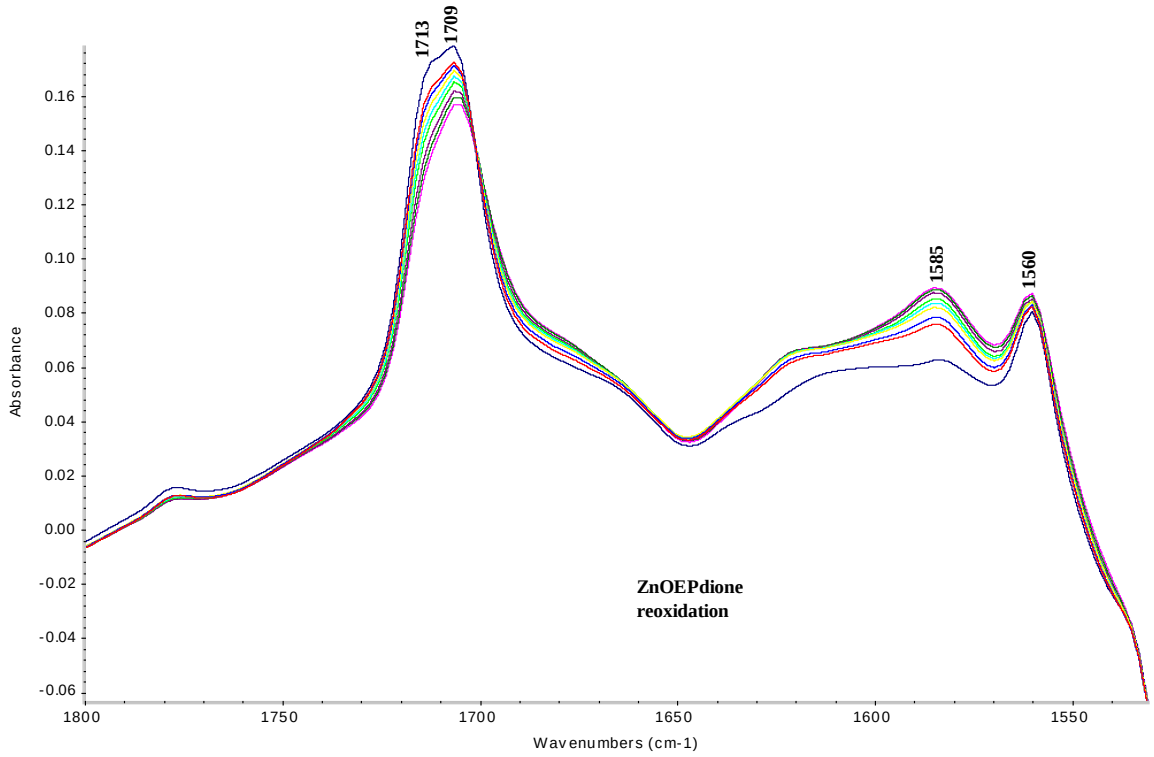

Figure 4-10. FTIR spectra of Zn-OEPdione with THF as reference 3.0 mM, in THF, 0.10 M TBAP by OTTLE spectroelectrochemistry, 32 scans

4.4. Conclusions

The reduction potential of ZnOEPone and ZnOEPdione are parallel with the findings of previous literature for H_2OEPone and H_2OEPdione of which reduction potentials decrease with the addition of a second carbonyl in the molecule. The sharp decrease in the Soret band and the appearance of a broadening band in the UV and visible region was the typical indication for a π anion formation.

The shift in the carbonyl band of 47 cm^{-1} for ZnOEPone compares with the shift of 32 cm^{-1} for FeOEPone and 33 cm^{-1} for CoOEPone. The latter two are thought to be metal centered reductions. Previous work by Wei showed a 38 cm^{-1} decrease in the νC=O

for H_2OEPone and new bands at 1551 and 1529 cm^{-1}. These are similar to ZnOEPone$^-$. For ZnOEPdione, the decrease in the νC=O is less but there was considerable broadening of the band. The smaller decrease may be due to increased delocalization of the electron density over two carbonyl groups. The shift in the carbonyl bond is smaller than expected.

Various studies of porphyrin complexes show the electron addition process can occur at the metal or on the macrocycle. In this particular case the electron addition is expected to occur at the macrocycle orbital because zinc is not redox active in the potential range utilized in our experiments. It was shown previously that ZnOEPone undergoes one-electron reduction at the macrocycle to generate a stable Zn(OEPone)$^-$ complex as revealed by UV-visible spectroscopy. Broad bands typical of π-anion radicals were observed for Zn(P)$^-$. The carbonyl band decreases significantly upon reduction, indicating substantial reduction of the macrocycle. ZnOEPdione reduction potential was -1.09 V which was expected taking into account that the dione complex has two electron withdrawing groups so it should reduce at a more positive potential. This means that a second carbonyl addition into the system influences the reduction potential. The FT-IR spectroelectrochemical data of porphinone and porphinedione show the carbonyl peak shift from 1709 cm^{-1} to 1662 cm^{-1} for the former compound, and from 1713 cm^{-1} to 1690 cm^{-1} for the latest, which is an unexpected value for a porphyrin centered process. A comparison of the FTIR results obtained upon reduction of the two zinc complexes is given in the Table 4-4 of this section. The carbonyl shift for ZnOEPone complex is 47 cm^{-1} and 23 cm^{-1} for ZnOEPdione. A comparison of ZnOEPdione infrared results with those of FeOEPdione data reveals that the carbonyl band for the zinc complex shifts to a

higher energy than for the iron complex. The two peaks at 1671 and 1655 cm^{-1} of medium intensity present in iron complex spectrum are absent in ZnOEPdione which displays new band at 1690 cm^{-1}.

Table 4-1.Cyclic voltammetry data for Zinc porphinone and Zinc porphinedione reduction

Compound	**Ipf, µA**	**Ipr, µA**	**Ipr/ipf**	**Epf, V**	**Epr, V**	**E1/2, V vs Ag/AgCl**
Zn-OEP	5.752	5.644	0.98	-1.78	-1.60	-1.69
Zn-OEPone	6.509	6.006	0.92	-1.34	-1.22	-1.28
Zn-OEPdione	2.334	2.964	1.26	-1.2	-0.99	-1.09

Solution conditions: Pt electrode, 0.80 mM in THF, with 0.10 M TBAP

Table 4-2.Comparison of the reduction potentials of free-base porphyrins and ZnOEP, Zn-OEPone and Zn-OEPdione

Compounds	Reduction potentials (V) E1/2	References
H_2OEP	-1.60	[180]
H_2-oxoOEC	-1.45	[180]
H_2TPP	-1.15	[182]
ZnOEP	-1.58	this work
Zn-OEPone	-1.17	this work
ZnTPP	-1.33	62
Zn-OEPdione	-0.98	this work

* Data were obtained vs. Ag/AgCl reference electrode. From comparion our valueas with literature values, our reference electrode was 0.11 V positive of the SCE values. Data in the table are versus SCE.

Table 4-3.UV-visible spectroelectrochemical results obtained during the reduction of Zn complexes, 0.80 mM in THF, with 0.10 M TBAP

Compounds	**Solvent**	**UV-visible spectra (nm)**	**Reference**
ZnOEP	THF	408, 538, 577	this work
ZnOEP $^{-}$	THF	451, 600-700	this work
ZnTPP	THF	455	62
ZnTPP^{-}	THF	680, 710, 790, 905	62
Zn-OEPone	THF	420, 620	this work
ZnOEP one^{-}	THF	450	this work
Zn-OEPdione	THF	390, 414, 440, 624	this work
Zn-OEPdione^{-}	THF	482, 688	this work

Table 4-4.Infrared spectroelectrochemistry of metal porphinones and porphinediones

Compound	**IR absorption signals, [cm^{-1}]**	**Reference**
ZnOEPone	1709, 1560	this work
Zn(OEPone) $^{-}$	1662, 1550, 1540	this work
Zn(OEPdione)	1713, 1707, 1583, 1560	this work
Zn(OEPdione)$^{-}$	1690, 1585, 1560	this work
Fe(III)OEPone	1719, 1563, 1536	174
Fe(II)OEPone	1703, 1550, 1530	174
Fe(OEPone)$^{-}$	1672, 1609, 1578, 1548	174
Fe(III)OEPdione	1717, 1580, 1560, 1543,1526	174
Fe(II)OEPdione	1703, 1547, 1524	174
Fe(OEPdione)$^{-}$	1671, 1655, 1648, 1640, 1593, 1562, 1535	174

Chapter 5 SPECTROELECTROCHEMICAL STUDIES OF MANGANESE PORPHINONE COMPLEXES

The structures of manganese octaethylporphinone and manganese octaethylporphinedione are shown in Scheme III. The carbonyl group on the porphyrin ring absorbs in the infrared region. The interaction between the central metal and the porphyrin ring, as well as reduction in the ring can be monitored by the shift in the carbonyl band in the infrared region.

Manganese porphyrin complexes have a significant importance because of their unique absorption spectra and mostly for their utility as model compounds for a general understanding of more complex metalloporphyrin spectra and structure. Previous studies of the reduction of manganese porphyrin complexes have indicated that manganese(III) complexes are reduced to manganese(II), and then to manganese(II) anion radical[102,103].

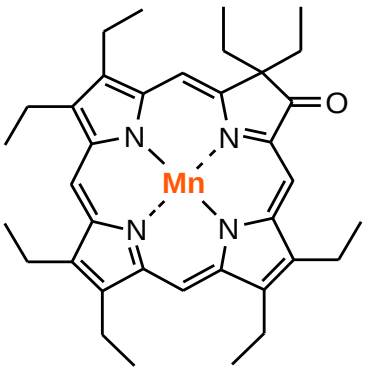

Manganese porphinone (MnOEPone)

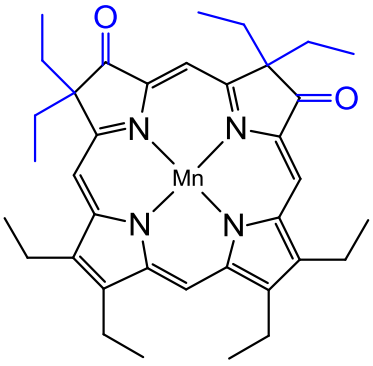

Manganese porphinedione (MnOEPdione)

Scheme III

In this chapter we report the electrochemical and spectroelectrochemical reduction of Mn(III)OEP, Mn(III)OEPone and Mn(III)OEPdione (Scheme III) in aprotic media. The complexes were analyzed by both cyclic voltammetry and UV-visible spectroelectrochemistry. The electron transfer processes were recorded at a platinum electrode in THF and 0.10 M TBAP.

5.1. Voltammetry of Manganese porphinone complexes

The reduction potentials of Mn(III)OEP, Mn(III)OEPone and Mn(III)OEPdione are presented in the Table 5-1. The $E_{1/2}$ value of Mn(III)OEPoneCl were observed at - 0.067 V and -1.11 V, and the peak to peak potential separation is greater than 58 mV (due to uncompensated solution resistance). The anodic to cathodic peak current ratio, i_{pc}/i_{pa} for the second reduction is 0.93 which indicates quasireversible electron transfer and stable reduction products. A typical voltammetric wave is shown in Figure 5-1. Cyclic voltammogram shows a peak at -0.7 V which might be due to surface effects.

Similar to Mn(III)OEPoneCl, Mn(III)OEPCl complex undergo two one- electron reductions (Figure 5-2). The first occurs at a potential of -0.29 V while the second process takes place at -1.27 V. The i_{pc}/i_{pa} ratio confirms a reversible reduction for the Mn(III)/Mn (II) (0.99) conversion and quasireversible process for Mn (II)/Mn (II)P^- conversion (0.93). In both cases an excess of Cl^- was added to ensure the presence of one type of axial ligand bonded to manganese(III). Without halide excess the reduction potential of the complex was shifted to a more negative potential due to changes in the reference electrode potential. The first reduction of Mn(III)OEPoneCl and

Mn(III)OEPCl illustrates that both processes occur at similar potentials while the second reduction process display less negative potential value for Mn(III)OEPoneCl because of the carbonyl group effect.

Mn(III)OEPdioneCl undergoes two one electron reductions at different scan rates. The compound display reversible and quasireversible reductions at -0.008 V and -1.48 V. The potential separation between the two processes is 1.4 V, which according to literature[43] suggests that they occur at different centers (metal vs porphyrin). The peak current ratio (i_{pc}/i_{pa}) was near unity for the first reduction and less than one for the second process suggesting a reversible and a quasireversible process respectively. The peak potential difference (E_{pa}-E_{pc}) for the first reduction was 0.10 V, broader than theory due to uncompensated resistance and the peak current increased linearly with $\nu^{1/2}$ at the scan rates investigated. This is an indication of diffusion controlled reversible one-electron transfer process (Figure 5-3).

A comparison of the first $E_{1/2}$ reduction potentials of Mn(III)OEPdioneCl with Mn(III)OEPoneCl and Mn(III)OEPCl shows that the metal reduction occurs at similar potential values for porphinone and porphinedione complexes and slightly less negative value was observed for the porphyrin complex. Introduction of the second carbonyl group in the molecule did not change significantly the reduction potential. In the case of the second reduction of manganese porphinedione, surprisingly the electron transfer occurs at a more negative potential than Mn(III)OEPoneCl and even Mn(III)OEPCl.

A comparison of these results with the ones previously obtained in our laboratory on iron porphyrin complexes shows a different order of reduction. The results reveal the ease of reduction in iron porphyrin series follows the order: Fe(2,4-OEPdione)Cl was

reduced easier than Fe(OEPone)Cl and Fe(OEP)Cl[180] while for manganese series, porphinedione is harder to be reduced than octaethylporphyrin and even more difficult when compared with porphinone.

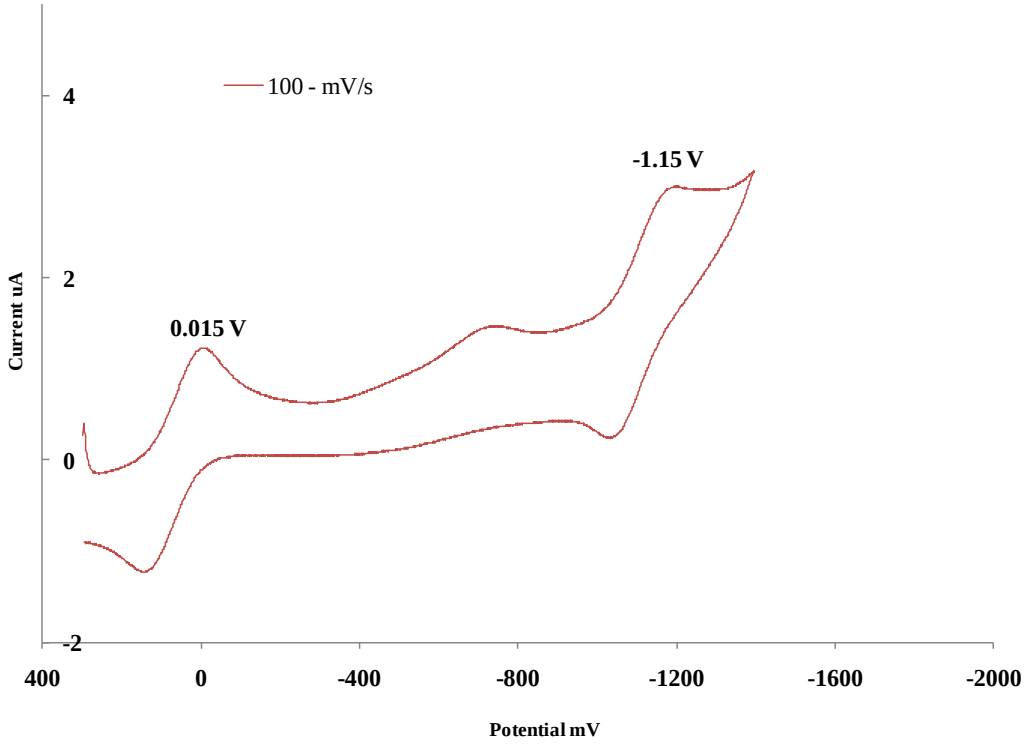

Figure 5-1. Cyclic voltammogram of Mn(III)OEPoneCl reduction. Solution conditions: 0.80 mM in THF, with 0.10 M TBAP electrolyte, WE: platinum, RE: Ag/AgCl

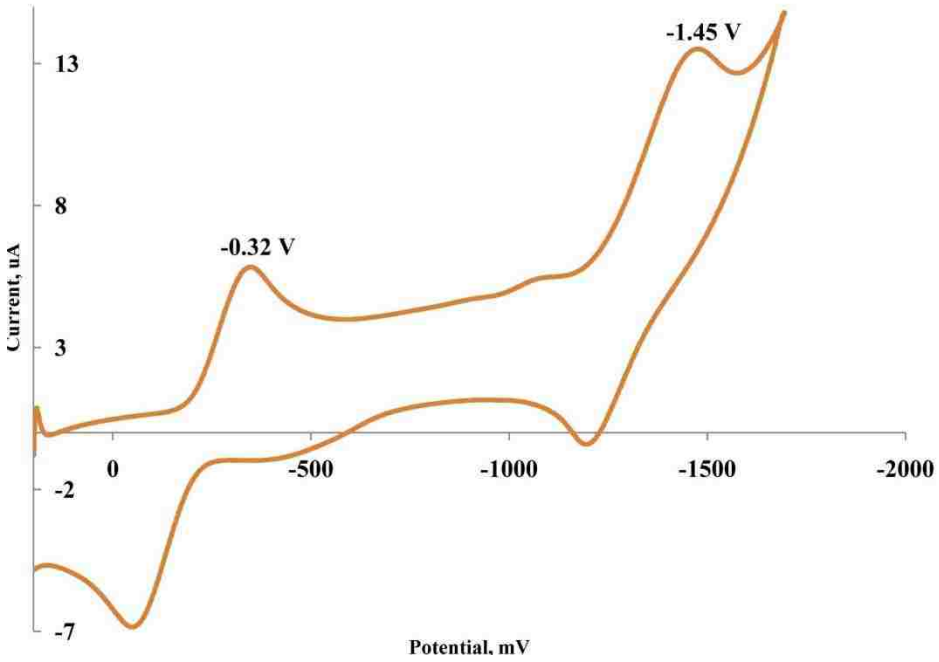

Figure 5-2. Cyclic voltammogram of Mn(III)OEPCl reduction. Solution conditions: 0.80 mM in THF, with 0.10 M TBAP electrolyte, WE: platinum, RE: Ag/AgCl

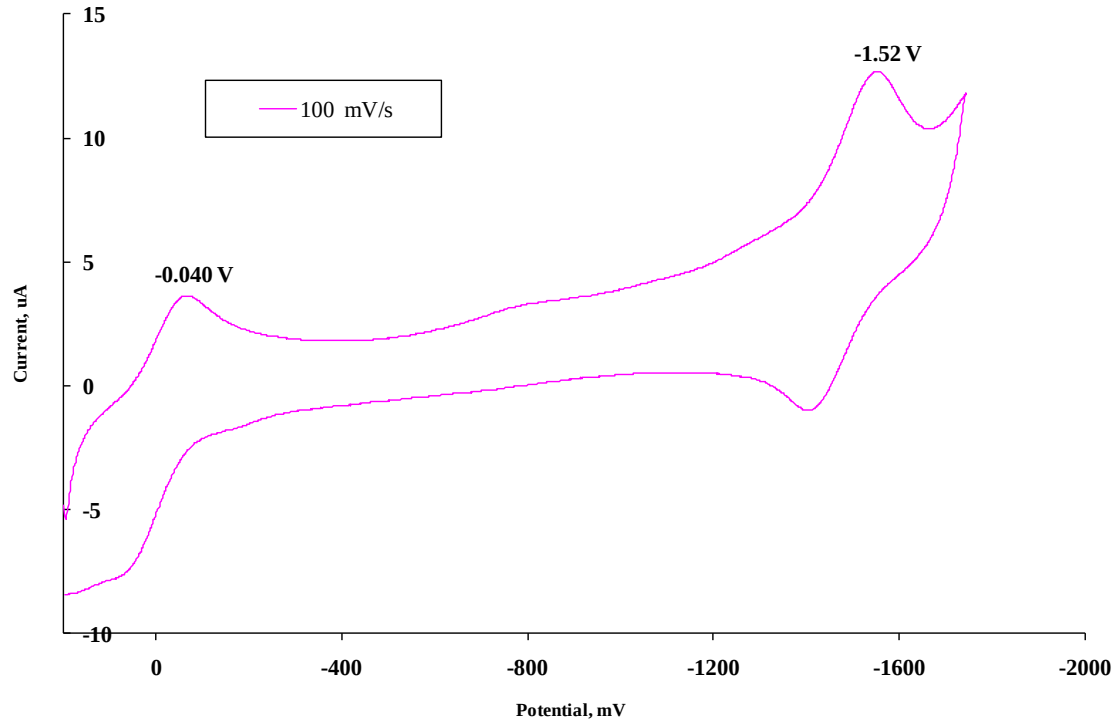

Figure 5-3. Cyclic voltammogram of Mn(III)OEPdioneCl reduction. Solution conditions: 0.80 mM in THF, with 0.10 M TBAP electrolyte, WE: platinum, RE: Ag/AgCl

5.2. Spectroelectrochemistry of Manganese porphinone complexes

Cyclic voltammetry technique provides insufficient insight to assure a certain process pathway (metal centered or porphyrin centered process); consequently the voltammetry results are supported with UV-visible, and IR spectroscopic data of the reduced product.

The electro-reduction of Mn(III)OEPoneCl, Mn(III)OEPdioneCl and Mn(III)OEPCl was analyzed by spectroelectrochemistry in order to characterize their reduced products. The electro-reduction process was performed in an OTTLE cell in THF containing 0.10 M TBAP and the changes in the visible spectra were recorded by controlled potential electrolysis.

Manganese(III)porphyrin complexes usually exhibit multiple Soret bands which arise from the interaction of the Mn orbitals and the porphyrin π*- orbital. Porphyrin (π) – metal (dπ) charge-transfer transitions are similar to porphyrin (π- π*) transitions. When the π-d charge-transfer and the π- π* Soret transitions occur at equivalent energies, they produce a "split Soret". The band at 600 nm is assigned to a CT transition π-dπ, the band at 550 nm is due to the ligand transitions π- π* and it can be related to a usual Q band[87].

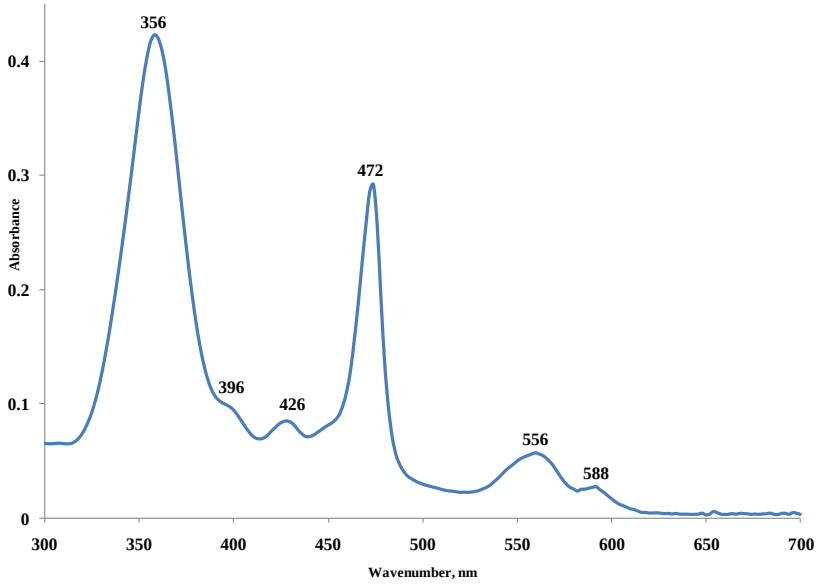

Figure 5-4. UV-Visible spectrum of Mn(III)OEPCl

The first reduction of Mn(III)OEPCl, is shown in Figure 5-6. The split Soret band (364-464 nm) decreases in intensity during the electrolytic process while a new band appears at 418 nm which corresponds to the Soret band of Mn(II) species. A further one electron reduction of the manganese octaethylporphyrin complex led to band broadening in the visible region and a featureless Q band (Figure 5-8). A comparison of the spectroelectrochemical results obtained from Mn(III)OEPCl and Mn(III)OEPoneCl with Mn(III)TPPCl reveals similarities in their spectra: split Soret band for Mn^{3+} in MnTPP shifts to higher wavenumber to give a "normal" Soret band in a Mn^{II}TPP complex.

The UV-visible spectrum of manganese octaethylporphinone illustrates the split Soret band at 364 nm and 478 nm and a Q band a 642 nm. The split B band characteristic for manganese complex decreases in intensity during electrolysis. Simultaneously a peak at 440 nm appears and the Q band at 642 nm shifts towards a lower wavelength (Figure 5-5). The isosbestic points indicate direct conversion to the manganous complex without intermediates. According to previous literature[105], the resulting spectrum

indicates a Mn(III)/Mn(II) reduction. The typical Mn(III) spectrum was regenerated by reoxidation, indicating that the one-electron reduction product was stable on the time scale of this experiment. This suggest that the compound passes from a Mn^{3+} state where there is a strong interaction between metal and the four pyrrole N which is relieved by back donation from metal to ligand to a Mn^{2+} state where metal-porphyrin π bonding is not favored and as a result the spectra of Mn(II) is "normal".

The second reduction of Mn(III)OEPone results in a red shift of the Soret band from 440 nm to 488 nm and the Q band at 624 nm becomes featureless (Figure 5-7). Band broadening is observed within visible region 600-700 nm suggesting formation of a π anion radical. The isosbestic points at 382, 426 and 624 nm indicate that no intermediates are formed during the electrolysis. The band broadening in the 450-550 nm and 700-900 nm regions suggests that the reduction process occurs at the macrocycle. Typical Mn(III) porphyrin spectrum resulted from the reoxidation of this second reduction product confirming the stability of the compound during experimental time scale.

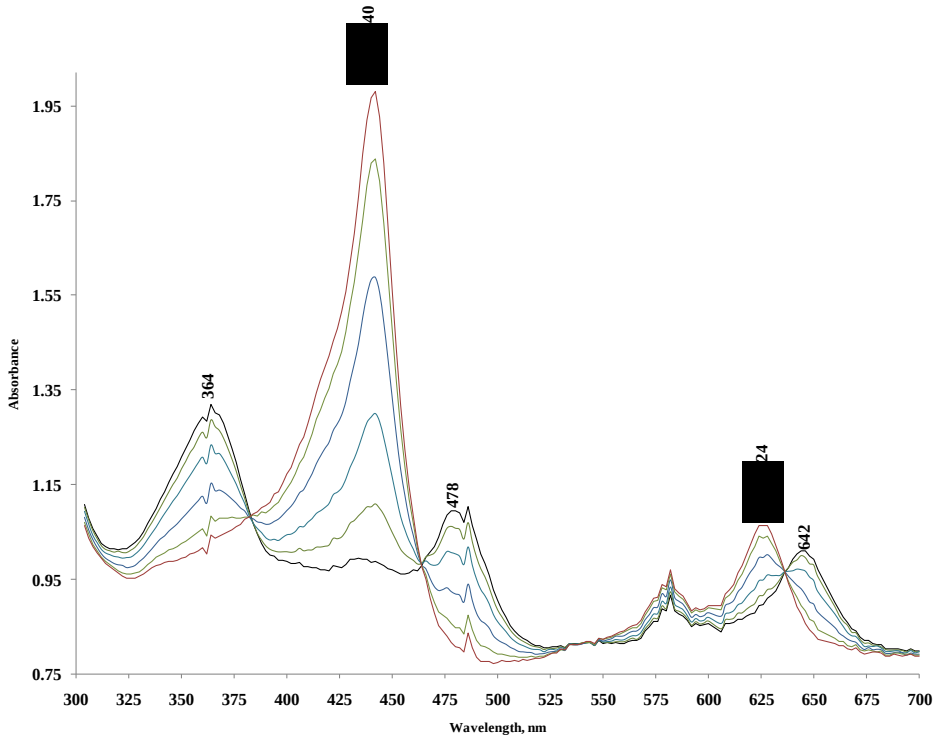

Figure 5-5. Thin-layer visible spectroelectrochemistry obtained during the reduction of Mn(III)OEPoneCl 0.80 mM in THF, with 0.10 M TBAP, potential region 0.4 V to -0.6 V

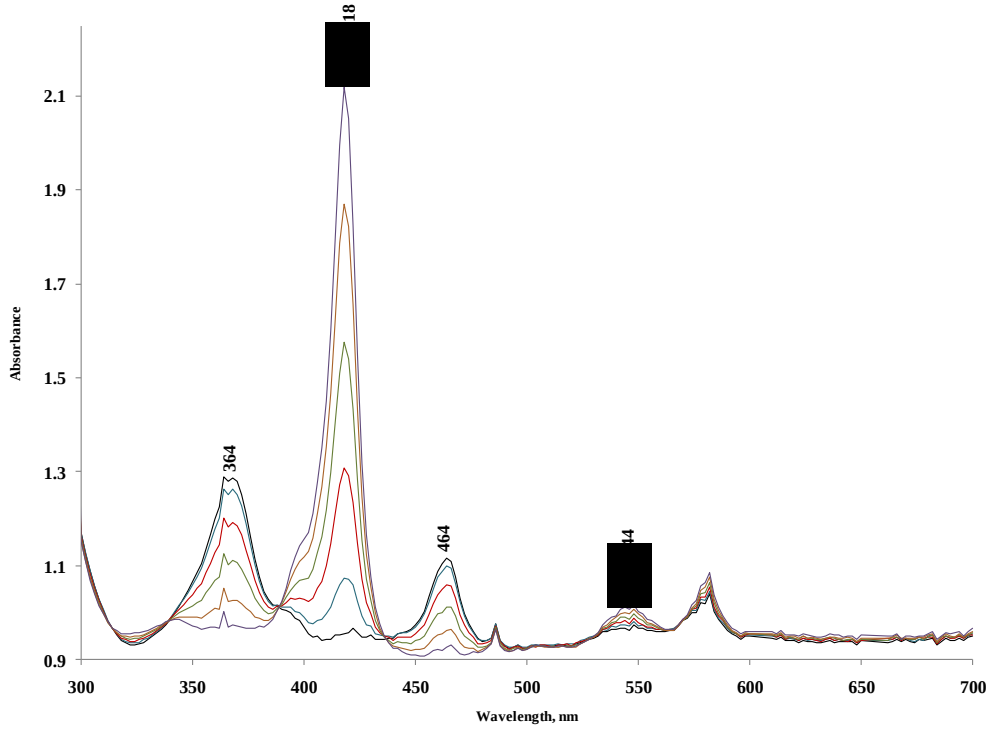

Figure 5-6. Thin-layer visible spectroelectrochemistry obtained during the reduction of Mn(III)OEPCl 0.80 mM in THF, with 0.10 M TBAP, potential region 0.4 V to -0.6 V

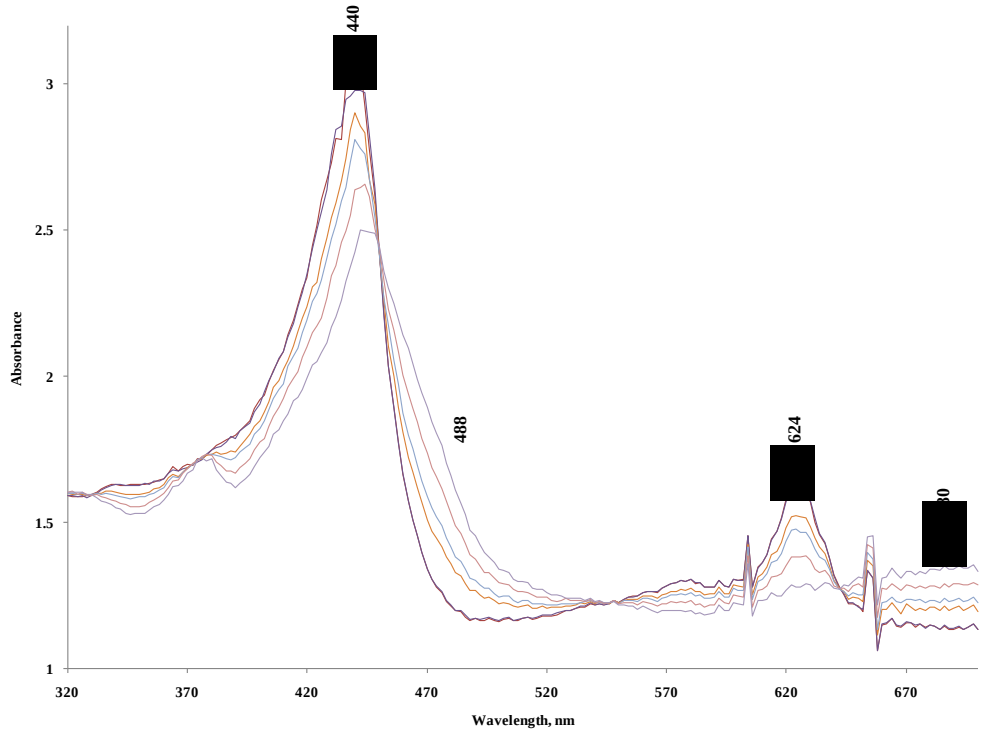

Figure 5-7. Thin-layer visible spectroelectrochemistry obtained during the reduction of Mn(II)OEPone 0.80 m<u>M</u> in THF, with 0.10 <u>M</u> TBAP, potential region -0.6 V to -1.5 V

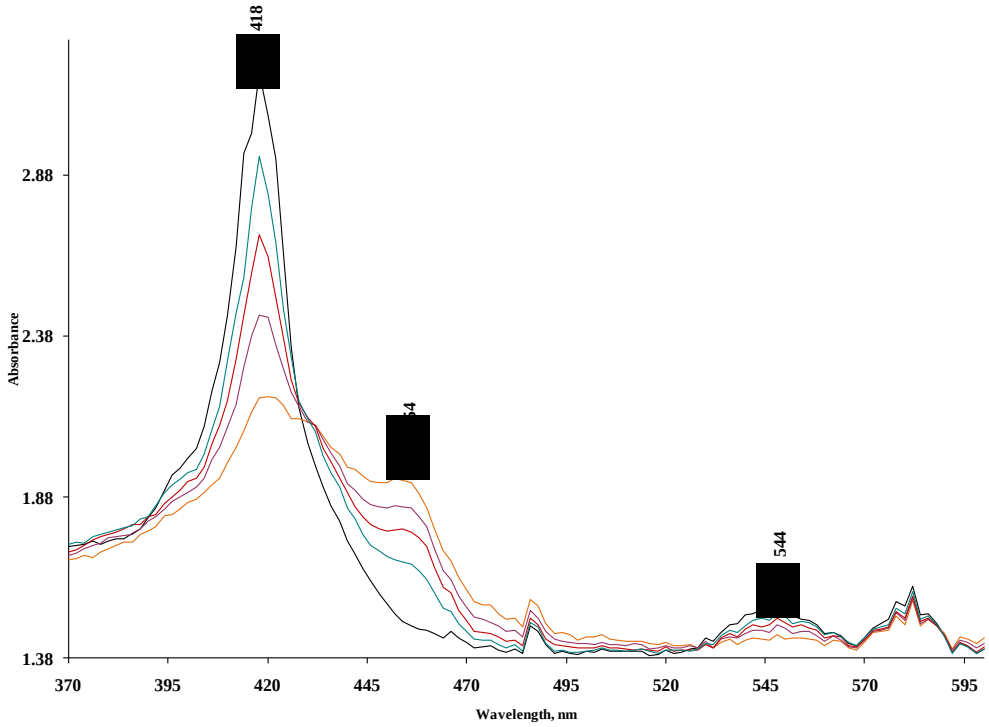

Figure 5-8. Thin-layer visible spectroelectrochemistry obtained during the reduction of Mn(II)OEP 0.80 m<u>M</u> in THF, with 0.10 <u>M</u> TBAP, potential region -0.6 V to -1.5 V

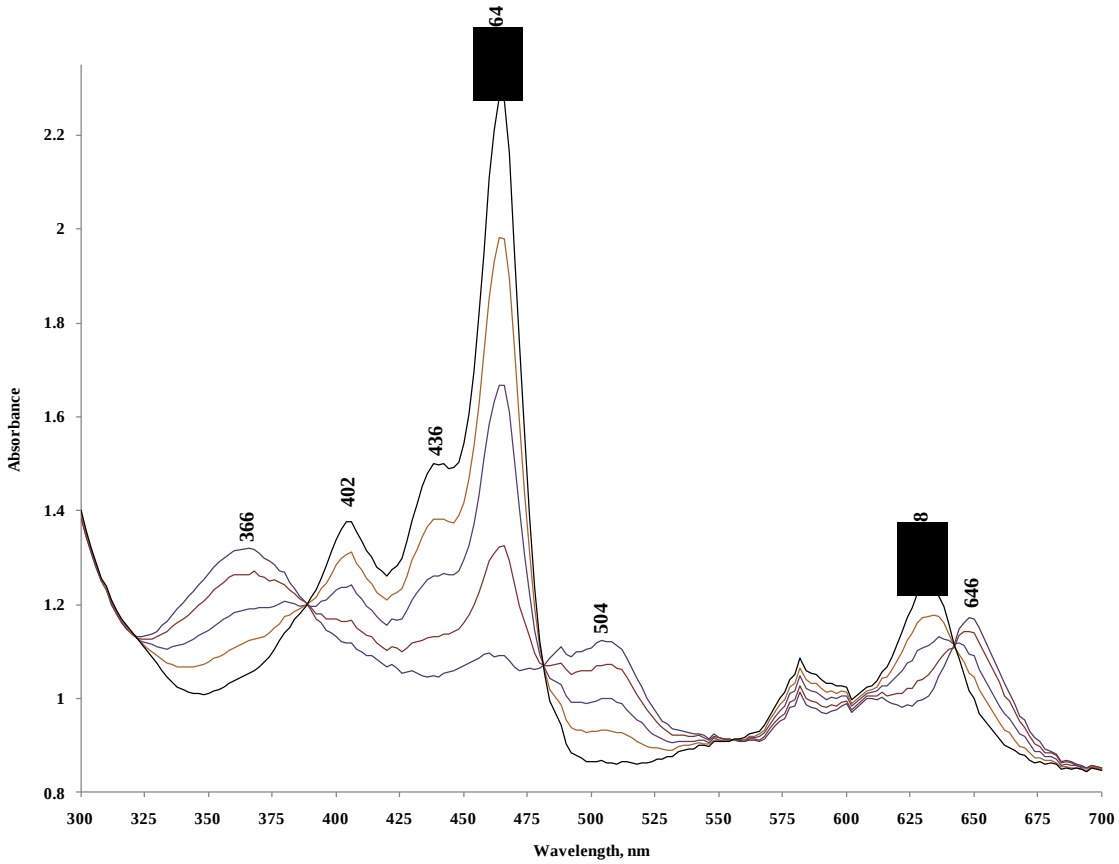

Figure 5-9. Thin-layer visible spectroelectrochemistry obtained during the reduction of Mn(III)OEPdioneCl 0.80 mM in THF, with 0.10 M TBAP, potential region 0.2 V to -0.6 V

The UV-visible spectral changes during the addition of a first electron to Mn(III)OEPdioneCl show a decrease in the intensity of the Soret band and new absorptions appear at 402, 436 and 464 nm. In the visible region the Q band records a blue shift with the peak at 628 nm. The absence of band broadening in the region of 700-800 nm and the presence of Q band after reduction is an indication of a metal centered process according to literature and previously discussed results. The presence of the isosbestic points suggests that intermediates are not produced (Figure 5-9).

The electroreduction of the Mn(II)OEPdione following the one electron addition to Mn(III)OEPdione, is shown in the Figure 5-10. The spectral features of the reduced

species are characterized by sharp decrease in Soret and Q bands. Band broadening is observed in both UV and visible region indicating the formation of a π anion radical, suggesting a ring-centered process. The process is reversible and by reoxidation of this species the Mn(II)OEPdione is recovered, this behavior indicating that intermediates were not formed.

The features observed on Fe porphyrins complexes upon first reduction process illustrates a red shift in the Soret band indicating Fe(II) species formation and a significant change in Soret and visible region upon addition of the second electron. A brief comparison of manganese complexes UV-visible spectra with the previous results published from our laboratory on iron porphyrin compounds indicates similar changes between the two metal complexes.

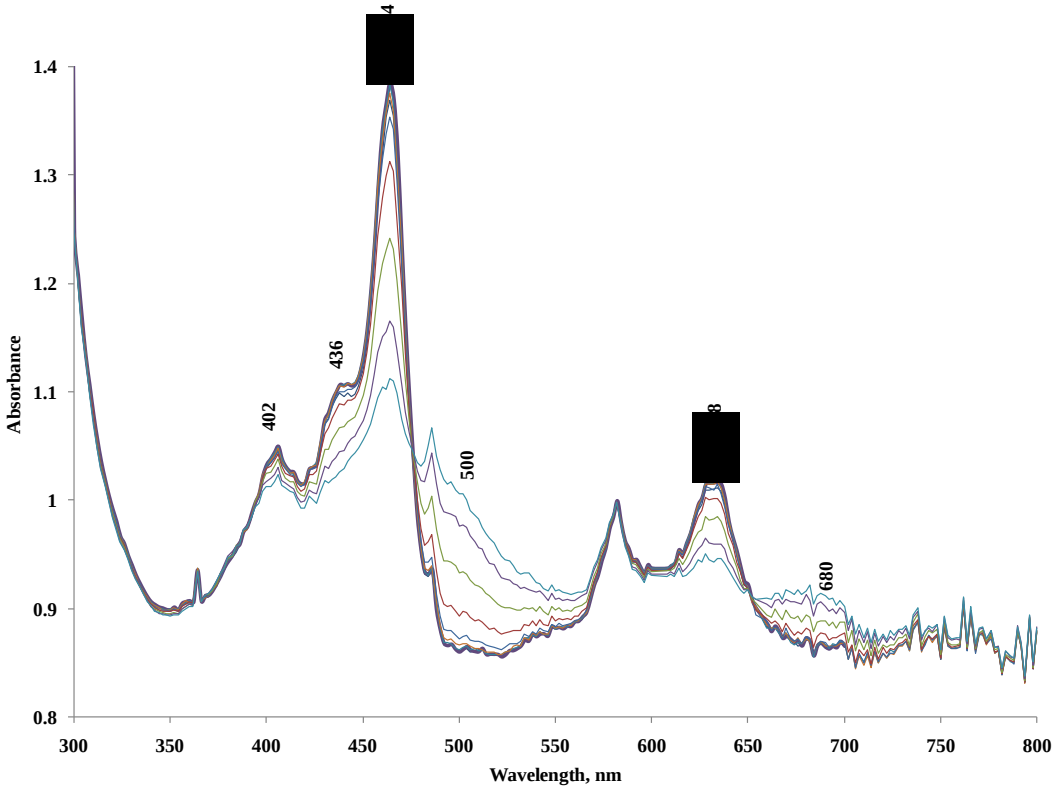

Figure 5-10. Thin-layer visible spectroelectrochemistry obtained during the reduction of Mn(II)OEPdione 0.80 mM in THF, with 0.10 M TBAP, potential region -0.6 V to -1.6 V

5.3. Thin layer FTIR of Manganese porphinone complexes

According to cyclic voltammetry and UV-visible results the electroreduction process that occurs between 0 and -1.5 V indicates two processes: one occurs at the metal center, another occurs at the porphyrin center. In order to confirm these results manganese complexes were assessed by thin-layer FTIR spectroscopic technique.

The FT-IR spectrum of Mn(III)-OEPone shows the carbonyl vibration at 1721 cm^{-1} (Figure 5-11). The C=O band shifted at 1706 cm^{-1} (15 cm^{-1}) upon reduction in anhydrous THF while the vibration band at 1578 cm^{-1} decreases in absorbance. This shift in carbonyl is similar to the shift observed for the Fe(III)-OEPone reduction (16 cm^{-1}) where the carbonyl vibration is weakened due to back-bonding from metal to porphinone. Upon reoxidation of the electrolyzed species (Figure 5-12) the C=O band at 1706 cm^{-1} returns to its original position indicating a stable compound, and the isosbestic points at 1780 and 1713 cm^{-1} suggesting that no intermediates were formed.

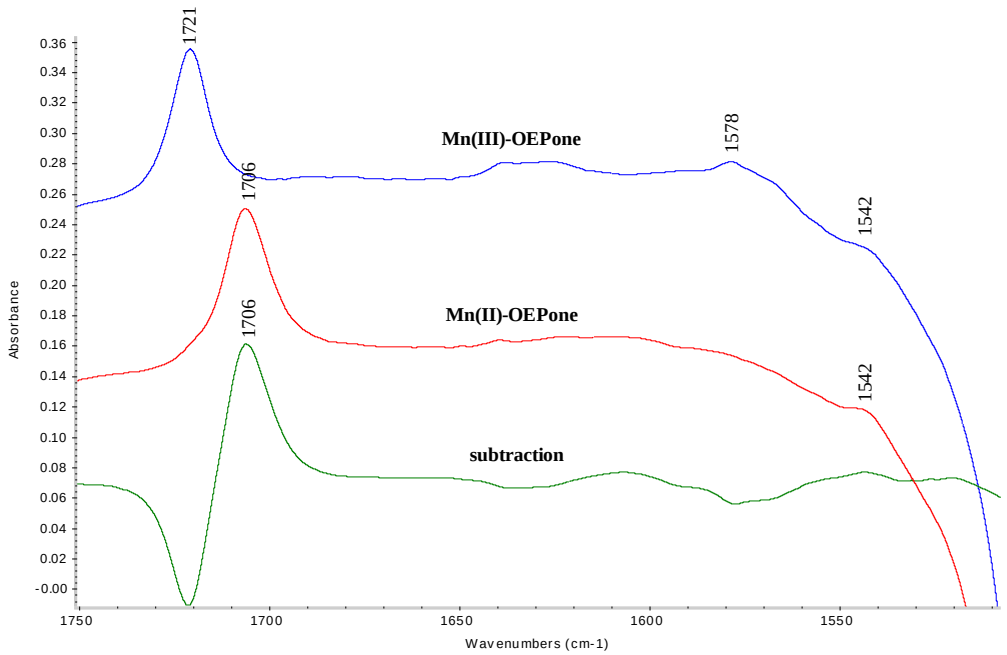

Figure 5-11. FTIR reduction spectra of Mn(III)-OEPoneCl 3.0 m<u>M</u>, in THF, 0.10 <u>M</u> TBAP by OTTLE spectroelectrochemistry, 32 scans

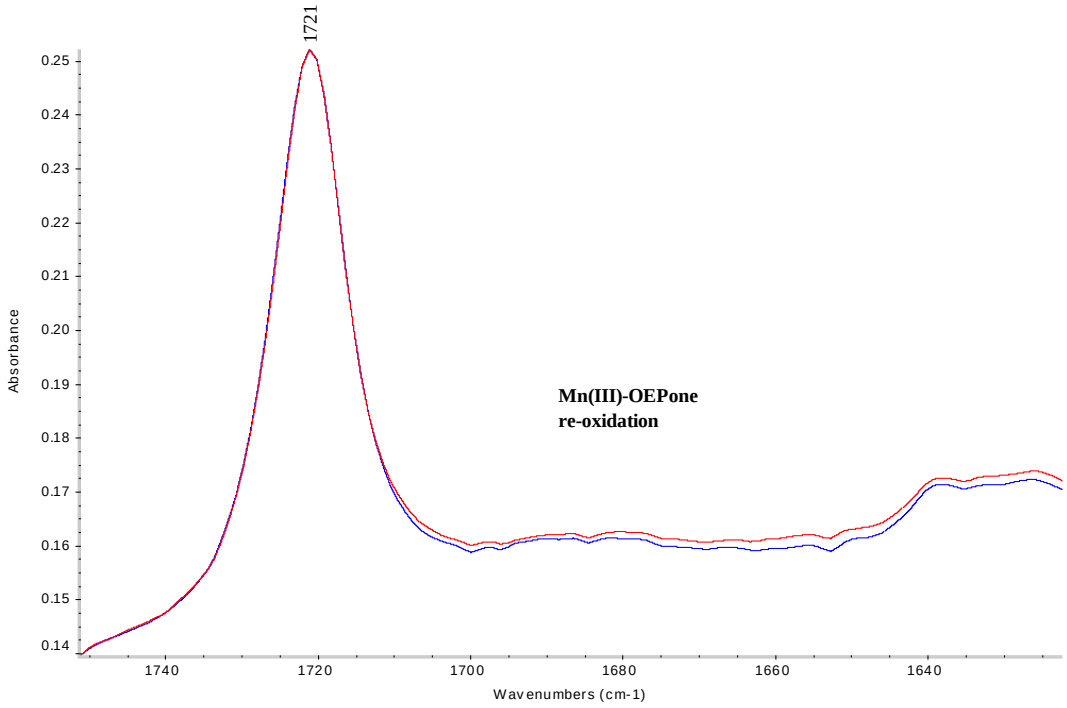

Figure 5-12. FTIR reoxidation spectra of Mn(III)OEPoneCl 3.0 m<u>M</u>, in THF, 0.10 <u>M</u> TBAP by OTTLE spectroelectrochemistry

Thin-layer FTIR spectroscopic data collected during the second electroreduction process of Mn(III)OEPone show the carbonyl shift from 1706 cm^{-1} to 1657 cm^{-1} (Figure 5-13). A shift of 49 cm^{-1} was observed and corresponded to a larger shift when compared to the one observed for the first reduction process of manganese porphinone. This shift is larger than that shift in the carbonyl band when Fe(II)OEPone was reduced (31 cm^{-1}). This is consistent with a radical anion formation. New bands are observed at 1543 cm^{-1}, 1538 cm^{-1} and 1530 cm^{-1}. Reoxidation of Mn(II)OEPone^{-} species result in typical spectra of Mn(III)OEPone (Figure 5-14). The shift in the carbonyl bond for ZnOEPone (47 cm^{-1}) is similar to the shift of MnOEPone (45 cm^{-1}) but larger than CoOEPone (33 cm^{-1}). In addition, the reduced species of MnOEPone displays two peaks in the porphyrin region at 1538 and 1530 cm^{-1} which are observed in ZnOEpone as well at 1550 and 1540 cm^{-1}. Therefore the reduction site in these compounds is the same.

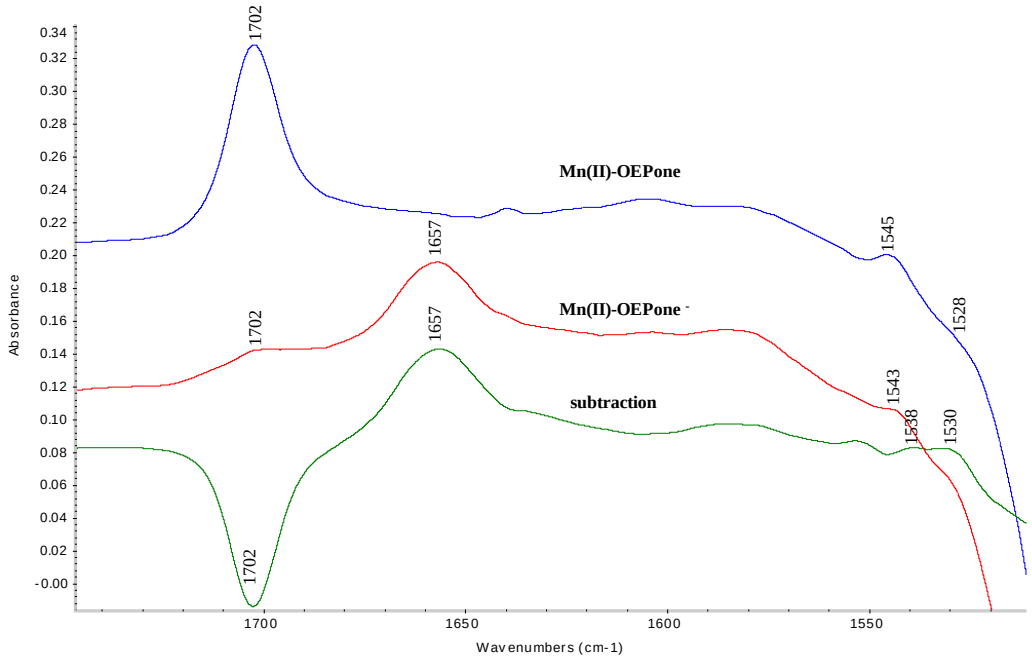

Figure 5-13. FTIR reduction spectra of Mn(II)-OEPoneCl 3.0 m<u>M</u>, in THF, 0.10 <u>M</u> TBAP by OTTLE spectroelectrochemistry, 32 scans

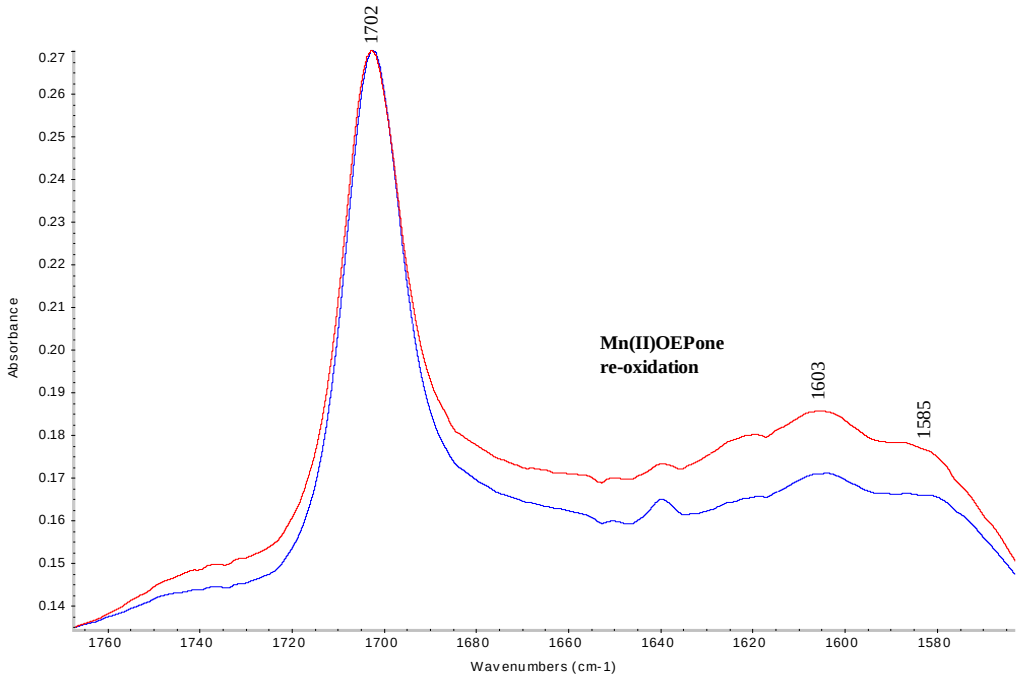

Figure 5-14. FTIR reoxidation spectra of Mn(II)-OEPoneCl 3.0 mM, in THF, 0.10 M TBAP by OTTLE spectroelectrochemistry.

The electrochemical results of Mn(III)OEPdioneCl reveals two one electron transfer processes that takes place at 0.0 V and -1.8 V. According to UV-visible results the former process is metal based while the latter is porphinone based process. In FT-IR analysis the two electron transfers were investigated separately as a function of reduction potential, primarily by the shift in the carbonyl band. The νC=O for porphinedione complex from 1725 cm^{-1} is shifted to 1706 cm^{-1} during the first reduction while the absorptions at 1595 cm^{-1} and 1572 cm^{-1} become featureless (Figure 5-15). Similar to Fe(III)OEPdioneCl first reduction had a small shift in carbonyl band (19 cm^{-1}) indicating a weakened C=O bond. Sweeping the potential from -0.6 V to -1.8 V for the second reduction process the carbonyl peak shifts from 1706 cm^{-1} to 1693 cm^{-1} a decrease of 13 cm^{-1} (Figure 5-16). New bands are observed at 1608 cm^{-1}, 1582 cm^{-1} and 1555 cm^{-1}. The addition of the second electron in the system leads to further increase in electron

density on the porphyrin but is not consistent with a radical anion formation. These shifts are less than those observed for Fe^{II}(OEPdione) (32 cm^{-1}) and Co^{II}(OEPdione) (28 cm^{-1}). This may indicate that Mn(OEPdione)$^-$ may be different from Mn(OEP)$^-$ and Mn(OEPone)$^-$. While the visible, infrared and voltammetry for Mn(OEP)$^-$ and Mn(OEPone)$^-$ are consistant with a π-anion radical, Mn(OEPdione)$^-$ is not and may be a Mn^I complex. In particular, the $E_{1/2}$ for Mn(OEPdione)/Mn(OEPdione)$^-$ is negative of Mn(OEPone)/Mn(OEPone)$^-$ and close to Mn(OEP)/Mn(OEP)$^-$. While a broad band was observed between 620- 700 nm for Mn(OEPone)$^-$, the band for Mn(OEPdione)$^-$ is sharper. Finally, the FTIR shift upon reduction is smaller.

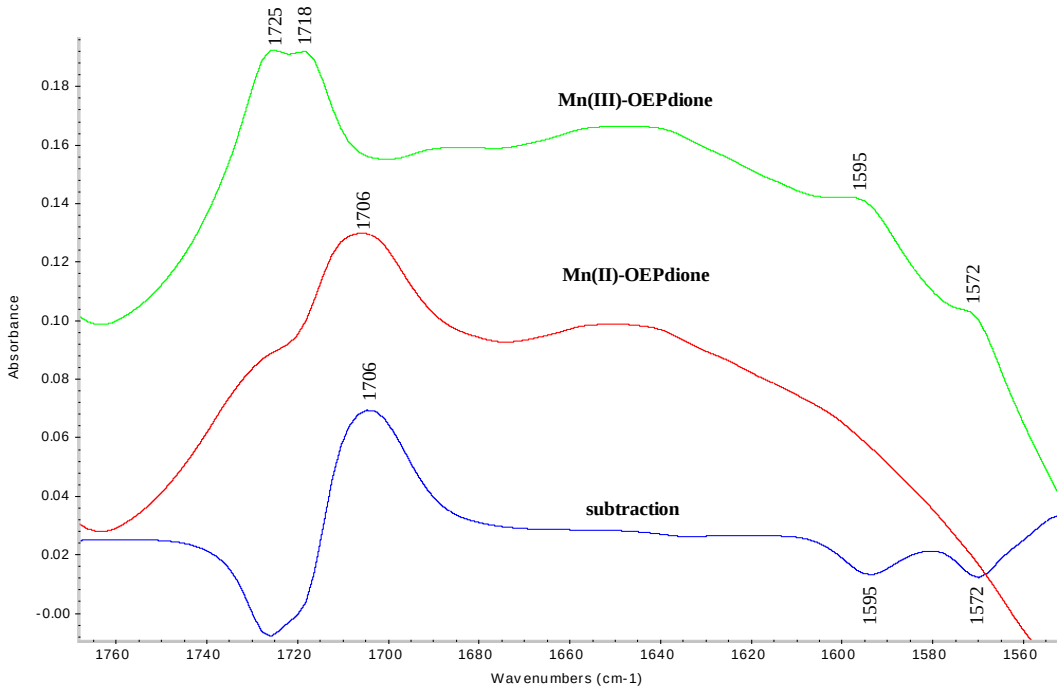

Figure 5-15. FTIR reduction spectra of Mn(III)OEPdioneCl 3.0 mM, in THF, 0.10 M TBAP by OTTLE spectroelectrochemistry, 32 scans

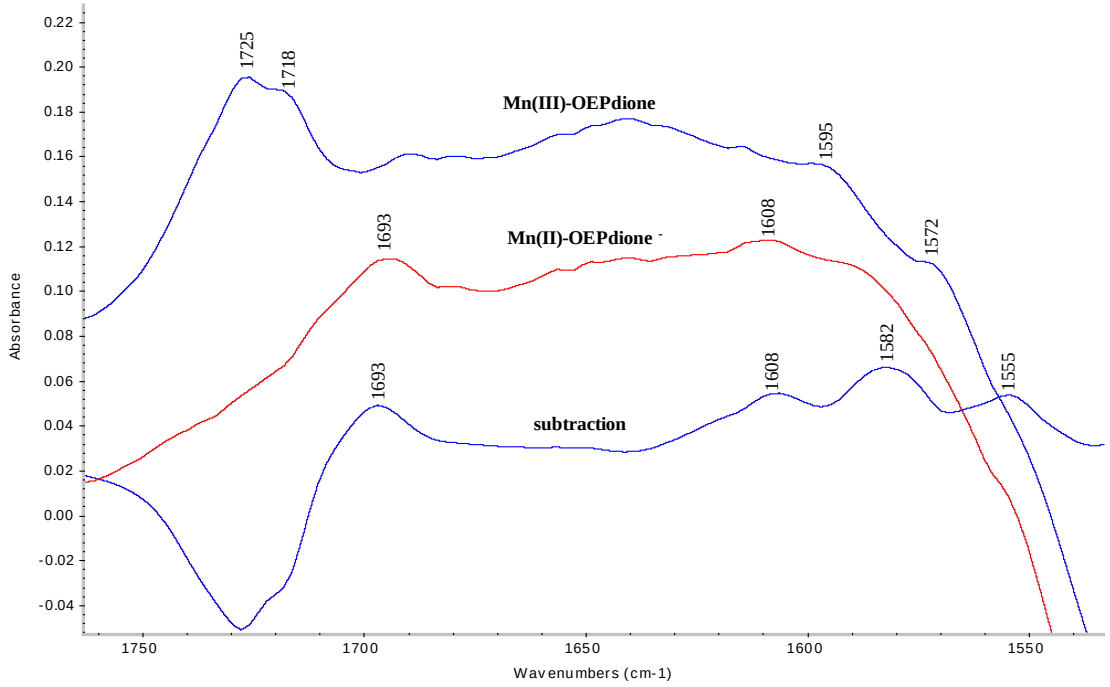

Figure 5-16. FTIR reduction spectra of Mn(II)OEPdione 3.0 mM, in THF, 0.10 M TBAP by OTTLE spectroelectrochemistry, 32 scans

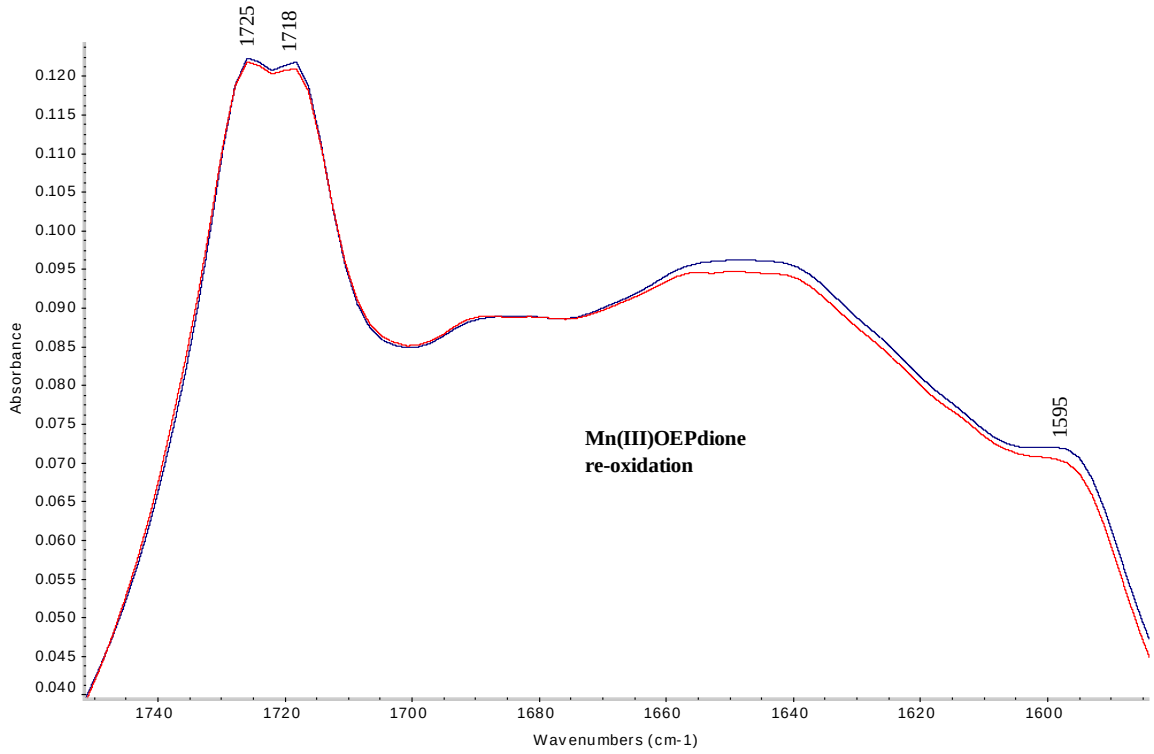

Figure 5-17. FTIR reoxidation spectra of Mn(III)-OEPdione 3.0 mM, in THF, 0.10 M TBAP by OTTLE spectroelectrochemistry.

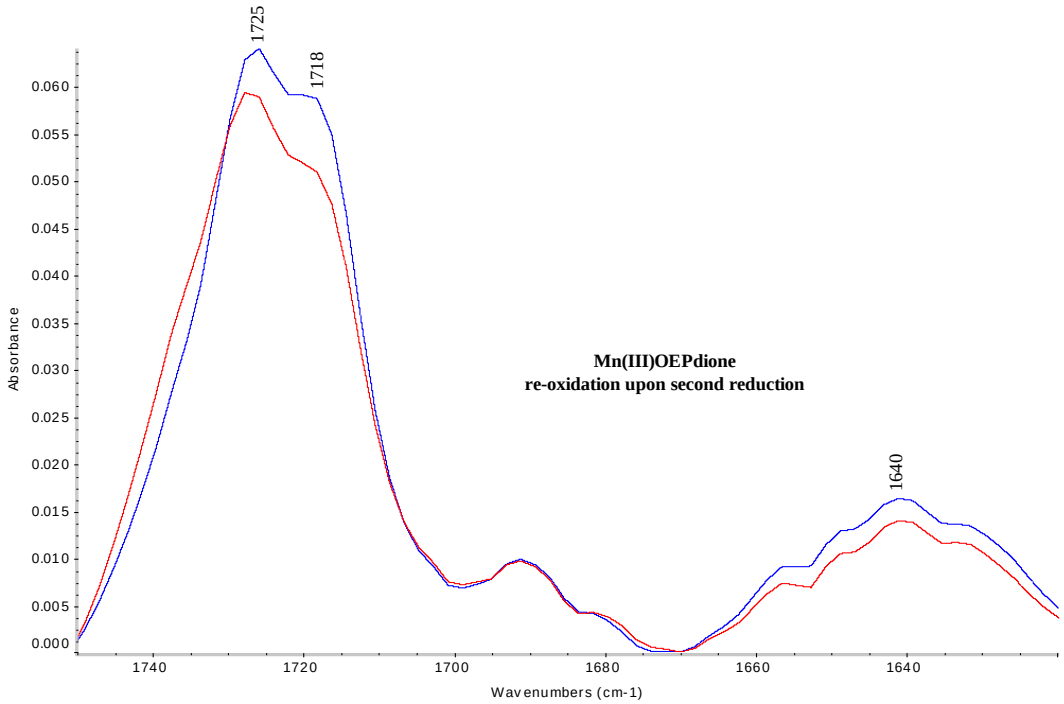

Figure 5-18.FTIR reoxidation spectra of Mn(III)-OEPdione upon second reduction 3.0 mM, in THF, 0.10 M TBAP by OTTLE spectroelectrochemistry.

5.4. Conclusions

The reduction of MnOEPone and MnOEPdione complexes occurred in two one electron transfer processes: one that is metal centered another that is believed to be porphyrin centered. The fact that the potential separation is ~ 1.4 V suggests that the sites of the electron transfer are different. The reduction potential for Mn(III)/Mn(II) electron transfer is comparable with the reduction potential of Fe(III)/Fe(II) which is attributed to be metal centered. The reduction potentials for the second electron addition were -1.11 V for MnOEPone and -1.48 V for MnOEPdione. This was different from FeOEPone and FeOEPdione where the $E_{1/2}$ for the dione was 80 mV positive of the porphinone complex. The UV visible spectra for the first reduction process for Mn(III)OEP, Mn(III)OEPone

and MnOEP(III)dione showed a shift from a split Soret band corresponding to a Mn^{3+} state to a "normal" Soret band. A small shift in Soret band is recorded for MnOEP and Mn(II)OEPone. Both manganese porphinone and porphinedione develop the characteristic band broadening and bleaching of Q bands indicating a porphyrin centered process. Further reduction of $Mn(OEPdione)^{-}$ could be observed at more negative potentials.

The νC=O for Mn(III)OEPoneCl is the highest energy for the M(III) complexes studied (1721 cm^{-1}). Addition of d-electrons (π-dπ backbonding) shifts the νC=O to lower energy (FeOEPoneCl, 1719 cm^{-1}, $CoOEPone^{+}$, 1714 cm^{-1}). Shifts of up to 19 cm^{-1} are typical for M(III)/M(II) reductions (19 cm^{-1} for Mn(III), 16 $cm^{-1}$for Fe(III), 4 cm^{-1} for Co(III)). The small shift for νC=O was explained for cobalt. A decrease in energy of 4-19 cm^{-1} after addition of electrons is an indication of a metal centered process. Formation of the π-anion is indicated by a 40-45 cm^{-1} decrease in νC=O. In addition new bands at about 1550/1530 cm^{-1} are seen for porphyrin π-anion radicals in this work.

In the porphyrin region, addition of electrons to the porphyrin rings gave rise small new bands which are also noted in ZnOEPone complex (MnOEPone 1538 cm^{-1}, 1530 cm^{-1}, ZnOEPone 1550 cm^{-1}, 1540 cm^{-1}). The shift in the νC=O band (45 cm^{-1}) and the new bands at lower energy is evidence for a porphyrin based process.

The νC=O for MnOEPdione also records the highest energy in the series compared (FeOEPdione 1717 cm^{-1}, $CoOEPdione^{+}$ 1712 cm^{-1}, MnOEPdione 1725 cm^{-1}) and the shift noted is comparable with iron and cobalt porphinediones (Fe(III) 14 cm^{-1}, Co(III) 3 cm^{-1}, Mn(III) 19 cm^{-1})). The νC=O for MnOEPdione also records the higher energy in the series compared (FeOEPdione 1717 cm^{-1}, $CoOEPdione^{+}$ 1712 cm^{-1},

MnOEPdione 1725 cm^{-1}) and the shift noted is comparable with iron and cobalt porphinediones (Fe(III) 14 cm^{-1}, Co(III) 3 cm^{-1}, Mn(III) 19 cm^{-1}).

Table 5-1.Selective FTIR data for porphyrin π anion radicals

Compound	**IR absorption signals, [cm^{-1}]**	**Reference**
Mn(II)-OEPone^{-}	1543, 1538, 1530	this work
Zn(OEPone) $^{-}$	1550, 1540	this work
H_2(OEPone)$^{-}$	1551, 1529	164

Table 5-2.Comparison of the reduction potentials of Manganese Porphyrin Complexes

Compounds	**Reduction $E_{pf,1}$ V**	**$E_{pr,2}$ V**	**Ep ½ V**	**Reduction $E_{pf,2}$ V**	**$E_{pr,2}$ V**	**Ep ½ V**
Mn(III)-OEPCl	0.100	0.042	- 0.29	-1.33	-1.20	-1.27
Mn(III)-OEPoneCl	0.015	0.119	0.067	-1.15	-1.06	-1.11
Mn(III)-OEPdioneCl	-0.040	0.056	0.008	-1.52	-1.43	-1.48

solution conditions: Pt electrode, 0.80 mM in THF, with 0.10 M TBAP

Table 5-3.Cyclic voltammetry data for Manganese porphinone and Manganese porphinedione

Compound	**Ipf2, µA**	**Ipr2, µA**	**Ipr/ipf**
Mn(III)-OEPCl	8.35	7.153	0.85
Mn(III)-OEPoneCl	1.517	1.411	0.93
Mn(III)-OEPdioneCl	6.397	5.981	0.94

Table 5-4.Thin-layer visible spectroelectrochemistry obtained during the reduction of Mn(III)OEP, Mn(III)-OEPone, Mn(III)-OEPdione 0.80 mM in THF, with 0.10 M TBAP

Compounds	**Solvent**	**UV-visible spectra (nm)**	**Reference**
Mn(III)OEP	THF	364, 464	this work
Mn(II)OEP	THF	418, 544	this work
Mn(II)OEP-	THF	454	this work
Mn(III)-OEPone	THF	364, 478, 642	this work
Mn(II)-OEPone	THF	440, 624	this work
Mn(II)-OEPone-	THF	488, 680	this work
Mn(III)-OEPdione	THF	366, 504, 646	this work
Mn(II)-OEPdione	THF	402(sh), 436(sh), 464, 628	this work
Mn(II)-OEPdione-	THF	530, 680	this work

Table 5-5.Infrared spectroelectrochemistry of metal porphinones and porphirinediones

Compounds	**IR wavelength (cm^{-1})**	**Reference**
Mn(III)-OEPone	1721, 1578, 1542	this work
Mn(II)-OEPone	1702, 1545, 1528	this work
Mn(II)-OEPone^{-}	1657, 1543, 1538, 1530	this work
Mn(III)OEPdione	1725, 1595, 1572	this work
Mn(II)-OEPdione	1706	this work
Mn(II)-OEPdione^{-}	1693, 1608, 1582, 1555	this work
Fe(III)-OEPone	1719, 1563, 1536	174
Fe(II)-OEPone	1703, 1550, 1530	174
Fe(OEPone)-	1672, 1609, 1578, 1548	174
Fe(III)OEPdione	1717, 1580, 1560, 1543,1526	174
Fe(II)OEPdione	1703, 1547, 1524	174
Fe(OEPdione)$^{-}$	1671, 1655, 1648, 1640, 1593, 1562, 1535	174

5.5. X ray analysis of Mn(III)OEPoneCl and Mn(III)OEPdioneCl

X-ray analysis of MnOEPoneCl and MnOEPdioneCl was performed and a summary of crystallographic parameters are given in Table 5-8.

In case of Mn(III)OEPoneCl black prisms and good diffraction were observed. However, the chiral molecule is statistically superimposed in the crystal with its mirror isomer (~10%) resulting in a global disorder: The crystal itself is centrosymmetric meaning that it represents a 1:1 racemic mixture of the enantiomers. The second axial position of Mn ions is blocked by alkyl groups of nearby molecules. Chloroform molecules populate pairwise big crystal cavities, apparently forming weak C-H…O bonds with carbonyl group of the ligand. There is a limited overlap of pi-system of nearby complex molecules in chains along z axis. In the pyramidal structure of Mn(III)OEPone, the axial chloride is coordinated to the metal at a distance of 2.368 Å and it is perpendicular to the porphyrin plane at an angle of 92.50 Ǻ. The manganese is above the plane of the four nitrogen atoms by -0.271 Å. The nitrogens are at a distance of 2.01 Å and 2.04 Å from the manganese. These distances can be contrasted with those of the manganese tetraphenyl porphyrin: Mn-Cl 2.36 Å; Mn-N 1.99 Å and 2.02 Å; Mn-N 0.27 Å and also iron tetraphenyl porphyrin: Fe-Cl 2.19 Å; Fe-N 2.05 Å; out of plane 0.38 Å[183]. The axial bond is similar to MnTPPCl but considerably longer than FeTPPCl (0.17 Å), the in plane bond is comparable with MnTPPCl and shorter than FeTPPCl by 0.04 Å.

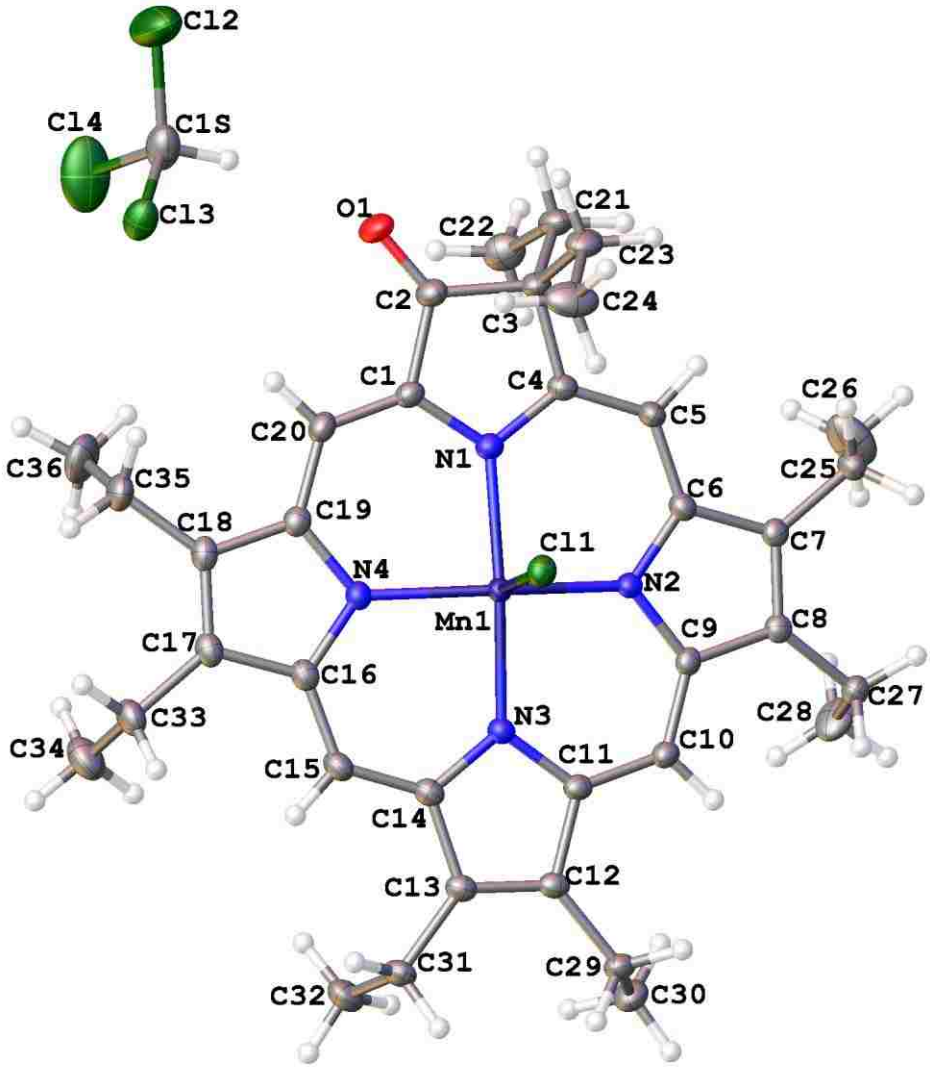

Figure 5-19. Mn(III)OEPoneCl

Table 5-6.Crystal data and structure refinement for Mn(III)OEPoneCl

Empirical formula	$C_{36.93785}H_{44.84652}Cl_{3.81355}MnN_4O$
Formula weight	751.00
Temperature/K	100.0
Crystal system	triclinic
Space group	P-1
a/Å, b/Å, c/Å	9.4036(3), 13.8954(5), 15.6166(6)
α/°, β/°, γ/°	107.683(3), 93.466(3), 107.325(3)
Volume/Å^3	1830.22(12)
Z	2
ρ_{calc}/mg mm^{-3}	1.363
μ/mm^{-1}	0.674
F(000)	785
Crystal size/mm^3	0.07 × 0.06 × 0.05
Theta range for data collection	3.4909 to 58.9602°
Index ranges	$-12 \leq h \leq 12$, $-18 \leq k \leq 18$, $-20 \leq l \leq 21$
Reflections collected	41159
Independent reflections	9273[R(int) = 0.0307]
Data/restraints/parameters	9273/219/633
Goodness-of-fit on F^2	1.065
Final R indexes [I>2σ (I)]	R_1 = 0.0372, wR_2 = 0.0860
Final R indexes [all data]	R_1 = 0.0494, wR_2 = 0.0941
Largest diff. peak/hole/e Å^{-3}	0.764/-0.362

Table 5-7.Comparison of selected distances (Å) and angles (deg) in Mn(III)OEPone

	Mn(III)OEPone
M-N_{sat}	2.013
M-N_{uns}	2.039
Cα-Cβ(O)	1.478
Cα-Cβ(Et2)	1.520
Cβ-$Cβ_{sat}$	1.506
Cβ-$Cβ_{sat}$	1.434
Cβ-$Cβ_{uns}$	1.365
N-Cα	1.378
Cα-Cm	1.378
Cβ-O	1.218
N-M-N_{adj}	89.001
N-M-N_{opp}	164.732
M-N-Cα	126.503
Cm-Cα-$Cβ_{sat}$	124.051
Cm-Cα-$Cβ_{uns}$	124.4
N-Cα-Cm	125.051
Cα-Cm-Cα	125.857
Cα-Cβ-C(Et2)	112.087
Cα-Cβ-Cβ(O)	101.665
N-Cα-$Cβ_{sat}$	110.916
N-Cα-$Cβ_{uns}$	110.827
Cα-Cβ-O	126.620
Cβ-Cβ-O	126.570
Cα-Cβ-CEt	125.342
Cβ-Cβ-CEt	123.365
Cα-N-$Cα_{sat}$	104.53
Cα-N-$Cα_{uns}$	107.882

The X-ray structure of Mn(III)OEPdioneCl has not been reported. Single crystal was grown and analyzed by X-ray. A summary of crystallographic parameters are given in Table 4-1. Black pyramids alongside with more solvent-dependent cubes were observed. The structure contains two crystallographically independent molecules with identical chemical structure. The molecule is chiral but the crystal is centrosymmetric, i.e. represents a racemic mixture. In the crystal, the molecules form centrosymmetric cyclic tetramers because of additional inter-molecular axial coordination Mn…O=C (Mn…O distances are 2.405 and 2.571 Å). Data were collected at 100 K, the complex crystallized in the space group C2/c with 16 formula units per unit cell.

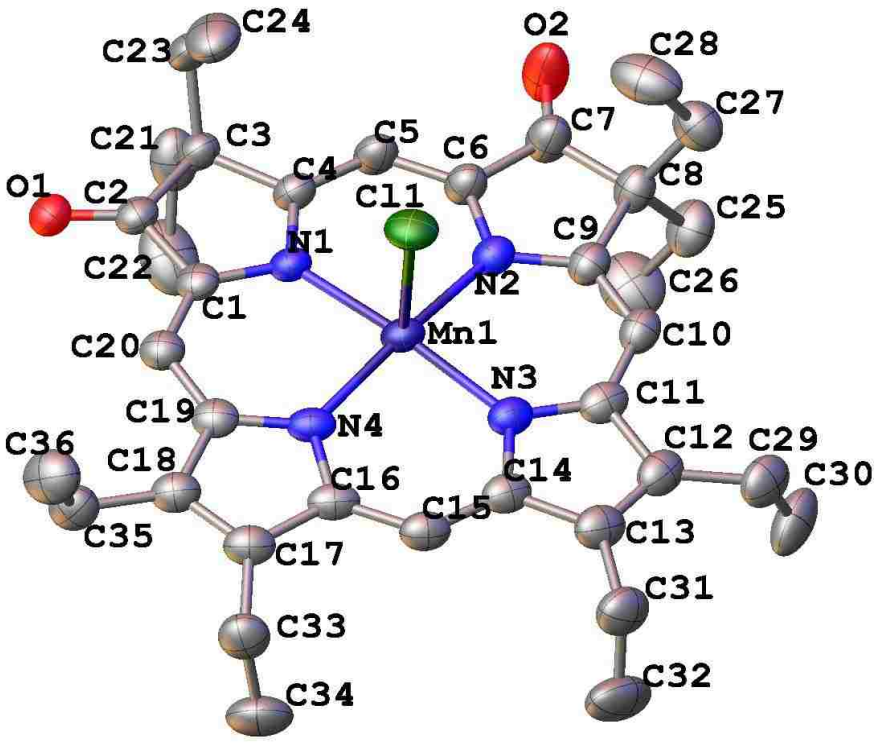

Figure 5-20. Mn(III)OEPdioneCl

In the pyramidal structure of Mn(III)OEPdioneCl, the axial chloride is coordinated to the metal at a distance of 2.37 Å and it is perpendicular to the porphyrin plane at an angle of 91.86 Å. The manganese is above the plane of the four nitrogen atoms by 0.167 Å towards the chlorine ion. Molecular structure of Mn(III)OEPdioneCl was analyzed and compared with previously reported data for FeOEPdioneCl and 2,4-OEPdione. Similar to iron dioxo complex, the Cβ-Cβ and Cα-Cβ bonds from the rings that hold oxygen atoms are elongated and smaller than those of free base. The Cβ-O distance is larger than that of 2,4 porphinedione due to the oxygen effect. The oxygen presence in the ring affects also the Cα-Cβ bonds to which they are attached. These are considerably shorter than the equivalent Cα-Cβ bonds in the same rings bearing the ethyl groups. Therefore the earlier statement[184] made by Chang and Fajer that the carbonyl groups are in conjugation with the π system of the macrocycle and affect the electronic properties is also valid for this complex.

Hence, the oxygen presence in the pyrroline rings leads to the elongation of Cβ-Cβ which produce a wider Cα-N-Cα bond angle and ultimately affects the Mn-N bonds by stretching. Clearly the Cα-N-Cα angles in the pyrrole rings are shorter. For comparison with iron complex these angles are larger but yet they are smaller than 2,4-isobacteriochlorin. The Mn-N distances are longer in the rings I and II when compared with III and IV; in addition they are smaller compared with the corresponding values from iron complex. Furthermore the Mn-N average distances for typical Mn (III) porphyrin complex is 2.01 Å which is close to our value 2.04 Å. The asymmetries in the Cα-Cβ-Cβ angles which open to 107.6 Å and 107.4 Å at C2 and C7 and to 100.42 Å and 100.6 Å at C3 and C8, are analogous to the respective angles in free-base and iron

complex. The manganese deviation from the plane of the nitrogens is 0.169 Å toward the chloride ion, which is considerable smaller compared with the 0.47 Å of the iron dione complex and also the axial bond is considerably longer, 0.16 Å thus follows the pattern observed in the comparison of MnTPPCl and FeTPPCl complexes.

Table 5-29 summarized the most relevant data for Mn(III)OEPone, Mn(III)OEPdione, Fe(III)OEPdione and 2,4-OEPdione. It can be observed that comparable Cβ-Cβ bonds in pyrroline rings are elongated when compared with the pyrroles rings in all compounds. The Cβ-O distances reflects keto functional groups in the molecule and the effect of the oxygen is reflected in attached Cα-Cβ which is shorter than the Cα-Cβ bonds which has ethyl groups attached. This indicates that carbonyl bond is in conjugation with the porphyrin system affecting its electronic properties.

Table 5-8. Comparison of selected distances (Å) for Mn(III)OEPone, Mn(III)OEPdione, Fe(III)OEPdione and 2,4-OEPdione

	Mn(III)OEPone	Mn(III)OEPdione	Fe(III)OEPdione	2,4OEPdione
Cβ- $C\beta_{sat}$	1.506	1.504	1.504	1.520
Cβ- $C\beta_{uns}$	1.365	1.365	1.372	1.381
Cα- Cβ (O)	1.478	1.464	1.484	1.483
Cα- $C\beta(Et_2)$	1.520	1.516	1.512	1.541
Cβ-O	1.218	1.225	1.219	1.207
M-N_{sat}	2.066	2.014	2.116	
M-N_{uns}	2.016	2.068	2.040	
Cα-N-$C\alpha_{sat}$	110.260	109.528	108.7	110.2
Cα-N-$C\alpha_{uns}$	104.8555	105.830	104.7	111.3

Table 5-9.Crystal data and structure refinement for Mn(III)OEPdione

Empirical formula	$C_{37.815385}H_{47.565385}Cl_{2.696155}MnN_4O_2$
Temperature / K	100.0
Crystal system	monoclinic
Space group	C2/c
a/Å, b/Å, c/Å	24.0979(4), 24.2775(4), 26.6322(4)
α/°, β/°, γ/°	90.00, 96.4976(15), 90.00
Volume/Å^3	15480.7(4)
Z	16
ρ_{calc}/mg mm^{-3}	1.271
μ/mm^{-1}	4.770
F(000)	6229
Crystal size/mm^3	0.14 × 0.06 × 0.04
Theta range for data collection	3.3376 to 147.782°
Index ranges	$-28 \leq h \leq 29$, $-30 \leq k \leq 28$, $-31 \leq l \leq 32$
Reflections collected	44599
Independent reflections	15255[R(int) = 0.0428]
Data/restraints/parameters	15255/25/942
Goodness-of-fit on F^2	1.038
Final R indexes [I>2σ(I)]	R_1 = 0.0575, wR_2 = 0.1539
Final R indexes [all data]	R_1 = 0.0801, wR_2 = 0.1707
Largest diff. peak/hole/eÅ^{-3}	1.144/-0.698

Table 5-10.Comparison of selected distances (Å) and angles (deg) in Mn(III)OEPdione, Fe(III)OEPdione and 2,4-OEPdione

	Mn(III)OEPdione	**Fe(III)OEPdione**	**2,4-OEPdione**
M-N_{sat}	2.014 (2)	2. 16 (6)	
M-N_{uns}	2.068 (2)	2.040 (6)	
Cα-Cβ(O)	1.464 (4)	1.484 (10)	1.483 (13)
Cα-Cβ(Et2)	1.516 (4)	1.512 (1)	1.541 (13)
Cα-$Cβ_{uns}$	1.434 (4)	1.436 (8)	1.417 (13)
Cβ-$Cβ_{sat}$	1.504 (4)	1.504 (10)	1.520 (13)
Cβ-$Cβ_{uns}$	1.365 (4)	1.372 (10)	1.381 (13)
N-Cα	1.369 (3)	1.379 (8)	1.369 (8)
Cα-Cm	1.377 (3)	1.372 (5)	.370 (11)
Cβ-O	1.225 (3)	1.219 (9)	1.207 (11)
N-M-N_{adj}	89.4 (8)	87.1 (6)	
N-M-N_{opp}	170.6 (8)	153.9 (2)	
M-N-Cα	124.4 (16)	126.1 (7)	
Cm-Cα-$Cβ_{sat}$	122.1 (2)	123.0 (11)	122.9 (4)
Cm-Cα-$Cβ_{uns}$	125.0 (2)	127.6 (4)	125.2 (7)
N-Cα-Cm	125.7 (2)	124.7 (6)	12 .2 (6)
Cα-Cm-Cα	126.1 (2)	127.4 (4	128.4 (13)
Cα-Cβ-C(Et2)	107.5 (2)	106.6 (5)	10 .0 (8)
Cα-Cβ-Cβ(O)	100.5 (2)	101.5 (6)	100.5 (8)
N-Cα-$Cβ_{sat}$	111.2 (2)	111.4 (7)	111.1 (9)
N-Cα-$Cβ_{uns}$	110.2 (2)	11 .1 (7)	106.1 (11)
Cα-Cβ-O	125.2 (3)	26.6 (7)	127.5 (0)
Cβ-Cβ-O	127.2 (3)	126.9 (7)	12 .6 (10)
Cα-Cβ-CEt	112.3 (4)	110.9 (7)	112.9 (5)
Cβ-Cβ-CEt	110.6 (4)	110.5 (5)	110.8 (8)
Cα-N-$Cα_{sat}$	109.5 (2)	108.7 (6)	110.2 (8)
Cα-N-$Cα_{uns}$	105.8 (2)	104.7 (6)	1 1.3 (8)

BIBLIOGRAPHY

[1] Milgrom, L. R., The colours of life : an introduction to the chemistry of porphyrins and related compounds; New York : Oxford University Press, **1997**, Chapter 1
[2] Doddrell, D.; Caughey, W. S. *J. Am. Chem. Soc.* **1972**, *94*, 2510
[3] Kadish, K. M.; *Prog. Inorg. Chem*.**1986**, *34*, 435-605
[4] Harrison, P. J.; Fookes, C. J. R.; Battersby, A. R.; *J. Chem. Soc. Chem. Comm.* **1981**, 797
[5] Scheer, H. "*The Porphyrins"*; Dolphin, D., Ed.; Academic Press: New York, **1979**, Vol II, Chapter 1
[6] Smith, K. M.; *"Porphyrins and metallo-porphyrins",* Smith, K. M., Ed., Elsevier Scientific, New York, **1975**, Chapters 2,14
[7] Felton, R.H. in *" The Porphyrins"*, Dolphyn, D., Ed.; Academic Press: New York **1978**, Vol. 5, pp 81
[8] Cocolios, P.; Kadish, K. M. *Israel J. Chem*. **1985**, *25*, 138
[9] Salehi, A; Oertling, W. A.; Babcock, G. T.; Chang, C. K. *J. Am. Chem. Soc*.**1986**, *108*, 5630
[10] Fuhrhop, J. H.; Mauzerall, D. *J. Am. Chem. Soc*.**1968**, *91*, 4174-4181
[11] Fuhrhop, J. H.; *Struct. Bonding*, **1974**, *1*, 18
[12] Chantrell S. J.; McAuliffe C. A.; Munn R. W.; Pratt A. C. *Coord Chem Rev.* **1975**, *16*, 259
[13] Shiomura E. T.; Phillippi H. M. Goff; Scholz W. F.; Reed A. C. *J. Am. Chem. Soc*. **1981**, *103*, 6778-6780.
[14] Hinman A. S.; Pavelich B. J., *Can. J. Chem.* **1987,** *65*, 919.
[15] Felton, R. H.; Dolphin, D.; Borg D. C.; Fajer, J. *J. Am. Chem. Soc.*, **1969,** *91*, 196
[16] Palmer, G. *"The Porphirins"*, Ed. Davis Dolphin, Vol 4, Academic Press, New York, **1978**, p-313-354.
[17] Lin, W. C. *"The Porphirins"*, Ed. Davis Dolphin, Vol 4, Academic Press, New York, **1978**, 355-375
[18] R. H. Felton, *"The Porphyrins"*, Ed. David Dolphin, Vol. 5, Academic Press, New York, **1978**, p 53-115
[19] D. G. David, *"The Porphyrins"*, Ed. David Dolphin, Vol. 5, Academic Press, New York, **1978**, p127-150.
[20] K. M Kadish, *Progress in Inorganic Chemistry*, **1986**, *34*, 437-604
[21] Kadish, K. M. *Prog. Inorg. Chem.* **1986**, *34*, 435-605
[22] Felton, R. H. *"The Porphyrins"*; D. Dolphin Ed.; Academic Press, New York, **1978**; Chapter 3
[23] Davis, D. G. *"The Porphyrins"*; D. Dolphin Ed.; Academic Press, New York, **1978**; Chapter 5
[24] Buchler, J. W.; Kokisch, W.; Smith, P. D. *Struct. Bonding* **1978**, *34*, 79
[25] Buchler, J. W.; *:Porphyrins and Metalloporphyrins"*; Smith, K. M. Ed.; Elsevier, New York, **1975**, Chapter 5
[26] Flits, W. *Adv. Heterocyclic Chem.* **1988**, *43*, 73; Scheer, H. *"The Porphyrins"* Ed. By Dolphin, D. Vol. 2, Chapter 1, Academic Press, New York, **1978**
[27] Peychal-Heiling, G.; Wilson, G. S. *Anal. Chem.* **1971**, *43*, 550
[28] Stolzenberg, A. M.; Speer, L. O.; Holm, R. H. *J. Am. Chem. Soc.* **1980**, *102*, 364

[29] Chang, C. K.; Hanson, L. K.; Richardson, R. F.; Young, R.; Fajer, J. *Proc. Natl. Acad. Sci. USA* **1981**, *78*, 2652
[30] Heath, G. A.; Low, M. R.; McQueen, R. C. S. *J. Chem. Soc. Perkin Trans. II* **1984**, 305
[31] Strauss, S. H.; Thompson, R. G.; *Inorg. Biochem.*, **1986**, *27*, 173
[32] Matinis, S. A.; Sotirious, C.; Chang, C. K.; Sligar, S. G. *Biochemistry* **1989**, *28*, 879
[33] Chang, C. K.; Barkigia, K. M.; Hanson, L. K.; Fajer, J. *J. Am. Chem. Soc.* **1986**, *108*, 1352
[34] Stolzenberg, A. M.; Glazer, P. A.; Foxman, B. M.; *Inorg. Chem.* **1986**, *25*, 983
[35] Strauss, S. H.; Thompson, R. G.; *Inorg. Biochem.*, 1986, *27*, 173
[36] Lanese, J. G.; Wilson, G. S. *J. Electrochem. Soc.* **1972**, *119*, 1039
[37] Balducci, G., Chottard, G, Gueutin, C., Lexa, D., Saveant J-M. *Inorganic Chemistry*, **1994,** *33*(9), 1972-1978
[38] Closs, G. L.; Closs, L. E. *J. Am. Chem. Soc.* **1963**, *85*, 818
[39] Furhop, J. H.; Kadish, K. M.; Davis, D. G.; *J. Am. Chem. Soc.* **1973**, *95*, 5140-5147
[40] Felton, R. H.; Owen, G. S.; Dolphin, D.; Fajer, J. *J. Am. Chem. Soc.* **1971**, *93*, 6332-6334
[41] Felton, R. H.; Linschitz, H. *J. Am. Chem. Soc.* **1966**, *88*, 1113-1116
[42] Felton, R. H.; Owen, G. S.; Dolphin, D.; Forman, A.; Borg, D. C.; Fajer, J. *Ann. N. Y. Acad. Sci.* **1973**, *206*, 504-515
[43] Zerner, M.; Gouterman, M. *Theoret. Chim. Acta*, **1966**, *4*, 44-63
[44] Zerner, M.; Gouterman, M. *Ionrg. Chem.* **1966**, *5*, 1699-1706
[45] Zerner, M.; Gouterman, M. Kobayaski, H. *Theoret. Chim. Acta* **1966**, *6*, 363
[46] Zerner, M.; Gouterman, M. *Theoret. Chim. Acta*, **1967**, *8*, 26
[47] Schaeffer, A. M.; Gouterman, M. *Theoret. Chim. Acta*, **1970**, *18*, 1
[48] Kadish, K. M.; Davis, D. G.; Furhop, J. H.; *Angew. Chem., Int. Ed. Engl.* ***1972***, *11*, 1014-1016
[49] Fajer, J.; Borg, D.C.; Forman, A.; Dolphin, D.; Felton, R. H. *J. Am. Chem. Soc.* **1970**, *92*, 3451-3459
[50] Fuhrhop, J. H.; Mauzerall, D. *J. Am. Chem. Soc.* **1969,** *91*, 4174-4181
[51] Felton, R. H.; Dolphin, D.; Borg, D. C.; Fajer, J. *J. Am. Chem. Soc.* **1969**,*91*, 196-198
[52] Fuhrhop, J. H.; Mauzerall, D. *J. Am. Chem. Soc*.**1968,** *90*, 3875-3876
[53] Kadish, K. M.; Rhodes, R. K.; *Inorg Chem* **1981**, *20*, 2961-2966
[54] Kadish, K. M.; Shiue, L. R. Rhodes, R. K.; Bottomley, L. A. *Inorg Chem* **1981**, *20*, 1274-1277
[55] Wolberg, A.; Manassen, J. *J. Am. Chem. Soc.*, **1970**, *92*, 2982-2991
[56] Kadish, K. M.; Shiue, L. R. *Inorg Chem* **1982**, *21*, 3623-3630
[57] Lanese, J. G.; Wilson, G. S. J. *Electrochem. Soc.* **1972**, *119*, 1039.
[58] Closs, G. L.; Closs, L. E. *J. Am. Chem. Soc.* **1963**, *85*, 818.
[59] Kadish, K.M.; Smith, K. M.; Guilard R. *"The porphyrin handbook "* Academic Press, **2000**
[60] Truxillo, L. A.; Davis, D. G. *Anal Chem.* **1975**, *47*, 2260-2267
[61] D'Souza, F.; Villard, A.; van Caemelbecke, E.; Franzen, M.; Boschi, T.; Tagliatesta, P.; Kadish, K. M. *Inorg Chem* **1993**, *32*, 4042- 4048
[62] Kadish, K. M.; Lin, X. Q,; Han, B. C. *Inorg Chem*, **1987**, *26*, 4161-4167
[63] Mu, X. H.; Lin, X. Q.; Kadish, K. M.; *Electroanal.* **1989**, 113-116

[64] Stanienda, A.; Biebl, G. Z. *Phys. Chem.* **1967**, *52*, 254-275
[65] Witlock, H. W.; Bower, B. K. *Tetrahedron Lett.* **1965**, 4827
[66] Kadish, K. M.; Bottomley, L. A.; Beroiz, D. *Inorg. Chem*. **1978,** *17*, 1124-1129
[67] Walker, F. A.; Beroiz, D.; Kadish, K. M.; *J. Am. Chem. Soc.* **1976**, *98*, 3484-3489
[68] Kageyama, H.; Hidai, M.; Uchida, Y. *Bull. Chem. Soc. Jpn.* **1972**, *45*, 2898-2902
[69] Kobayashi, H.; Hara, T.; Kaizu, Y. *Bull. Chem. Soc. Jpn.* **1972**, 2148-2155
[70] Kadish, K. M.; Davis, D. G.; *Ann. N. Y. Acad. Sci.* **1973**, *206*, 495-503
[71] Kadish, K. M.; Thompson, L. Z.; Beroiz, D.; Bottomley, L. A. *ACS Symposium Series* **1977**, *38*, 51
[72] Kadish, K. M.; *Iron Porphyrin*, Part 2, Lever, A. B. P.; Gray, H. B., Eds.; Addison Wesley: Reading, MA, **1983**, 161
[73] Kadish, K. M. *Progress in Inorganic Chemistry*, Vol. 34, Lippard, S. J., Ed.; John Wiley&Sons, New York, **1986**, 435
[74] Kadish, K. M., Ed.; *Electrochemical and Spectrochemical Studies of Biological Redox Componnents (ACS Advances in Chemistry Series 201)*, ACS, Washinghton, D. C., **1983**
[75] Constant, L. A.; Davis, D. G. *Anal. Chem.* **1975**, *47*, 2253-2260
[76] Kadish, K. M.; Morrison, M. M. Constant, L. A.; Dickens, L.; Davis, D. G. *J. Am. Chem. Soc.* **1976**, *98*, 8387-8390
[77] Bottomley, L. A.; Kadish, K. M. *Inorg. Chem.* **1981**, *20*, 1348-1357
[78] Timkovich, R., Cork, M. S., Taylor, P. V. J. Biol. Chem. **1984**, *259*, 1577-1585
[79] Richardson, P. F., Chang, C. K., Spaulding, L. D., Fajer, J. *J. Am. Chem. Soc.*, **1979,** *101*, 7736-7738.
[80] Liu, L. *Dissertation thesis* **1991**
[81] (a) O. H. Kao; J. H. Wang, *Biochemistry*, **1965**, *4*, 342. (b) L. Latos-Grazynski; R-J. Cheng; G. N. La Mar; A. L. Balch, *J. Am. Chem, Soc.* **1982,** *104*, 5992. (c). Y. Hatefi, *Ann. Rev. Biochem.* **1985,** *54*, 1015. (d) F.S. Mathewss, *Prog. Biophys. Mol. Biol.* **1985,** *45*, 1
[82] M. Gouterman, *"The Porphyrins"*, Ed. David Dolphin, Vol. 3, Academic Press, New York, **1978**, pg-165.
[83] L. J. Boucher, *Coord. Chem. Reviews*, **1972,** *7*, 289.
[84] (a) J.E. Falk, "Porphyrins and Metalloporphyrins", Elsevier, Amsterdam, **1964**. (b) J. H. Fuhrhop, Struct. Bonding, **1974,** *18*, 1. (c). S. J. Chantrell; C.A. McAuliffe; R.W. Munn; A. C. Pratt, *Coord. Chem. Rev*. **1975,** *16*, 259.
[85] Hu, Q. *Dissertation thesis* **1999**
[86] Manassen, J.; Wolberg, A.; *J. Amer. Chem. Soc.*, **1970**, *92*, 2982
[87] Falk, J. E.; *"Porphyrins and Metalloporphyrins"* Elsevier, New York, N. Y., **1964**.
[88] Felton, R. H. Fajer, J.; Berg, D. C.; Dolphin, D.; *J. Amer. Chem. Soc.*, **1970**, *92*, 3451.
[89] Lanese, J. G.; Wilson, G. S.; *J. Electrochem. Soc.* **1972**, *119* (8), 1039-1043
[90] Clack, D. W.; Hush, n. S. *J. Am. Chem. Soc*. **1965**, *87*, 238-4242
[91] Felton, R. H.; Linschitz, H. *J. Am. Chem. Soc*. **1966**, *88*, 1113-1116
[92] Lanese, J. G.; Wilson, G. S. *J. Electrochem. Soc*. **1972**, *119*, 1039
[93] Wolberg, A.; Manassen, J. *J. Am. Chem. Soc* **1970**, *92*, 2982-2991
[94] M. Calvin, *Rec. Pure Appl. Chem.*, **1965**, *15*, 1.
[95] J. Zaleski, *J. Physiol. Chem.*, **1904**, *43*, 11.
[96] J. F. Taylor, *J. Bid. Chem.*, **1940**, *135*, 569

[97] Loach, P.A.; Calvin, M.; *Biochemistry*, **1963**, *2*, 361.
[98] Boucher, L.J.; *J. Amer. Chem. Soc.*, **1970**, *90*, 6640.
[99] Fuhrhop, J. H.; Kadish, K. M.; Davis, D. G. *J. Am. Chem. Soc.*, **1973**, *95*, 5140-5147
[100] Morehouse, K.M.; Neta, P. *J. Phys. Chem.* **1984**, *88*, 1575-1579.
[101] Guldi,D.M.; Kumar, M.; Neta, P. *J. Phys. Chem.* **1992**, *96*, 9576-9581.
[102] Kadish, K. M.; Kelly, S. *Inorg. Chem.*, **1979**, *18* (11), 2968-2971
[103] Boucher, L. J. *J. Am. Chem. Soc.*, **1970**, *92*, 2725-2730
[104] Swistak, C.; Mu, X. H.; Kadish, K. M. *Inorg. Chem.* **1987**, *26*, 4360-4366
[105] Tagliateste, P.; Li, J.; Autret, M.; Van Caemelbecke, E.; Villard, A.; D'Souza, F.; Kadish, K. M. *Inorg. Chem.* **1996**, *35*, 5570-5576
[106] Kadish,K.M; Rhodes, R. K. *Inorg. Chem*. **1983,** *22*, 1090-1094
[107] Kadish,K.M; Boisselier-Cocolios, B.; Simonet, B., Chang, D., Ledon, H., and Cocolios, P., *Inorg Chem.*, **1985**, *24*, 2148-2156
[108] Teraoka, J., Hashimoto, S., Mori, M. Kitagawa, T., *J. Am. Chem. Soc.*, **1987**, *109*, 180-184
[109] Hickman, D., Shirazi, A., Goff, H. M., *Inorg. Chem.*, **1985**, *24*, 563-566
[110] (a) D.F. Evans, *J. Chem. Soc*. 1959, 2003. (b) A. Wolberg; J. Manassen, J. Am. Chem. Soc. **1970**, *92*, 2982.
[111] D. Kim; L. A. Miller, G, Rakhit; T. G. Spiro, *J. Phys. Chem*. **1986,** *90*, 3320.
[112] (a) R.S. Alger, *Electron Paramagnetic Resonance, Techniques and Applications,*Interscience Wiley, NY, **1968**. (b). A. Abragam and B. Bleaney, *Electron Paramagnetic Resonance of Transition Ions,* Oxford Press, London, **1970**.
[113] T. Kitagawa and Y. Ozaki, *Struct. Bonding*, **1987**, *64*, 71-114
[114] K.. Nakamoto, *Infrared and Raman Spectra of Inorganic and Coordination Compounds,* 4th edition; Wiley-Interscience Publication, NY, **1986**.
[115] E.T. Shimomura; M.A. PhilHppi; H. M. Goff; W.F. Scholz; C.A. Reed, J. Am. Chem, Soc. **1981,** *103*, 6778-6780.
[116] (a)A. S. Hinman; B. J. Pavelich; K. McGarty, *Can. J. Chem.* **1988**, *66*, 1589. (c) D. H. Jones and A,S. Hinman, J. Chem. Soc. Dalton Trans. **1992**, (9), 1503-1508. (d) A. S. Hinman; T, Olonwyolemi, *Can. J. Chem.* **1993**, *71*, 1975.
[117] A. S. Hinman; B. J, Pavelich; A. E. Komdo; S. Pons, *J. Electroanal. Chem,* **1987**, *234*, 145.
[118] Gasyna, Z.; Stillman, M. J. *Inorg. Chem.* **1990**, *29*, 5101.
[119] Salehi, A.; Oertling, W.A.; Babcock, G.T.; Chang, C.K. *J. Am. Chem. Soc.* **1986,** *108*, 5630.
[120] Reed, C. A ,, *Electrochemical and Spectrochemical Studies of Biologica1 Redox Components* (ACSAdvances in Chemistry Series 201), Kadish, K.M. Ed., ACS, Washington, D.C., **1983**.
[121] Kadish, K.M.; Larson, G.; Lexa, D.; Momenteau, M.; *J. Am. Chem. Soc.* **1975**, *97*, 282-288.
[122] Lexa, D.; Momenteau, M.; Mispelter, J.; *Biochim. Biophys. Acta,* **1974**, *338*, 151.
[123] Yamaguchi, K.; Morishima, I.; *Inorg. Chem.* **1992**, *31*, 3216.
[124] Axolabehere, E.; Geneieve, C.; Lexa, D.; *New J. Chem.* **1994**, *18*, 889.
[125] Srivatsa, G.S.; Sawyer, D.T.; Boldt, N. J.; Bocian, D.F.; *Inorg. Chem.* **1985**, *24*, 2133.
[126] Donohoe, R.J.; Atamian, M.; Bocian, D.F.; *J. Am. Chem. Soc.* **1987**, *109*, 5593.

[127] Teroka, J.; Hashimoto, S.; Sugimoto, H.; Mori, M.; Kitagawa, T.; *J. Am. Chem. Soc.* **1987**, *109*, 180
[128] Rodgers, R.R.; Reed, R.A.; Su, Y.O.; Spiro, T.G.; *Inorg. Chem.* **1992**, *31*, 2688.
[129] Sinyakov, G.N.; Shulga, A.M.; *J. Mol. Struc.* **1993**, *295*, 1.
[130] Hickman, D.L.; Shirazi, A,; Goff, H.M.; *Inorg. Chem.* **1983**, *24*, 563.
[131] Felton, R.H.; Davis, D.G. *The Porphyrins*, Vo1.5, Dolphin, D. Ed., Academic, New York **1978**, Chapt. 3, 4.
[132] Fuhrhop, J.H. *Porphyrins and Metalloporphyrins*, Smith, K. Ed., Elsevier, New York **1975**, Chapter 14.
[133] Hinman, A. S.; Jones, D. H.; *J. Chem. Soc. Dalton Trans.* **1992**, 1503-1508
[134] Heheman, W. R.; Burnett, J. N.; Murray, R. W. *Anal. Chem.* **1968**, *40*, 1970.
[135] Helneman, W. R.; Burnett, J. N.; Murray, R. W. *Anal. Chem.* **1968**, *40*, 1974.
[136] Kreishman, G. P.; Anderson, C. W.; Su, C. H.; Haisali, H. B.; Heineman, W. R. *Bioelectrochem. Bioenerg.* **1978**, *5*, 196.
[137] Meyer, M. L.; DeAngelis, T. P.; Heineman, W. R. *Anal. Chem.* **1977**, *49*, 602.
[138] Yildiz, A.; Kissinger, P. T.; Reilley, C. N. *Anal. Chem.* **1988**, *40*, 1018.
[139] Norris, B. J.; Meckstroth, M. L.; Heineman, W. R. *Anal. Chem.* **1976**, *48*, 630.
[140] Petek, M.; Neal. T. E.; Murray, R. W. *Anal. Chem.* **1971**, *43*, 1069.
[141] Kenyhercz, T. M.; DeAngelis, T. P.; Norris, B. J.; Heineman, W. R.; Mark, H. B. *J. Am. Chem. Soc.* **1978**, *98*, 2469.
[142] Stargardt, J. F.; Hawkridge, F. M.; Landrum, H. L. *Anal. Chem.* **1978**, *50*, 930.
[143] Rhodes, R. K.; Kadish, K. M., unpublished work, University of Houston, **1979-1980**.
[144] Kadish,K. M.; Rhodes, R. K.;*Anal. Chem*. **1981**, *53*, 1539-1541
[145] X. Q. Lin and K. M. Kadish *Anal. Chem.* **1985**, *57*, 1498-1501
[146] X. Q. Lin and K. M. Kadish *Anal. Chem.* **1986**, *58*, 1493-1497
[147] Ashley, K.; Pons, B. S. *Chem Rev*, **1988**, *88*, 673
[148] Korzeniewski, C. *Crit. Rev. Anal. Chem.* **1997**, *27*, 81
[149] Zhang, H.; *Master Thesis*, Marquette University, **2000**
[150] Hu, S.; Lin, C.-Y.; Blackwood, Jr., M. E.; Mukherjee, A.; Spiro, T. G. *J. Phys. Chem.* **1995**, *99*, 9694-9701.
[151] Reed, R. A.; Purello, R.; Prendergast, K.; Spiro, T. G. *J.Phys.Chem.* **1991**, *95*, 9720-9727.
[152] Lin, C.-Y.; Spiro, T. G. *Inorg.Chem.* **1996**, *35*, 5237-5243.
[153] Blackwood, M. E. Jr.; Lin, C.-Y.; Cleary, S. R.; McGlashen, M. L.; Spiro, T. G. J. Phys. Chem. A **1997**, *101*, 255-258.
[154] Perng, J.; Bocian, D. F. *J. Phys. Chem.* **1992**, *96*, 4804-4811.
[155] Stolzenberg, A. M.; Spreer, L. 0.; Holm, R. H. *J. Am. Chem. Soc.* **1980**, *102*, 364-370.
[156] Chang, C. K.; Fajer, J. *J. Am. Chem. Soc*. **1980**, *102*, 848-851
[157]. Stolzenberg, A. M.; Strauss, S. H.; Holm, R. H. *J. Am. Chem. Soc.* **1981**, *103*, 4763-4778.
[158] Richardson, P. F.; Chang, C. K.; Hanson, L. K.; Spaulding, L. D.; Fajer, J. *J. Phys. Chem.* **1979**, *83*, 3420-3424.
[159] Fujita, E.; Fajer, J. *J. Am. Chem. Soc.* **1983**, *105*, 6743-6745.
[160] Sullivan, E. P.,Jr.; Grantham, J. D.; Thomas, C. S.; Strauss, S. H. *J. Am. Chem. Soc.* **1991**, *113*, 5264-5270.

[161] Barkigia, K. M.; Chang, C. K.; Fajer, J.; Renner, M. W. *J. Am. Chem. Soc.* **1992**, *114*, 1701-1707.
[162] Cai, L. S.; Holm, R. H. *J. Am. Chem. Soc.* **1994**, *116*, 7177-7188.
[163] Liu, Y.; Ryan, M. D. *Inorg. Chim. Acta* **1994**, *225*, 57-66.
[164] Zhongcheng, Wei.; PhD thesis, Marquette University **1998**
[165] Chang. C. K.; Sotiriou C. *J. Org. Chem.* **1987**, *52*, 926
[166] Chang. C. K.; Sotiriou C. *J. Org. Chem.* **1985**, *50*, 4989
[167] Chang. C. K.; Wu, W.; *J. Am. Chem. Soc.* **1987**, *109*, 3149
[168] Alder, A. D.; Longo, F. R.; Finareli, J. D.; Goldmacher, J.; Assour, J.; Korsakoff, L. *J. Org. Chem.* **1967**, *32*, 467
[169] Stolzenberg, A. M.; Glazer, P. A.; Foxman, B. M.; *Inorg. Chem.* **1986**, *25*, 983
[170] Dolphin, D. *The Porphyrins* vol. I, pp. 414, New York, **1978**
[171] Chang, C. K.; Sotiriou, C.; Wu, W. *J. Chem. Soc. Chem. Commun.* **1986**, 1213
[172] Chang. C. K.; Timkovich, R.; Wu, W. *Biochemistry* **1986**, *25*, 8447
[173] Kadish K. M., Lin X. Q., *Anal. Chem.* **1985**, *57*, 1498-1501
[174] Wei, Z.; Ryan, M. D. *Inorg. Chem.* **2010,** *49* (15), 6948-6954.
[175] Doppelt, P.; Fischer, J.; Weiss, R. *Inorg. Chem.* **1984,** *23*, 2958-2962.
[176] Sazou, D.; Araullo-McAdams, C.; Han, B. C.; Franzen, M. M.; Kadish, K. M. *J. Am. Chem. Soc.* **1990,** *112* (22), 7879-7886
[177] Zhu, W.; Sintic, M.; Ou, Z.; Sintic, P. J.; McDonald, J. A.; Brotherhood, P. R.; Crossley, M. J.; Kadish, K. M. *Inorg. Chem.* **2010,** *49* (3), 1027-1038.
[178] Arraullo, C.; Kadish, K. M.; *Inorg. Chem.* **1990**, *29*, 2749-2757.
[179] Shirazi, A.; Goff, H. M. *Inorg. Chem.* **1982,** *21* (9), 3420-3425.
[180] Liu, Y. PhD thesis, Marquette University **1991**
[181] Bocian, D. F., private communication **1992**
[182] Giraudeau, A.; Ruhlmann, L.; ElKahef, L.; Gross, M.; *J. Am. Chem. Soc.*, **1996**, *118*, 2969-2979
[183] Boucher, L. J.; *Coord. Chem. Rev.*, **1972**, *7*, 289
[184] Chang, C. K.; Barkigia, K. M.; Renner, M. W.; *J. Am. Chem. Soc.* **1992,** *114*, 1701-1707